Doctoral Dissertation (Shinshu University)

Study on control of oscillation behaviors for hydrogel microspheres

(ハイドロゲル微粒子の体積振動挙動の制御に関する研究)

March 2022

Graduate School of Textile Science & Technology

Kohei Inui

乾　滉平

Table of Contents

3. Chapter 2

"The Belousov-Zhabotinsky Reaction in Thermoresponsive Core-Shell Hydrogel Microspheres with a Tris(2,2'-bipyridyl)ruthenium Catalyst in the Core"

3.1 Introduction

3.2 Experimental section

3.3 Results and discussion

3.3.1 Microgel synthesis

3.3.2. Oscillation study using various microgels

3.3.3. Temperature-controlled On-Off switching behavior of the BZ reaction in microgels

3.4. Conclusions

3.5. References

4. Summary

5. Acknowledgements

1. Introductory Remarks

1.1 Background

In nature, various spontaneous rhythmic phenomena, e.g., occurrences with temporal periodicity and spatio-temporal patterns, are observed.[1,2] In biological systems, one example of temporal periodicity is the heartbeat. Cardiomyocytes achieve contraction and relaxation movements via oscillatory behavior, such as the association/dissociation of the actin–myosin protein interaction[3-5] using the decomposition energy of adenosine triphosphate (ATP). At the macroscopic scale, the heart, which is composed of cardiomyocytes, is responsible for pumping blood and contributing to the maintenance of vital activity. As another example, the spatio-temporal patterns of proteins in cells also play an important role in biological functions. The ability of a cell to move is regulated by spatio-temporal patterns; cell migration occurs via the patterns of actin-binding proteins and cell division via those of Min proteins.[6-8] As illustrated by these phenomena, the autonomous motions of biological systems are sustained by rhythmic phenomena in the chemical reactions of the biomolecules. The important mechanisms of self-regulation, environmental adaptability, and self-repair in biological systems can be studied to provide insight for the design of artificial materials. In recent years, research toward the construction of artificial cells[9] or biomolecular robots[10-13] using biomolecules as components has been developed. However, since living systems are complicated phenomena, it is not easy to clarify the mechanisms that occur within these. Therefore, research in the field of synthetic molecular chemistry is conducted to provide general insights via artificial models and to create biomimetic autonomous materials.

This research has involved synthetic compounds including metal catalysts,[14-16] supramolecules,[14,15,17,18] polymers,[14-17] and particles.[14,15,19-22] It focuses on synthesizing and organizing molecular building blocks at the microscale to create molecular systems that autonomously convert energy with high efficiency. This could lead to the development of artificial molecular robots and autonomous materials via synthetic chemistry.[14,15] Biological phenomena provide inspiration for the development of new autonomous materials, but the synthesis of these artificial systems must be achieved in a controlled and predictable way. In this regard, it is challenging to mimic living systems, where organized behavior is controlled by spatio-temporal structures on various size scales.

In the field of colloids, synthetic nanometer-to-micrometer-sized particles are studied.[14,15,19-22] Groups of these particles can form macroscopic spatio-temporal

patterns via responsiveness to stimuli driven by external energy such as light and magnetic and/or electric fields, as well as spontaneous functionalization through chemical reactions.[19-22] The use of synthetic particles makes it possible to obtain regularity in collective motions by designing single particles with energy-conversion mechanisms.[19-22] Therefore, it should be possible to artificially create models of the collective motions that occur in nature and autonomous materials that exhibit movements like those of living systems. In particular, colloidal systems with particles that exhibit periodic behavior have been studied using chemical reactions (**Table 1**).[23-45] The particles are designed so that the interaction between them is changed via the stimulus-responsiveness of the surfaces of the particles.[23-34] Here, programmed chemical reaction networks are designed with a feedback mechanism that works to return the system to its normal internal state.[23-45] For example, modifying the surface of the particles with azobenzene, which undergoes a photoisomerization reaction, allows the dispersion/aggregation states of the particles to be controlled by light stimulation.[24-34] In other systems, the oscillatory motion of the particles is regulated by a cycle of reversible reactions that depend on the pH in a buffer, using the hydrolysis of an ester or carbodiimide-based substrates.[35-42] However, in these systems it is necessary to supply an external stimulus or substrate, and thus the lack of sustainability of the periodic control is a problem.[23-42] Therefore, an autonomously pulsating pH system controlled by external equipment, i.e., a continuous stirred-tank reactor, using pH-responsive particles that response to the concentration of hydrogen ions was invented.[43] Without external input, the construction of autonomous cycles in a chemical reaction network would not be easy unless it was based on the use of biomolecules such as enzymes and ATP.[44,45] Thus, the main focus of the studies using artificial colloids has been to control time-periodic motion using the chemical reaction network. Colloidal materials that mimic biological functions such as autonomy and environmental adaptability are still under development.

One class of synthetic particles is hydrogel microspheres (microgels), which are soft and deformable.[46-50] Microgels that are composed of temperature-responsive polymers such as poly *N*-isopropylacrylamide (pNIPAm)[51,52] exhibit a lower critical solution temperature (LCST), and their physicochemical properties can be changed reversibly by changing the external environment, such as the temperature or pH.[53,54] Unlike hard inorganic particles, microgels are open systems swollen by water, which allows chemical substrates to diffuse into their interior or exterior. Microgel systems that exhibit periodic motion, i.e., microgels that convert chemical energy into mechanical motion, have been reported.[55-64] One design strategy for such systems

involves the immobilization of transition-metal-based catalysts such as [ruthenium(II)tris(2,2′-bipyridine)][PF_6]$_2$ ([**1**][PF_6]$_2$) in pNIPAm microgels. The microgels are dispersed in a reaction solution, and the periodic oxidation/reduction reaction of the metal complex site is allowed to proceed. Since the change in the oxidation/reduction state is converted into a change of the hydrophilicity/hydrophobicity of the gels, the microgels can spontaneously generate volume oscillation. It is thus possible to control this autonomous oscillation behavior continuously at regular intervals without external stimuli (**Table 1**; p(NIPAm-*co*-[**1**][PF_6]$_2$)). Here, the Belousov–Zhabotinsky (BZ) reaction,[65-71] an oscillating chemical reaction that imitates the metabolic reaction of a living system,[72] is used to control the time periodicity. Furthermore, these systems show rhythms and patterns similar to biological phenomena such as the heartbeat.[69,70] Therefore, the oscillating behavior of microgels generated by the BZ reaction can be used for understanding and imitating biological phenomena.

The application of the BZ reaction to polymeric materials has been investigated on various scales. On the scale of linear polymers, Ishiwatari et al. applied this reaction to an electrolyte polymer in 1984.[73] The polymer was part of the substrate for the BZ reaction and was thus involved in oscillating behavior. In bulk gels larger than a millimeter, Yamaguchi et al. applied the BZ reaction to a polyacrylamide bulk hydrogel in 1991.[74] This represented the first report of the study of the BZ reaction using a water-swollen three-dimensional polymer network as a medium. The effects of substrate diffusion in an environment where the catalyst is immobilized in a polymer network, as well as spatio-temporal patterns due to the size and shape of the gel, on the oscillatory behavior of the BZ reaction were discussed. Subsequently, Yoshida et al. used a polymer with an LCST, pNIPAm, in 1996.[75] In the BZ reaction solution, it was revealed that the pNIPAm gel showed a change in volume phase transition temperature (VPTT) in synchronization with the BZ reaction. A gel that beats autonomously under certain conditions, like a heart, using the chemical energy of the BZ reaction was proposed for the first time.

In addition to their gel properties, microgels also have colloidal properties. By adapting microgels using the BZ reaction, Suzuki et al. first achieved the characteristic oscillating behavior of a colloidal dispersion system in 2008.[55] Oscillation waveforms were observed via the time-dependent change in the transmittance caused by the difference in light-scattering intensity between the swollen and deswollen states. Under conditions in which the microgels are in the dispersed state, the amplitude of the oscillation waveform varies due to the difference in the size of the microgels in the

oxidized/reduced states. On the other hand, under certain conditions, where microgels aggregate, a dramatic change in turbidity occurs due to the decrease in colloidal stability caused by the deswelling of the microgels. Thus, the dispersing/flocculating oscillation of the microgels was found to be synchronized with the time-periodic changes in the colloidal stability of the particles in addition to the swelling/deswelling oscillation of the gels. The microgels also show unusual functionality at the macroscopic level, where they produce a collective motion. Focusing on living systems, for example, the heart can be regarded as an assembly of cardiomyocytes, and the micro-movement of actin and myosin in the individual cardiomyocytes causes periodic beats.[2-5] Inspired by this phenomenon, it was found that a macrogel assembled from the microgels exhibited a large volume amplitude analogous to a heartbeat.[61] The macrogel was created by centrifugal concentration of the microgel dispersion and chemical bonding of the microgels. When the dispersing/flocculating oscillation of the microgels occurred, the volume amplitude of the macrogel increased. By constructing a higher structure from the microgels, macroscopic motion that cannot be achieved with conventional gels was realized. In addition to this oscillatory behavior, the effects on the cross-linking density of the microgels,[56] initial substrate concentration in the BZ reaction,[57] periodic viscosity changes of the microgel dispersion,[58,59] and introduction of a core–shell structure to the oscillating microgels[60] have been investigated. Microgels can be regarded as the smallest unit with a three-dimensional polymer network structure, i.e., volume. From the viewpoint of microgel design, the author speculated that it might be possible to control the volumetric oscillation behavior driven by the BZ reaction.

As described above, oscillating microgels exhibit periodic behavior that changes their volume (swelling/deswelling oscillation) and colloidal stability (dispersing/flocculating oscillation). These phenomena occur via mechanisms in which the reaction substrate diffuses into the gels and chemical reactions are transformed into oscillatory motion. In biological phenomena, there are important rhythms that maintain activities such as the heartbeat and brain waves. In cell tissues such as cardiomyocytes, reaction networks are formed via biomolecules and the interaction of proteins.[2] Therefore, if the microgels can be used as components to control substrate diffusion inside the three-dimensional structure of the particles, it could be possible to control the oscillatory behavior of the system via a precise chemical network, like in biological tissue. Furthermore, there should be sufficient room for improvement in these systems to achieve superior functionalization similar to that of living organisms in terms of designing the microgel component. If such imitation becomes possible using microgels, they could be used to create models of rhythmic phenomena in nature and applied in

advanced bioinspired materials.

Table 1. Colloidal oscillation systems controlled by chemical reaction.

Particles	Diameter (nm)	Chemical reaction	Stimulus/ Substrate	Sustainability of periodic control	Oscillation period	Ref.
PEG-*b*-pSt[a] vesicles	300–700	Catalytic decomposition of hydrogen peroxide	Temperature	Need to supply external stimuli	~16 min	23
TiO_2	200–2,500		Light		~50–~100 s	24,25
AgCl	1,000–2,300	Dissolution of AgCl			~17 s	26
gold, silver, Fe_3O_4, silica, pSt	5–5,000	Azobenzene isomerization			100 s	27–30
gold, silica, pMMA[b]	6–920	Spiropyran isomerization			~70 s	31–34
gold, Fe_3O_4, silicon nanocrystals	4–15	Esterification of carboxylic acids	EDC[f]	Need to supply substrates	~4–~26 h	35,36
p(NIPAm-*b*-MMA)	750		DMS[g]		~ 80 min	37
gold	4	Hydrolysis	Esters		~24–~36 h	38
p(OEGMA-*co*-DEAEMA)[c]	400–800		Urea		~10 min–~10 h	39–41
pSt, PEO-*b*-PCD[d] micelles	20–70	Complexation of ATP and polymers	ATP		~20–~60 min	42
p(NIPAm-*co*-AAc[e])	150–700	Acidity of carboxylic acids	H^+	Controlled with CSTR[h]	~100 min	43
PEG-*b*-pSt polymersomes	200	Enzymatic reaction	ATP, glucose	Autonomous cyclic reaction network	~70–~130 min	44,45
p(NIPAm-*co*-[**1**][PF_6]$_2$)	40–4,300	Redox of metal complex catalyst	The BZ reaction		~7–500 s	55–64

[a] PEG-*b*-pSt: poly(ethylene glycol)-*b*-poly(styrene), [b] pMMA: poly(methyl methacrylate),
[c] p(OEGMA-*co*-DEAEMA): oligo(ethylene glycol) methyl ether methacrylate-*co*-diethylaminoethyl methacrylate,
[d] PEO-*b*-PCD: poly(ethylene oxide)-*b*-functional block appended with biguanidine-cyclodextrin side units,
[e] AAc: acrylic acid, [f] EDC: 1-(3-dimethylaminopropyl)-3-ethylcarbodiimide, [g] DMS: dimethyl sulfate,
[h] CSTR: continuous stirred-tank reactor.

1.2 Outline

The author has investigated the control of the BZ reaction through the design of the microgels and thus developed new functionalities based on oscillation control. The oscillation behavior of the microgels can be controlled via the BZ reaction, which depends on the temperature and the substrate concentration.[55,57] On the other hand, the

oscillation behavior of the BZ reaction such as oscillation period, oscillation amplitude, and oscillation duration are affected by the physicochemical properties of the microgels.[56,60,61,64] Therefore, it is important to design the microgels and optimize the BZ reaction in order to control the oscillation behavior. The physicochemical properties of the microgels, such as gel size, swelling degree, and colloidal stability, can be designed by changing the chemical composition or synthetic method.[46-50,76,77] Furthermore, the introduction of a core–shell structure enables sophisticated structural design of the microgel properties, including the particle morphology, microgel interactions, multi-stimulus responsiveness, and the uptake and release of substrates.[78-85] In this thesis, the effects of chemical composition and microgel structure on the BZ reaction were investigated. Finally, precise control of the oscillation behavior was achieved via the development of functionalized microgels.

In **chapter 1**, the author reports the development of microgels that exhibit high-frequency oscillation similar to that of the heartbeat. Biological phenomena exhibit various oscillation periods, such as the ~1 s period of the heartbeat and the ~24 h circadian rhythm. Control of the oscillation period of microgels is important for imitating and understanding biological phenomena. When the BZ reaction is carried out under high-temperature or high-substrate-concentration conditions, the chemical reaction rate increases, and thus, a shortened oscillation period would be expected. However, under these conditions, conventional microgels tend to aggregate irreversibly. Therefore, by investigating the chemical composition of the microgels to obtain microgels that show high colloidal stability, short-period oscillation was successfully achieved.

In **chapter 2**, the author reports the development of microgels for which the oscillation can be switched on or off by changing the temperature. One of the important functions of biological systems is recognizing and adapting to changes in the external environment. The ability of a cell to move is regulated by spatio-temporal patterns induced in cell tissues. Similarly, control of the rhythm and pattern of the BZ reaction is important because it is directly linked to the oscillation behavior of the microgels. However, since the reaction substrate continuously diffuses into the gels, the oscillation itself cannot be stopped or restarted. Therefore, by developing microgels with a temperature-responsive hydrogel shell that can regulate the substrate diffusion into the core, on–off switching of the oscillation in response to changing temperature was realized.

1.3 References

1. Vicsek, T.; Zafeiris, A. Collective motion, *Physics Reports* **2012**, *517*, 71-140.

2. Alberts, B.; Johnson, A. D.; Lewis, J.; Morgan, D.; Raff, M.; Roberts, K.; Walter, P. *Molecular Biology of the Cell*, W. W. Norton & Company: New York, 2014.

3. Pringle, J. W. S. The Croonian Lecture, 1977 - Stretch Activation of Muscle: Function and Mechanism. *Proc. R. Soc. London, Ser. B* **1978**, *201*, 107–130.

4. Warshaw, D. M. Throttling Back the Heart's Molecular Motor. *Science* **2016**, *351*, 556–557.

5. Robison, P.; Caporizzo, M. A.; Ahmadzadeh, H.; Bogush, A. I.; Chen, C. Y.; Margulies, K. B.; Shenoy, V. B.; Prosser, B. L. Detyrosinated Microtubules Buckle and Bear Load in Contracting Cardiomyocytes. *Science* **2016**, *352*, aaf0659.

6. Blanchoin, L.; Boujemaa-Paterski, R.; Sykes, C.; Plastino., J. Actin dynamics, architecture, and mechanics in cell motility. *Physiol. Rev.* **2014**, *94*, 235-263.

7. Garbett, D.; Bisaria, A.; Yang, C.; McCarthy, D. G.; Hayer, A.; Moerner, W. E.; Svitkina, T. M.; Meyer, T. T-Plastin reinforces membrane protrusions to bridge matrix gaps during cell migration. *Nature. Commun.* **2020**, 11, 4818.

8. Vecchiarelli, A. G.; Li, M.; Mizuuchi, M.; Hwang, L. C.; Seol, Y.; Neuman, Keir C.; Mizuuchi, K. Membrane-bound MinDE complex acts as a toggle switch that drives Min oscillation coupled to cytoplasmic depletion of MinD. *Proc. Natl. Acad. Sci. U.S.A.* **2016**, *113*, E1479.

9. Xu, C.; Hu, S.; Chen, X. Artificial cells: from basic science to applications. *Mater. Today* **2016**, *19*, 516–532.

10. Needleman, D.; Dogic, Z. Active Matter at the Interface Between Materials Science and Cell Biology. *Nat. Rev. Mater.* **2017**, *2*, 17048.

11. Ricotti, L.; Trimmer, B.; Feinberg, A. W.; Raman, R.; Parker, K. K.; Bashir, R.; Sitti, M.; Martel, S.; Dario, P.; Menciassi, A. Biohybrid Actuators for Robotics: A Review of Devices Actuated by Living Cells. *Sci. Robot.* **2017**, *2*, eaaq0495.

12. Sato, Y.; Hiratsuka, Y.; Kawamata, I.; Murata, S.; Nomura, A. M. Micrometer-sized molecular robot changes its shape in response to signal molecules *Sci. Robot.*, **2017**, *2*, eaal3735.

13. Keya, J. J.; Suzuki, R.; Kabir, A. M. R.; Inoue, D.; Asanuma, H.; Sada, K.; Hess, H.; Kuzuya, A.; Kakugo, A. DNA-Assisted Swarm Control in a Biomolecular Motor System. *Nat. Commun.* **2018**, *9*, 453.

14. Merindol, R.; Walther, A. Materials learning from life: concepts for active, adaptive and autonomous molecular systems *Chem. Soc. Rev.*, **2017**, *46*, 5588–5619.

15. Zhang, X.; Chen, L.; Lim, K. H.; Gonuguntla, S.; Lim, K. W.; Pranantyo, D.; Yong, W. P.; Yam, W. J. T.; Low, Z.; Teo, W. J.; Nien, H. P.; Loh, Q. W.; Soh, S. The Pathway to Intelligence: Using Stimuli-Responsive Materials as Building Blocks for Constructing Smart and Functional Systems. *Adv. Mater.* **2019**, *31*, 1804540.

16. He, X.; Aizenberg, M.; Kuksenok, O.; Zarzar, L. D.; Shastri, A.; Balazs, A. C.; Aizenberg, J. Synthetic homeostatic materials with chemo-mechano-chemical self-regulation. *Nature* **2012**, *487*, 214–218.

17. Fukino, T.; Yamagishi, H.; Aida, T. Redox-Responsive Molecular Systems and Materials. *Adv. Mater.* **2017**, *29*, 1603888.

18. Ikegami, T.; Kageyama, Y.; Obara, K.; Takeda, S. Dissipative and Autonomous Square-Wave Self-Oscillation of a Macroscopic Hybrid Self-Assembly under Continuous Light Irradiation *Angew. Chem. Int. Ed.* **2016**, *55*, 8239–8243.

19. Katuri, J.; Ma, X.; Stanton, M. M.; Sánchez, S. Designing Micro- and Nanoswimmers for Specific Applications. *Acc. Chem. Res.* **2017**, *50*, 2–11.

20. Lin, Z.; Gao, C.; Chen, M.; Lin, X.; He, Q. Collective Motion and Dynamic Self-Assembly of Colloid Motors. *Curr. Opin. Colloid Interface Sci.* **2018**, *35*, 51–58.

21. Fernández-Medina, F.; Ramos-Docampo, M. A.; Hovorka, O.; Salgueiriño, V.; Städler, B. Recent Advances in Nano- and Micromotors. *Adv. Funct. Mater.* **2020**, *30*, 1908283.

22. van Ravensteijn, B. G. P.; Voets, I. K.; Kegel, W. K.; Eelkema, R.

Out-of-Equilibrium Colloidal Assembly Driven by Chemical Reaction Networks. *Langmuir* **2020**, *36*, 10639–10656.

23. Tu, Y.; Peng, F.; Sui, X.; Men, Y.; White, P. B.; van Hest., J. C. M.; Wilson, D. A. Self-propelled supramolecular nanomotors with temperature-responsive speed regulation. *Nature Chemistry* **2017**, *9*, 480–486.

24. Singh, D. P.; Choudhury, U.; Fischer, P.; Mark, A. G. Non-Equilibrium Assembly of Light-Activated Colloidal Mixtures. *Adv. Mater.* **2017**, *29*, 1701328.

25. Hong, Y.; Diaz, M.; CórdovaFigueroa, U.M.; Sen, A. Light driven titanium dioxidebased reversible microfireworks and micromotor/micropump systems. *Adv. Funct. Mater.* **2010**, *20*, 1568–1576.

26. Ibele, M.; Mallouk, T. E.; Sen, A.; Schooling behavior of light powered autonomous micromotors in water. *Angew. Chem. Int. Ed.* **2009**, *48*, 3308–3312.

27. Klajn, R.; Wesson, P. J.; Bishop, K. J. M.; Grzybowski, B. A. Writing Self-Erasing Images Using Metastable Nanoparticle “Inks”. *Angew. Chem., Int. Ed.* **2009**, *48*, 7035–7039.

28. Wei, Y.; Han, S.; Kim, J.; Soh, S.; Grzybowski, B. A. Photoswitchable Catalysis Mediated by Dynamic Aggregation of Nanoparticles. *J. Am. Chem. Soc.* **2010**, *132*, 11018–11020.

29. Zhao, H.; Sen, S.; Udayabhaskararao, T.; Sawczyk, M.; Kucanda, K.; Manna, D.; Kundu, P. K.; Lee, J. W.; Král, P.; Klajn, R. Reversible Trapping and Reaction Acceleration within Dynamically Self-Assembling Nanoflasks. *Nat. Nanotechnol.* **2016**, *11*, 82–88.

30. Kathan, M.; Hecht, S. Photoswitchable Molecules as Key Ingredients to Drive Systems Away from the Global Thermodynamic Minimum. *Chem. Soc. Rev.* **2017**, *46*, 5536–5550.

31. Vialetto, J.; Anyfantakis, M.; Rudiuk, S.; Morel, M.; Baigl, D. Photoswitchable Dissipative Two-Dimensional Colloidal Crystals. *Angew. Chem., Int. Ed.* **2019**, *58*, 9145–9149.

32. Klajn, R. Spiropyran-Based Dynamic Materials. *Chem. Soc. Rev.* **2014**, *43*, 148– 184.

33. Ueda, M.; Kudo, K.; Ichimura, K. Photochromic Behaviour of a Spirobenzopyran Chemisorbed on a Colloidal Silica Surface. *J. Mater. Chem. 1995*, *5*, 1007–1011.

34. Bell, N. S.; Piech, M. Photophysical Effects between Spirobenzopyran-Methyl Methacrylate-Functionalized Colloidal Particles. *Langmuir* **2006**, *22*, 1420–1427.

35. Van Ravensteijn, B. G. P.; Hendriksen, W. E.; Eelkema, R.; Van Esch, J. H.; Kegel, W. K. Fuel-Mediated Transient Clustering of Colloidal Building Blocks. *J. Am. Chem. Soc.* **2017**, *139*, 9763–9766.

36. Grötsch, R. K.; Angı, A.; Mideksa, Y. G.; Wanzke, C.; Tena-Solsona, M.; Feige, M. J.; Rieger, B.; Boekhoven, J. Dissipative Self-Assembly of Photoluminescent Silicon Nanocrystals. *Angew. Chem., Int. Ed.* **2018**, *57*, 14608–14612.

37. Samanta, D.; Klajn, R. Aqueous Light-Controlled Self-Assembly of Nanoparticles. *Adv. Opt. Mater.* **2016**, *4*, 1373–1377.

38. Grötsch, R. K.; Wanzke, C.; Speckbacher, M.; Angl, A.; Rieger, B.; Boekhoven, J. Pathway Dependence in the Fuel-Driven Dissipative Self-Assembly of Nanoparticles. *J. Am. Chem. Soc.* **2019**, *141*, 9872–9878.

39. Heuser, T.; Steppert, A. K.; Molano Lopez, C.; Zhu, B.; Walther, A. Generic Concept to Program the Time Domain of Self-Assemblies with a Self-Regulation Mechanism. *Nano Lett.* **2015**, *15*, 2213–2219.

40. Che, H.; Buddingh, B. C.; van Hest, J. C. M. Self-Regulated and Temporal Control of a "Breathing" Microgel Mediated by Enzymatic Reaction. *Angew. Chem., Int. Ed.* **2017**, *129*, 12755–12759.

41. Che, H.; Cao, S.; van Hest, J. C. M., Feedback-Induced Temporal Control of "Breathing" Polymersomes To Create Self-Adaptive Nanoreactors. *J. Am. Chem. Soc.* **2018**, *140*, 5356−5359.

42. Hao, X.; Sang, W.; Hu, J.; Ya, Q. Pulsating Polymer Micelles via ATP-Fueled Dissipative Self-Assembly. *ACS Macro Lett.* **2017**, *6*, 1151−1155.

43. Varga, I.; Szalai, I.; Mészaros, R.; Gilányi, T. Pulsating pH-Responsive Nanogels. *J. Phys. Chem. B* **2006**, *110*, 20297–20301.

44. Nijemeisland, M.; Abdelmohsen, L. K. E. A.; Huck, W. T. S.; Wilson, D. A.; van Hest., J. C. M., A Compartmentalized Out-of-Equilibrium Enzymatic Reaction Network for Sustained Autonomous Movement. *ACS Cent. Sci.* **2016**, *2*, 843−849.

45. Dehne, H.; Reitenbach, A.; Bausch, A. R. Transient Self-Organisation of DNA Coated Colloids Directed by Enzymatic Reactions. *Sci. Rep.* **2019**, *9*, 7350.

46. Pelton, R. Temperature-sensitive Aqueous Microgels. *Adv. Colloid Interface Sci.* **2000**, *85*, 1–33.

47. Plamper, F. A.; Richtering, W. Functional Microgels and Microgel Systems. *Acc. Chem. Res.* **2017**, *50*, 131–140.

48. Suzuki, D.; Horigome, K.; Kureha, T.; Matsui, S.; Watanabe, T. Polymeric Hydrogel Microspheres: Design, Synthesis, Characterization, Assembly and Applications. *Polym. J.* **2017**, *49*, 695–702.

49. Plamper, F. A.; Richtering, W. Functional Microgels and Microgel Systems. *Acc. Chem. Res.* **2017**, *50*, 131–140.

50. Karg, M.; Pich, A.; Hellweg, T.; Hoare, T.; Lyon, L. A.; Crassous, J. J.; Suzuki, D.; Gumerov, R. A.; Schneider, S.; Potemkin, I. I.; Richtering, W. Nanogels and Microgels: From Model Colloids to Applications, Recent Developments, and Future Trends. *Langmuir* **2019**, *35*, 6231–6255.

51. Heskins, M.; Guillet, J. E. Solution Properties of Poly(*N*-isopropylacylamide) *J. Macromol. Sci. Chem. A.* **1968**, *2*, 1441–1455.

52. Schild, H. G. Poly(*N*-isopropylacrylamide): Experiment, Theory and Application. *Prog. Polym. Sci.* **1992**, *17*,163–249.

53. Umeda, Y.; Kobayashi, T.; Hirai, T.; Suzuki, D. Effects of pH and Temperature on Assembly of Multiresponsive Janus Microgels. *Colloid. Polym. Sci.* **2011**, *289*, 729–737.

54. Kureha, T.; Aoki, D.; Hiroshige, S.; Iijima, K.; Aoki, D.; Takata, T.; Suzuki, D. Decoupled Thermo- and pH-responsive Hydrogel Microspheres Cross-linked by Rotaxane Networks. *Angew. Chem., Int. Ed.* **2017**, *57*, 15393–15396.

55. Suzuki, D.; Sakai, T.; Yoshida, R. Self-Flocculating/Self-Dispersing Oscillation of Microgels. *Angew. Chem., Int. Ed.* **2008**, 47, 917–920.

56. Suzuki, D.; Yoshida, R. Temporal Control of Self-Oscillation for Microgels by Cross-Linking Network Structure. *Macromolecules* **2008**, *41*, 5830–5838.

57. Suzuki, D.; Yoshida, R. Effect of Initial Substrate Concentration of the Belousov−Zhabotinsky Reaction on Self-Oscillation for Microgel System. *J. Phys. Chem. B* **2008**, *112*, 12618–12624.

58. Suzuki, D.; Taniguchi, H.; Yoshida, R. Autonomously Oscillating Viscosity in Microgel Dispersions. *J. Am. Chem. Soc.* **2009**, *131*, 12058–12059.

59. Taniguchi, H.; Suzuki, D.; Yoshida, R. Characterization of Autonomously Oscillating Viscosity Induced by Swelling/Deswelling Oscillation of the Microgels. *J. Phys. Chem. B* **2010**, *114*, 2405–2410.

60. Suzuki, D.; Yoshida, R. Self-Oscillating Core/Shell Microgels: Effect of a Crosslinked Nanoshell on Autonomous Oscillation of the Core. *Polym. J.* **2010**, *42*, 501–508.

61. Suzuki, D.; Kobayashi, T.; Yoshida, R.; Hirai, T. Soft Actuators of Organized Self-Oscillating Microgels. *Soft Matter* **2012**, *8*, 11447–11449.

62. Matsui, S.; Kureha, T.; Nagase, Y.; Okeyoshi, K.; Yoshida, R.; Sato, T.; Suzuki, D. Small-Angle X-ray Scattering Study on Internal Microscopic Structures of Poly(*N*-isopropylacrylamide-*co*-tris(2,2′-bipyridyl))ruthenium(II) Complex Microgels. *Langmuir* **2015**, *31*, 7228–7237.

63. Minato, H.; Murai, M.; Watanabe, T.; Matsui, S.; Takizawa, S.; Kureha, T.; Suzuki, D. The Deformation of Hydrogel Microspheres at the Air/Water Interface, *Chemical Communications* **2018**, *54*, 932–935.

64. Matsui, S.; Inui, K.; Kumai, Y.; Yoshida, R.; Suzuki, D. Autonomously Oscillating Hydrogel Microspheres with High-Frequency Swelling/Deswelling and Dispersing/Flocculating Oscillations. *ACS Biomater. Sci. Eng.* **2019**, *5*, 5615–5622.

65. Zaikin, A. N.; Zhabotinsky, A. M. Concentration Wave Propagation in Two-Dimensional Liquid-Phase Self-Oscillating System. *Nature* **1970**, *225*, 535–537.

66. Field, R. J.; Koros. E.; Noyes R. M. Oscillations in Chemical Systems. II. Thorough Analysis of Temporal Oscillation in the Bromate-Cerium-Malonic Acid System. *J. Am. Chem. Soc.* **1972**, *94*, 8649–8664.

67. Zhabotinsky, A. M.; Zaikin, A. N. Autowave Processes in a Distributed Chemical System. *J. Theor. Biol.* **1973**, *40*, 45–61.

68. Field, R. J.; Burger, M. *Oscillations and Travelling Waves in Chemical Systems*; John Wiley & Sons, Inc.: New York, 1985.

69. Toth, R.; Taylor, A. F. The Tris(2,2′-bipyridyl)ruthenium-Catalysed Belousov–Zhabotinsky Reaction. *Prog. React. Kinet. Mech.* **2006**, *31*, 59–115.

70. Yoshida, R.; Sakai, T.; Hara, Y.; Maeda, S.; Hashimoto, S.; Suzuki, D.; Murase, Y. Self-Oscillating Gel as Novel Biomimetic Materials. *J. Controlled Release* **2009**, *140*, 186–193.

71. Epstein, I. R.; Xu, B. Reaction-Diffusion Processes at the Nano- and Microscales. *Nat. Nanotechnol.* **2016**, *11*, 312–319.

72. Bertram, R.; Budu-Grajdeanu, P.; Jafri, M. S. Using Phase Relations to Identify Potential Mechanisms for Metabolic Oscillations in Isolated β-cell Mitochondria. *Islets* **2009**, *1*, 87–94.

73. Ishiwatari, T.; Kawagishi, M.; Mitsuishi, M. Oscillatory reactions in polymer systems. *J. polym. sci., Polym. chem. ed.* **1984**, *22*, 2699–2704.

74. Yamaguchi, T.; Kuhnert, L.; Nagy-Ungvarai, Z.; Mueller, S. C.; Hess, B. Gel systems for the Belousov-Zhabotinskii reaction. *J. Phys. Chem.* **1991**, *95*, 5831–5837.

75. Yoshida, R.; Takahashi, T.; Yamaguchi, T.; Ichijo, H. Self-oscillating gel. *J. Am. Chem. Soc.*, **1996**, *118*, 5134-5135.

76. Agnihotri, P.; Raj, R.; Kumar, D.; Dan, A. Short Oligo(ethylene glycol) Chain Incorporated Thermoresponsive Microgels: From Structural Analysis to Modulation of Solution Properties. *Soft Matter* **2020**, *16*, 7845–7859.

77. Ma, X.; Cui, Y.; Zhao, X.; Zheng, S.; Tang, X. Different deswelling behavior of temperature-sensitive microgels of poly(*N*-isopropylacrylamide) crosslinked by polyethyleneglycol dimethacrylates. *J. Colloid Interface Sci.* **2004**, *276*, 53–59.

78. Nayak, S.; Lyon, L. A. Soft nanotechnology with soft nanoparticles. *Angew. Chem., Int. Ed.* **2005**, *44*, 7686–7708.

79. Lu, Y.; Ballauff, M. Thermosensitive core–shell microgels: from colloidal model systems to nanoreactors. *Prog. Polym. Sci.* **2011**, *36*, 767–792.

80. Smith, M. H.; Lyon. L. A. Multifunctional Nanogels for siRNA Delivery *Acc. Chem. Res.* **2012**, *45*, 985–993.

81. Hellweg, T. Responsive core–shell microgels: Synthesis, characterization, and possible applications. *J. Polym. Sci. Part B: Polym. Phys.* **2013**, *51*, 1073–1083.

82. Suzuki, D.; McGrath, J. G.; Kawaguchi, H.; Lyon, L. A. Colloidal Crystals of Thermosensitive, Core/Shell Hybrid Microgels. *J. Phys. Chem. C* **2007**, *111*, 5667–5672.

83. Hu, X.; Tong, Z.; Lyon, L. A. Multicompartment Core/Shell Microgels *J. Am. Chem. Soc.* **2010**, *132*, 11470–11472.

84. Richtering, W.; Potemkin, I. I.; Trautwein. C. Could multiresponsive hollow shell–shell nanocontainers offer an improved strategy for drug delivery? *Nanomedicine* **2016**, *11*, 2879–2883.

85. Gelissen, A. P. H.; Scotti, A.; Turnhoff, S. K.; Janssen, C.; Radulescu, A.; Pich, A.; Rudov, A. A.; Potemkin, I. I.; Richtering, W., An anionic shell shields a cationic core allowing for uptake and release of polyelectrolytes within core–shell responsive microgels. *Soft Matter* **2018**, *14*, 4287–4299.

2. Chapter 1

"High-Frequency Swelling/Deswelling Oscillation of Poly(Oligoethylene Glycol) Methacrylate Based Hydrogel Microspheres with a Tris(2,2'-bipyridyl)ruthenium Catalyst"

*Part of this work was published in Inui, K.; Saito, I.; Yoshida, R.; Minato, H.; Suzuki, D. *ACS Applied Polymer Materials*, **2021**, *3*, 3298–3306.
Reprinted with permission from Copyright (2021) American Chemistry Society.

2.1 Introduction

In biological systems, spatio-temporal phenomena, e.g., the pulsation of cardiac muscle cells and signal transduction via the activity of nerve cells, involving biomolecular colloids such as proteins are achieved autonomously.[1] At the microscale, the association–dissociation reactions of molecular motors, i.e., actin and myosin filaments that use the decomposition energy of adenosine triphosphate, enable the continuous beating of the human heart with a period of ~1 s.[2-4]

The prospect of creating biomimetic and autonomous materials using natural molecular motors, which convert chemical fuel into mechanical movement to achieve complex and advanced functions is a fascinating research topic.[5-7] Imitating the autonomous system of living organisms, self-driven particles that move by consuming energy and show similarities to biological phenomena related to collective motion have been studied.[8-13] For instance, the chemical reactions of metal-complex catalysts and external stimuli such as light and pH have been used as energy sources, and the resulting collective motions in the system have been investigated (e.g., dispersion/flocculation and propelled motion).[8-13] Such systems can be expected to discover applications as models to develop a universal law of collective motion in biological systems,[5,8,9] and as advanced bioinspired materials for chemical reactions,[10-12] artificial muscles,[6] and self-healing.[5,13]

Microgels are a class of artificial colloids. These soft and deformable particles are composed of cross-linked three-dimensional networks swollen by water, and their typical size ranges from several tens of nanometers to several micrometers.[14-17] One of the most fascinating properties of microgels is their stimulus-responsiveness, i.e., the physicochemical properties such as hydrophilicity/hydrophobicity, surface-charge density and volume change in response to external stimuli such as temperature, pH, or light.[18,19] Suzuki et al. have already developed autonomously oscillating microgels that periodically swell/deswell or disperse/flocculate in the absence of an external

stimulus.[20-29] In these microgels, [ruthenium(II)tris(2,2′-bipyridine)][PF_6]$_2$ ([**1**][PF_6]$_2$), which is a catalyst for the BZ reaction,[30-36] is covalently bound to a thermo-responsive polymer backbone such as pNIPAm.[37,38] The BZ reaction can be considered as analogous to metabolic reactions such as the tricarboxylic acid cycle in cellular organisms.[39] By dispersing the microgels in the reaction solution, the catalyst periodically alternates between the reduced ([**1**]$^{2+}$) and oxidized states ([**1**]$^{3+}$) in a cyclic reaction network. Thus, the microgels show oscillatory swelling/deswelling and assembly/disassembly behavior[20-22] as they spontaneously convert chemical into mechanical energy. The oscillations of these microgels are useful in, e.g., rheology modifiers,[23,24] self-oscillating micropumps,[26,28] and high-performance catalytic carriers.[29]

The activity of living systems is controlled precisely and at high speed, as exemplified by the human heartbeat and brain waves.[1-4] In terms of energy conversion, the response of microgels to external stimuli is expected to be rapid due to their colloidal dimensions (*cf.* the Tanaka–Fillmore equation).[40] However, the induction of responses to external stimuli such as temperature or pH requires external equipment or the addition of a large amount of energy to change the environment of the dispersion medium.[41,42] Therefore, establishing precise and rapid control over the stimulus response of microgels remains challenging. During the development of oscillating microgels, various methods of controlling the oscillation period have been investigated. For instance, in order to increase their VPTT and ensure colloidal stability, the hydrophilic acrylamide monomer has been copolymerized with pNIPAm-based microgels. When they were dispersed at high temperature (~50 °C), a short oscillation period (~7 s) was acieved.[28] On the other hand, the oscillation period of the BZ reaction can be shortened to ~0.1 s by optimizing the reaction conditions (e.g., temperature and the substrate concentration).[43] In the context of microgels, pH-responsive microgels with rapid switching (within ~2 s) have been reported, and the enhanced response speed has been discussed in terms of their chemical composition and reaction kinetics.[44] Based on the above facts, the oscillation period of the microgels could likely be shortened to ~1 s, which is the length of the human heartbeat cycle. If such a fast stimuli-response potential of the microgels could be realized, it can be expected that microgels find applications in actuators with motion similar to the human heartbeat.

In the present study, the author created new autonomously oscillating microgels with poly(oligoethylene glycol) methacrylate (pOEGMA) as the thermo-responsive microgel backbone. The author hypothesized that the BZ reaction conditions could be adapted to take advantage of the lower critical solution temperature

(LCST) of pOEGMA (~64 °C), which is much higher than that of conventional pNIPAm (~32 °C), to achieve a short period comparable to that of the human heartbeat (~1 s). The author focused on the effect of the molecular weight of the poly(ethylene glycol) cross-linker on the progress of the BZ reaction and the swelling/deswelling oscillation behavior of the microgels. Finally, the microgels were organized to create a macrogel that acted as an autonomously oscillating actuator with a period comparable to that of the human heartbeat.

2.2 Experimental Section

Materials

Oligoethylene glycol methacrylate (OEGMA, M_n = 300 g/mol, 98%), ethylene glycol dimethacrylate (EGDMA, M_n = 200 g/mol, 98%), poly(ethylene glycol) dimethacrylate (pEGDMA550, M_n = 550 g/mol, 98%), poly(ethylene glycol) dimethacrylate (pEGDMA750, M_n = 750 g/mol, 98%), glutaraldehyde solution (GA, 50 wt.% in H_2O), and poly(vinyl alcohol) (PVA, M_w = 9,000–10,000, 80% hydrolyzed) were purchased from Sigma Aldrich and used as received. 2,2′-Azobis(2-methylpropinamidine)dihydrochloride (V-50, 95%), sodium chloride (NaCl, 99.5%), malonic acid (MA, 98%), sodium bromate ($NaBrO_3$, 99.5%), nitric acid (HNO_3, 16 M), cerium(III) sulfate *n*-hydrate ($Ce(SO_4)\cdot nH_2O$, 78–88%), and cerium(IV) sulfate tetrahydrate ($Ce(SO_4)_2\cdot 4H_2O$) were purchased from Wako Pure Chemical Industries and used as received. [Ruthenium(II)tris(2,2′-bipyridine)][PF_6]$_2$ ([**1**][PF_6]$_2$) monomer and [ruthenium(II)(4-vinylinyl-4′-methyl-2,2′-bipyridine)bis(2,2-bipyridine)][PF_6]$_2$ were synthesized according to a previously reported procedure.[45] Distilled and ion-exchanged (EYELA, SA-2100E1) water was used in all experiments.

Synthesis of the Oscillating Microgels

According to previously reported procedure,[20] the oscillating pOEGMA microgels were synthesized by a surfactant-free aqueous free radical precipitation polymerization. The polymerization was performed in a three-necked round-bottom flask (50 mL) equipped with a condenser, a mechanical stirrer, and a nitrogen gas inlet. The OEGMA monomer (0.6480 g; 96 mol%), [**1**][PF_6]$_2$ monomer, as well as the EGDMA (0.0090 g, 2 mol%), pEGDMA550 (0.0248 g, 2 mol%), or pEGDMA750 (0.0338 g, 2 mol%, 2 mol%) cross-linker were dissolved in deionized water (28 mL). The monomer solution (75 mM) was heated to 90 °C under constant stirring (250 rpm) and a stream of nitrogen. After sparging with nitrogen for 30 min to remove any

dissolved oxygen, the polymerization was initiated by adding V-50 (0.0163 g, 2 mM) dissolved in deionized water (2 mL). After 4 h, the microgel dispersion was cooled in an ice bath to stop the polymerization. In order to remove any impurities, the following purification process was conducted twice: The microgels obtained were purified by centrifugation (15 °C, 10 min, 415,000 g; HITACHI, himac CS 100 GX), decantation, and redispersion in water. Subsequently, the dispersion was dialyzed for 5 days with daily water replacements. The obtained microgels are denoted as ORu(E), ORu(pE550), and ORu(pE750). Here, O, Ru, E, pE550, and pE750 represent OEGMA, [**1**][PF_6]$_2$, EGDMA, pEGDMA550, and pEGDMA750, respectively.

Observation of the Synthesized Microgels

In order to confirm the formation of microgels and to evaluate their size, the microgel images were observed using transmission electron microscopy (TEM, JEOL2010, operated at 200 kV). Samples were prepared by dropping microgel dispersions (1 μL, ~0.001 wt%) on a carbon-coated copper grid (Okenshoji Co., Ltd.), and dried at room temperature. Using the software package Image J (version 1.51, National Institutes of Health, USA), the diameter of the microgels was calculated (N = 50).

Measurement of the Amount of [1][PF_6]$_2$ in the Microgels

The amount of [**1**][PF_6]$_2$ in the microgels was examined to confirm the incorporation of [**1**][PF_6]$_2$ in the microgels. According to previously reported procedure, the amount of [**1**][PF_6]$_2$ that remains in the supernatant after centrifugation of the dispersion was measured using UV-vis spectroscopy (JASCO, V-630 iRM).[20] The measurement wavelength was set to 460 nm, which corresponds to the absorbance maximum of [**1**]$^{2+}$.[20] After 10 min of thermal equilibration, the measurement was carried out at 25 °C.

Measurement of the Critical Flocculation Temperature of the Microgels

The critical flocculation temperature (CFT) was examined as a function of the NaCl concentration in order to evaluate the tolerance of the microgels toward ionic strength. The temperature dependence of the optical transmittance of the microgel dispersions was monitored using UV-vis spectroscopy at various NaCl concentrations between 0 and 2500 mM. The measurements were conducted at 25–70 °C (heating rate: 0.5 °C/min) under constant stirring (800 rpm). The [**1**][PF_6]$_2$ concentration in the microgels was adjusted to 100 μM in all systems. The measurement wavelength was set

at 570 nm, which corresponds to the isosbestic point of $[\mathbf{1}]^{2+}$ and $[\mathbf{1}]^{3+}$, to eliminate any effects of the absorption of the Ru complex on the transmittance.[20]

Measurements of the Hydrodynamic Diameter (D_h) of the Microgels

The temperature dependence of the hydrodynamic diameters (D_h) of the microgels was measured using dynamic light scattering (DLS, Malvern instruments Ltd., Zetasizer Nano S). The D_h values between 25 and 70 °C were calculated based on the obtained diffusion coefficient using the Stokes–Einstein equation (Zetasizer software v 6.12). The microgel concentration was 0.005 wt%, and microgels were dispersed in solutions of either 910 mM HNO_3/10 mM Ce^{4+} or 880 mM HNO_3/10 mM Ce^{3+} to fix the microgels in the reduced $[\mathbf{1}]^{2+}$ and oxidized $[\mathbf{1}]^{3+}$ states, respectively. An average value of 3 sets of 15 measurements with a 30 s acquisition time was used for the intensity autocorrelation.

Measurements of the Oscillation Waveforms of the Microgels

The oscillation of the microgels was monitored by UV-vis spectroscopy of the turbidity changes of the microgels that are synchronized with the BZ reaction. For that purpose, a mixture of the microgel dispersion ($[[\mathbf{1}][PF_6]_2]$ = 100 μM), HNO_3 (500–2500 mM), and $NaBrO_3$ (50–250 mM) was poured into a sample holder. After 10 min of thermal equilibration, the BZ reaction was initiated by adding the MA solution (25–1000 mM; final liquid volume: 2.5 mL). The measurement wavelength was set to 570 nm and the measurements were carried out under constant stirring (800 rpm) between 25 °C and 65 °C. From the obtained waveforms, the oscillation period and amplitude were calculated based on the average value of the second and sixth oscillations.

Preparation of a Macrogel Composed of the Microgels

The assembled microgels are trapped by the physical entanglement of PVA and retain the shape of the macrogel.[46] A mixture (500 μL) of the microgel dispersion (1.0 wt%) and an aqueous PVA solution (1 wt%) was poured into a centrifuge tube, shaken at 300 rpm and 15 °C for 5 minutes, and then centrifuged at 10,000 g for 5 minutes at 15 °C. After removing 480 μL of the supernatant, 1 μL of GA (50 wt%) was added to the remaining sediment, and the mixture was shaken at 300 rpm and 15 °C for 5 minutes to cause the formation of an acetal bond between PVA and GA and thus induce gelation.[47] The mixture was then poured into a silicone mold (1 mm × 1 mm × 0.1 mm) to assemble the microgels and thus form the macrogel.

Observation of the Swelling/deswelling Oscillation of the Macrogel

The swelling/deswelling oscillation of the macrogel was examined using an optical microscope (LZ-LEDT, Kenis) equipped with a digital camera (ImageX Earth Type S2.0M, Kikuchi-Optical Co., Ltd.). The macrogel was immersed in an aqueous solution (2 mL) that contained HNO_3 (1000 mM) and $NaBrO_3$ (200 mM). After 30 min of thermal equilibration at 37 °C, an MA solution (100 mM) was injected to initiate the BZ reaction. Images of the oscillation behavior of the macrogel was collected in increments of 0.25 s using the software package ImageX Earth Type S-2.0 M, Version 3.0.5 and evaluated by a spatiotemporal analysis.

2.3 Results and discussion

2.3.1 Microgel synthesis

To shorten the oscillation period of the microgels, it is necessary to either elevate the temperature and/or increase the substrate concentration of the BZ reaction. However, irreversible aggregation of the microgels might occur at high temperatures near the VTT and under high-ionic-strength conditions.[28] Under high-substrate concentrations, interparticle electrostatic repulsion of the microgels makes the microgels even more hydrophobic.[20] Hence, microgels with higher VTTs are required not only to conduct the BZ reaction under colloidally stable conditions, but also to enable the swelling/deswelling oscillation of the microgels at higher temperature.[28]

In the present study, the author chose poly(oligoethylene glycol) methacrylate (pOEGMA) as the microgel backbone (**Figure 2-1(a)**). Similar to pNIPAm, pOEGMA exhibits thermoresponsive properties with LCST-type behavior; its LCST values can be varied from 26 to 90 °C by adjusting the number of ethylene oxide units.[48,49] Furthermore, the hydrated pOEGMA microgel surface exhibits good colloidal stability due to the increase in steric hindrance.[29,50,51]

Oscillating pOEGMA microgels that contain the catalyst [**1**][PF_6]$_2$ were synthesized via a surfactant-free aqueous radical precipitation polymerization. As the microgel backbone, the author chose pOEGMA with an LCST of 64 °C, as it is suitable for aqueous precipitation polymerization at 90 °C, i.e., below the boiling point of water. Additionally, the author investigated how cross-linkers that differ with respect to molecular weight of the poly(ethylene glycol) affect the progress of the BZ reaction and the swelling/deswelling oscillation behavior of the microgels. Microgels were synthesized using various molecular weights of the cross-linker poly(ethylene glycol) (E (M_w = 200) for EGDMA; pE550 (M_w = 550) for pEGDMA; pE750 (M_w = 750) for pEGDMA) (**Table 2-1**) in order to control the oscillation behavior (e.g., the amplitude

and oscillation period) of the microgels. As the deswelling ratio of microgels increases remarkably with increasing poly(ethylene glycol) chain length,[51-53] the cross-linkers of the microgels would be expected to affect the size of the microgels and substrate diffusion into the microgels. TEM images of representative ORu(E), ORu(pE550), and ORu(pE750) microgels after drying at room temperature are shown in **Figure 2-1(b)**. None of the three microgels exhibited secondary particles and uniform particles were obtained given the coefficient of variation of the microgel diameters (CV = ~10%). The amount of the catalyst [**1**][PF_6]$_2$ in all the microgels was almost identical (**Table 2-1**) and the color of the catalyst was visible in all the microgel dispersions (**Figure 2-1(c)**). To confirm that the oscillating pOEGMA microgels exhibit high ionic tolerance, the dependence of the CFT of the pOEGMA microgels (ORu(pE550)) on the NaCl concentration was evaluated between concentrations of 0 and 2500 mM (**Figure 2-2**). In a previous study, it was reported that oscillating pNIPAm microgels exhibit a CFT of 32 °C in the presence of 100 mM NaCl,[20] whereas the oscillating pOEGMA microgels in this study can tolerate up to 2500 mM NaCl at the same CFT. This series of tests demonstrated that the obtained microgels would enable the BZ reaction to be conducted at high temperature and high substrate concentration and should thus be able to exhibit a short oscillation period.

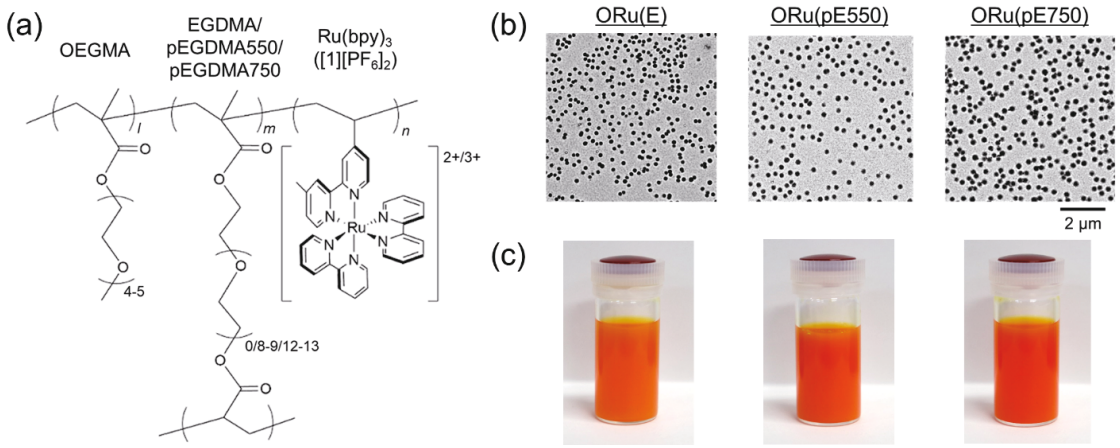

Figure 2-1. (a) Chemical structure of the oscillating pOEGMA microgels used in this study. (b) TEM images of the dried microgels at room temperature (~25 °C). (c) Photographs of dispersions of the microgels.

Table 2-1. Synthetic conditions, diameters (D),[a] and [**1**][PF_6]$_2$ content of the microgels.

	OEGMA (mol%)	EGDMA (mol%)	pEGDMA550 (mol%)	pEGDMA750 (mol%)	[1][PF_6]$_2$ (mol%)	D (nm)[a] (CV/%)	[1][PF_6]$_2$ introduced (mol%)
ORu(E)	96	2			2	181±18 (10.1%)	0.97
ORu(pE550)	96		2		2	254±23 (8.8%)	0.90
ORu(pE750)	96			2	2	272±25 (9.2%)	0.86

[a] Determined from TEM images of the dried microgels at room temperature (~25 °C).

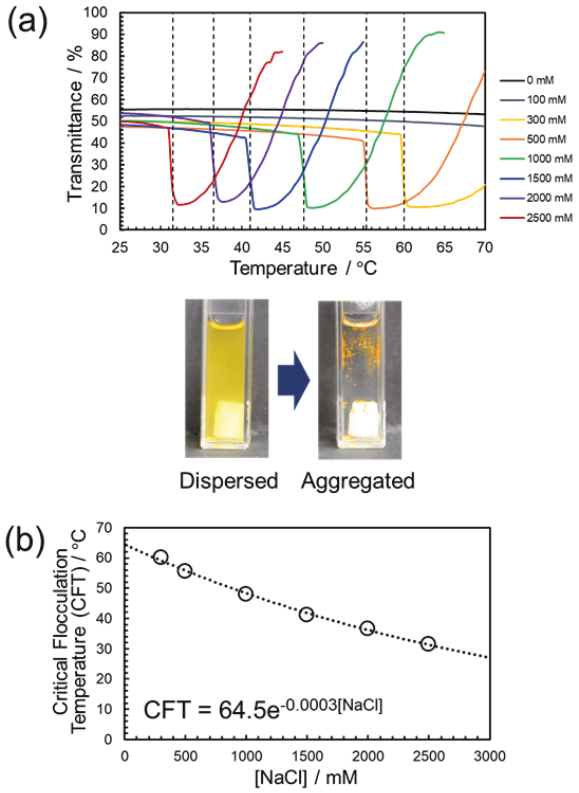

Figure 2-2. (a) Temperature dependence of the optical transmittance of the pOEGMA oscillating microgels (ORu(pE550)) at various NaCl concentrations and (b) CFT dependence of the microgels on the NaCl concentration as measured using UV-vis spectroscopy.

Subsequently, the temperature dependence of the hydrodynamic diameter (D_h) of the microgels was measured using dynamic light scattering (DLS) to confirm that the variation of the microgel size was synchronized with the BZ reaction. The molecules of [**1**][PF_6]$_2$ in the microgels were fixed in either the reduced state ([**1**]$^{2+}$) or the oxidized state ([**1**]$^{3+}$) using a reducing or oxidizing agent,[20] respectively. The ionic strength of each microgel dispersion was set to 1000 mM, which is the same as that in the BZ reaction. As can be seen in **Figure 2-3**, the size variation was confirmed for the microgels containing the reduced or the oxidized catalyst. It should also be noted here that all the microgels flocculated near the LCST of pOEGMA (~64 °C) in the reduced [**1**]$^{2+}$ state, while the microgels in the oxidized [**1**]$^{3+}$ state maintained their colloidal stability at higher temperature. These results indicate that the VTT behavior of pOEGMA is related to its redox state, which is comparable to conventional pNIPAm.[20-22] In the reduced [**1**]$^{2+}$ or oxidized [**1**]$^{3+}$ states, the D_h values of the deswollen microgels near the LCST of pOEGMA (~64 °C) were almost identical. On the other hand, among the swollen microgels below the LCST, the D_h values increased with increasing molecular weight of the cross-linker. The hydrophilic side chains that consist of ethylene oxide units for cross-linker can be expected to be involved in the swelling behavior of the microgels.[51-53] Based on these results, it can also be expected that the cross-linkers affect not only the density of the polymer network in the microgels, but also their oscillatory behavior during the BZ reaction.

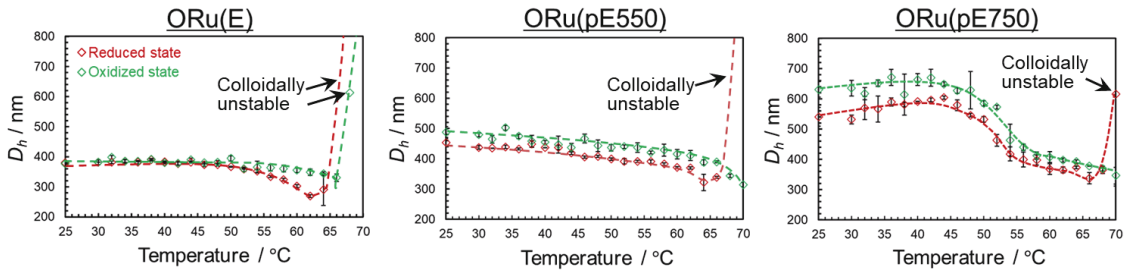

Figure 2-3. Temperature dependence of the hydrodynamic diameter (D_h) of the ORu(E), ORu(pE550), and ORu(pE750) microgels in the reduced [**1**]$^{2+}$ (in 910 mM HNO_3/10 mM Ce^{3+} solution) and oxidized [**1**]$^{3+}$ (in 880 mM HNO_3/10 mM Ce^{4+} solution) states.

2.3.2 Investigation of the oscillatory behavior under the BZ reaction conditions

Next, the BZ reaction was performed using the obtained microgels and the oscillatory behavior was examined by UV-vis spectroscopy of the optical transmittance. In the cases where oscillation behavior was observed, the oscillation began after an induction period. The oscillation period of the BZ reaction at different substrate concentrations and temperatures was evaluated based on the transmittance waveforms (**Figure 2-4**).

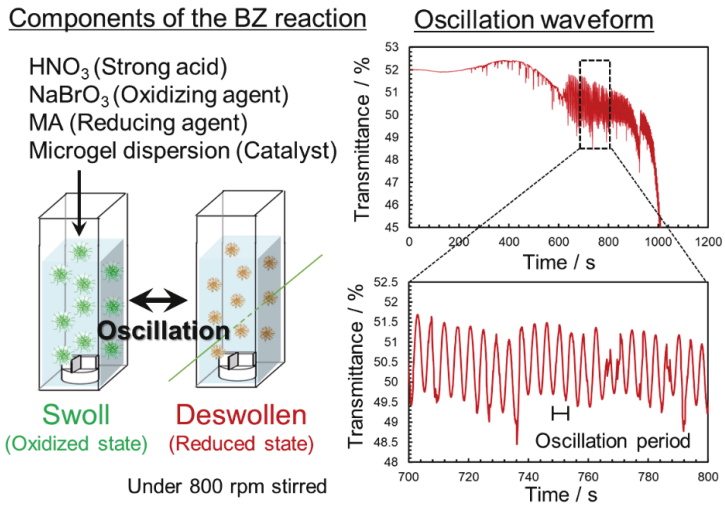

Figure 2-4. Procedure for the BZ reaction and a typical oscillation waveform (ORu(pE550); [**1**][PF_6]$_2$ = 100 μM; [HNO_3] = 850 mM; [$NaBrO_3$] = 150 mM; [MA] = 100 mM; 55 °C).

First, the substrate concentration (HNO_3, $NaBrO_3$, and MA) dependence of the oscillation behavior of the pOEGMA microgels (ORu(pE550)) was evaluated. The temperature was fixed at 55 °C, where the dispersion stability of the microgels was maintained sufficiently. Oscillatory behavior occurred in the ranges of 500-2000 mM for [HNO_3], 50-200 mM for [$NaBrO_3$], and 25-150 mM for [MA] (**Figures 2-5**, **2–6**, and **2-7**). The oscillation periods determined from the waveforms showed linear relationships with the substrate concentrations, which were used to determine the chemical reaction rate equations (**Figure 2-8**).[54] Furthermore, the oscillation period decreased with increasing substrate concentration. Surprisingly, a short oscillation period of ~4.0 s, which represents the shortest period reported to date, was observed under some high-substrate-concentration conditions. These results indicate that oscillation behavior with a short period can be precisely controlled by varying the substrate concentration.

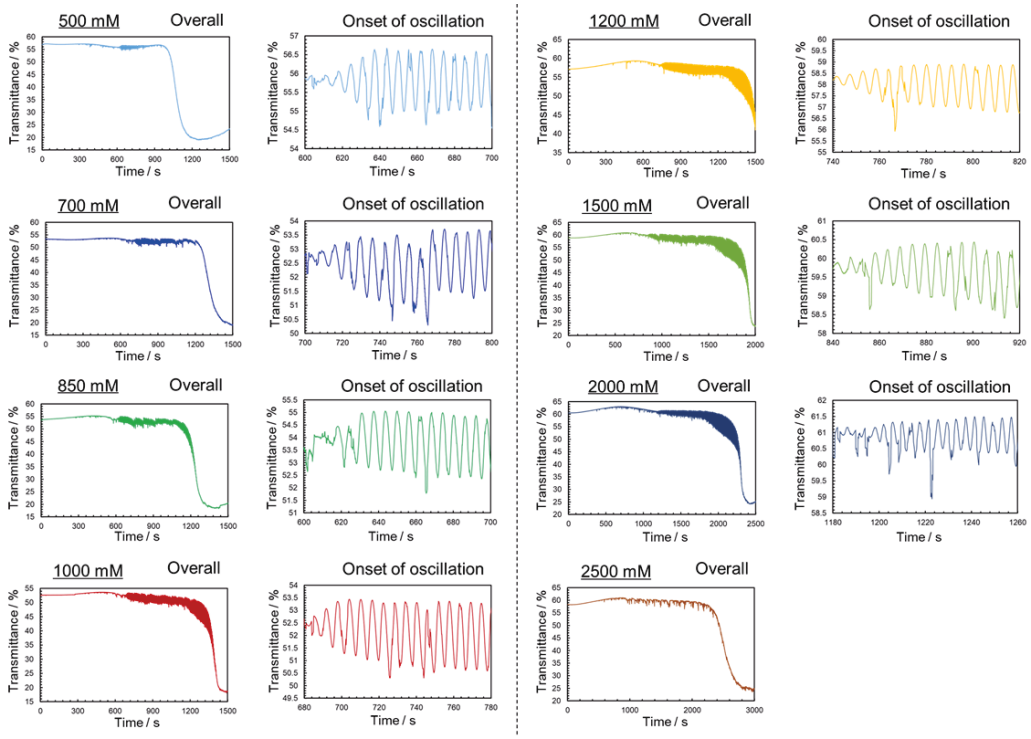

Figure 2-5. Dependence of the oscillation waveforms of the ORu(pE550) microgels on the nitric acid concentration ([HNO_3]). [**1**][PF_6]$_2$ = 100 μM; [$NaBrO_3$] = 150 mM; [MA] = 100 mM; 55 °C.

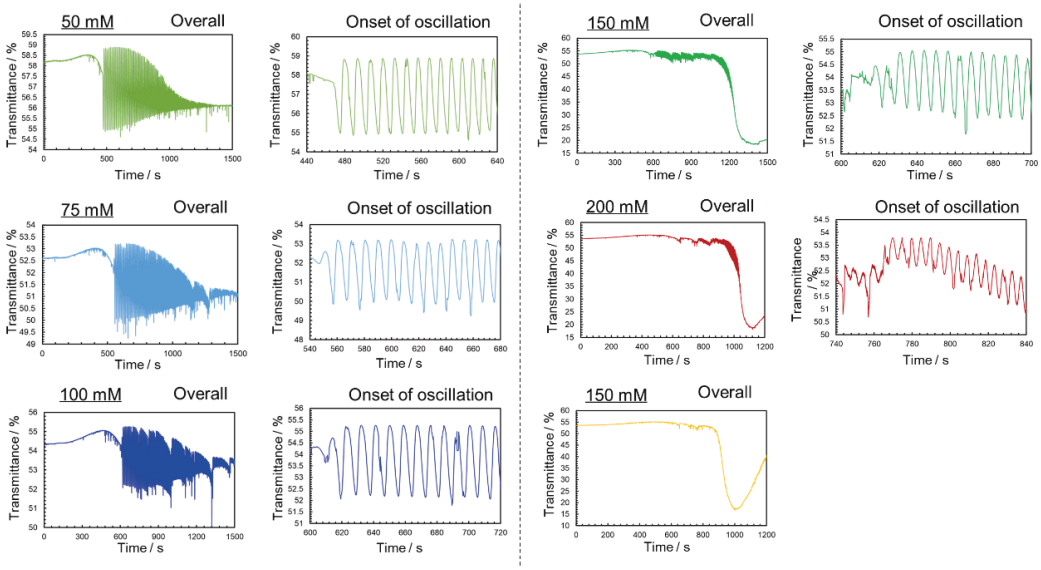

Figure 2-6. Dependence of the oscillation waveforms of the ORu(pE550) microgels on the $NaBrO_3$ concentration ([$NaBrO_3$]). [**1**][PF_6]$_2$ = 100 μM; [HNO_3] = 850 mM; [MA] = 100 mM; 55 °C.

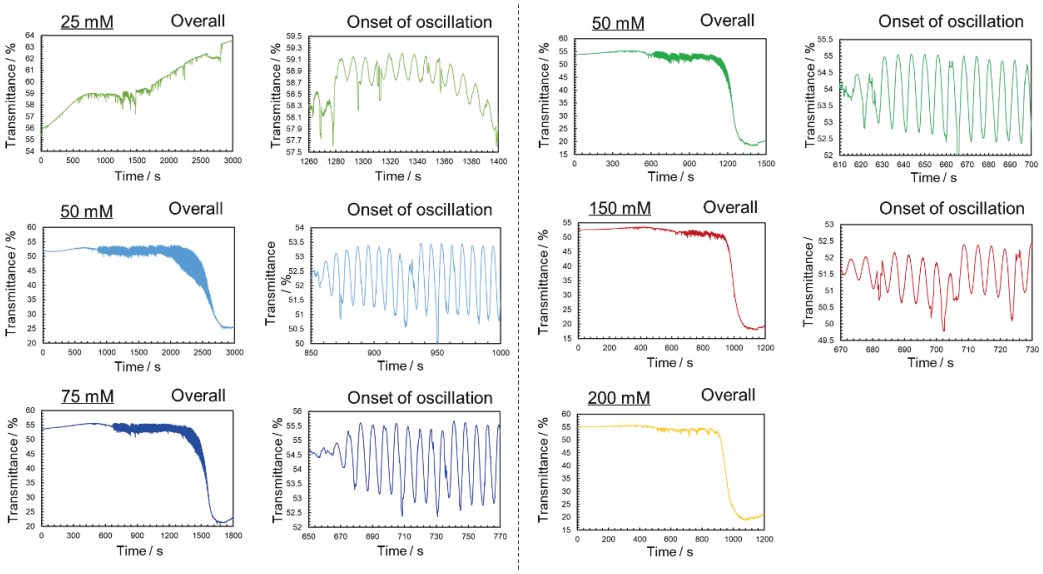

Figure 2-7. Dependence of the oscillation waveforms of the ORu(pE550) microgels on the malonic acid concentration ([MA]). [**1**][PF_6]$_2$ = 100 μM; [HNO_3] = 850 mM; [$NaBrO_3$] = 150 mM; 55 °C.

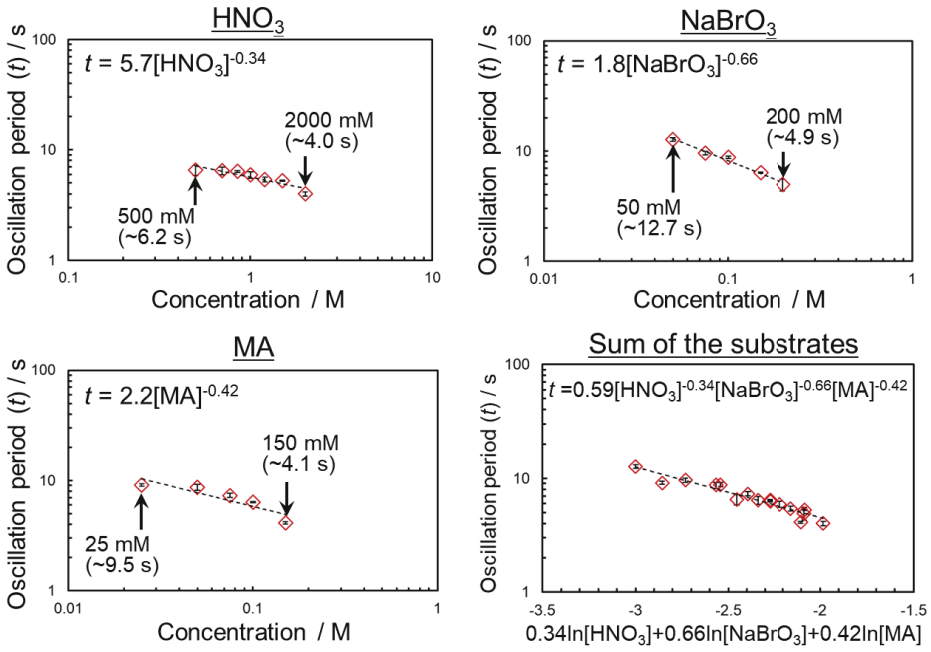

Figure 2-8. Linear relationship between the oscillation period and the concentration of the BZ reaction substrates: HNO_3, $NaBrO_3$, and MA, as well as the sum of all the substrate concentrations. The BZ reaction was conducted at standard reference conditions ([**1**][PF_6]$_2$ = 100 μM; [HNO_3] = 850 mM; [$NaBrO_3$] = 150 mM; [MA] = 100 mM; 55 °C), and the concentration of the specified substrate was varied.

Subsequently, the temperature dependence of the oscillatory behavior of the microgels (ORu(E), ORu(pE550), and ORu(pE750)) was evaluated. The substrate concentrations were fixed at [HNO_3] = 850 mM, [$NaBrO_3$] = 150 mM, and [MA] = 100 mM, where the dispersion stability of the microgels was maintained sufficiently. Oscillation was observed in the range from 25 °C to approximately the flocculation temperature of the microgels in the reduced [**1**]$^{2+}$ state (**Figures 2-9**, **2-10**, and **2-11**). When the oscillation period obtained from the waveforms and temperature were plotted using the Arrhenius equation (1), a linear relationship was observed (**Figure 2-12**).[20,21,25,28,29,55]

$$\ln F_{osc} = \ln A_{osc} - E_{osc}/RT \qquad (1)$$

where F_{osc} is the frequency of the oscillation, A_{osc} is the collision factor, E_{osc} is the apparent activation energy, R is the gas constant (R = 8.314 J K^{-1} mol^{-1}), and T is the temperature in Kelvin. Higher temperatures corresponded to shorter oscillation periods, with the shortest oscillation period being ~3.2 s. Thus, the rapid oscillation can be controlled not only by the substrate concentration, but also by the temperature. The values of E_{osc} and A_{osc} decrease with increasing molecular weight of the cross-linker (ORu(E): E_{osc} = 71.4 kJ mol^{-1}, A_{osc} = 5.55 × 10^{10} s^{-1}; ORu(pE550): E_{osc} = 62.1 kJ mol^{-1}, A_{osc} = 1.40 × 10^{9} s^{-1}; ORu(pE750): E_{osc} = 57.4 kJ mol^{-1}, A_{osc} = 2.39 × 10^{8} s^{-1}), which may suggest that the reaction efficiency also depends on the chemical composition of the microgels.[56] Especailly, the values for ORu(pE750) were close to those for the catalyst alone, i.e., without the microgels. Hence, the microgel cross-linkers can be expected to affect the ease of substrate diffusion and the chemical reaction, as these values can be expected to correlate to the density of the polymer network in the microgels. Furthermore, the amplitude of the change in transmittance was evaluated and found to be higher for microgels with higher molecular weight of the cross-linker (**Figure 2-13**). This result is most likely due to the increased microgel size or colloidal stability of the microgels, as discussed for the redox state experiments (**Figure 2-3**). Based on these results, the author anticipated that a shorter oscillation period could be obtained by optimizing the BZ conditions and the chemical composition of the microgels.

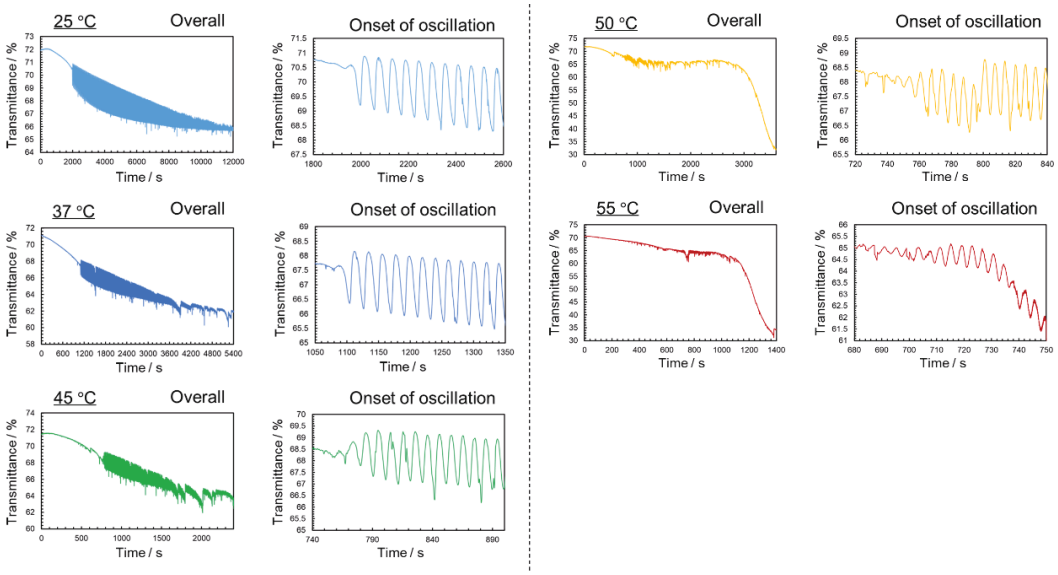

Figure 2-9. Dependence of the oscillation waveforms of the ORu(E) microgels on the temperature. [**1**][PF_6]$_2$ = 100 μM; [HNO_3] = 850 mM; [$NaNO_3$] = 150 mM, [MA] = 100 mM.

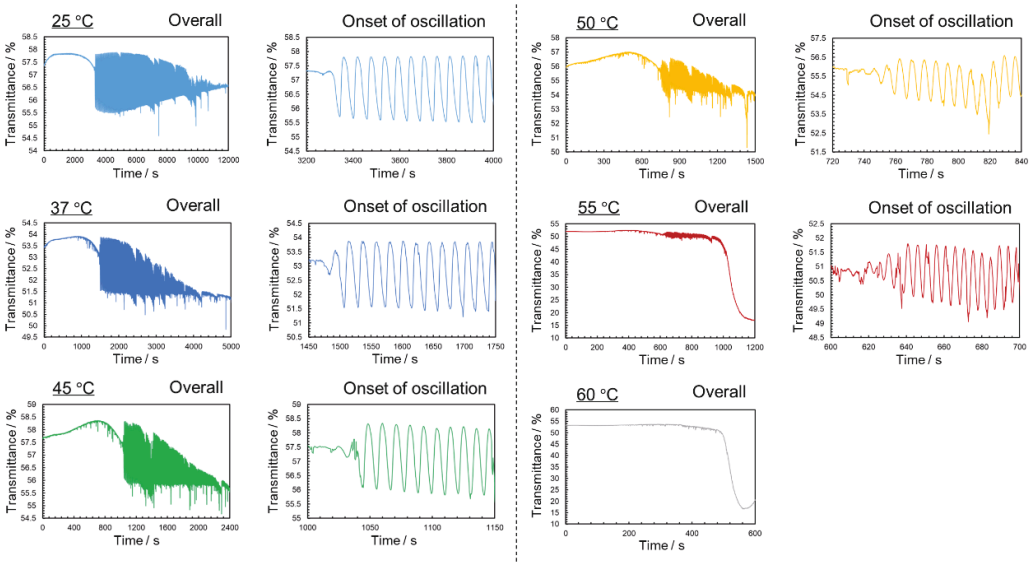

Figure 2-10. Dependence of the oscillation waveforms of the ORu(pE550) microgels on the temperature. [**1**][PF_6]$_2$ = 100 μM; [HNO_3] = 850 mM; [$NaNO_3$] = 150 mM, [MA] = 100 mM.

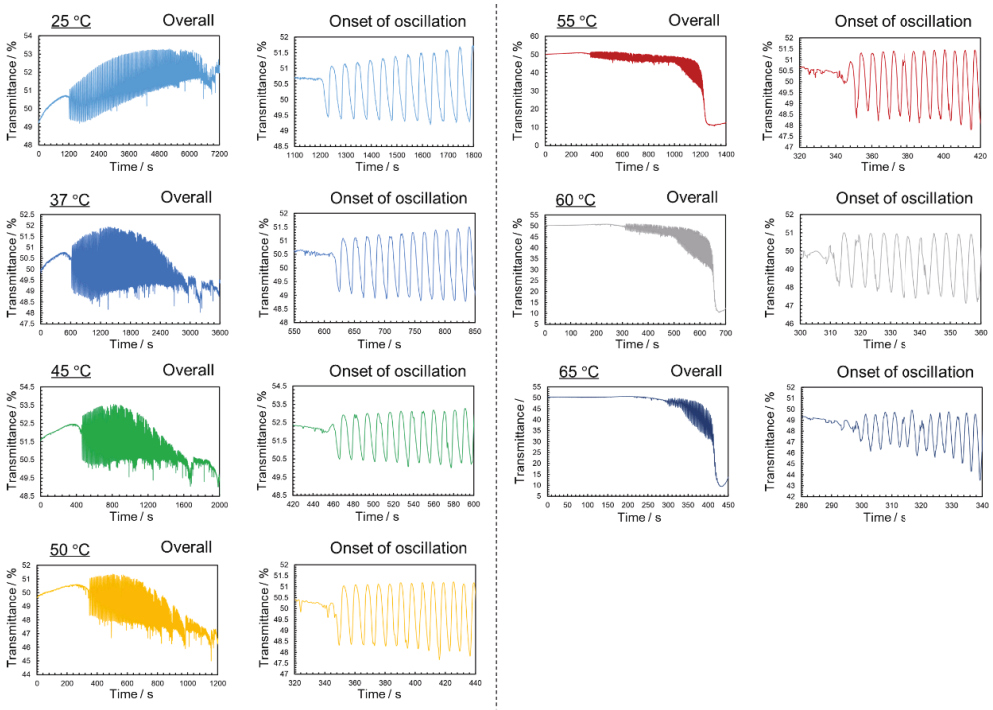

Figure 2-11. Dependence of the oscillation waveforms of the ORu(pE750) microgels on the temperature. [**1**][PF_6]$_2$ = 100 μM; [HNO_3] = 850 mM; [$NaNO_3$] = 150 mM, [MA] = 100 mM.

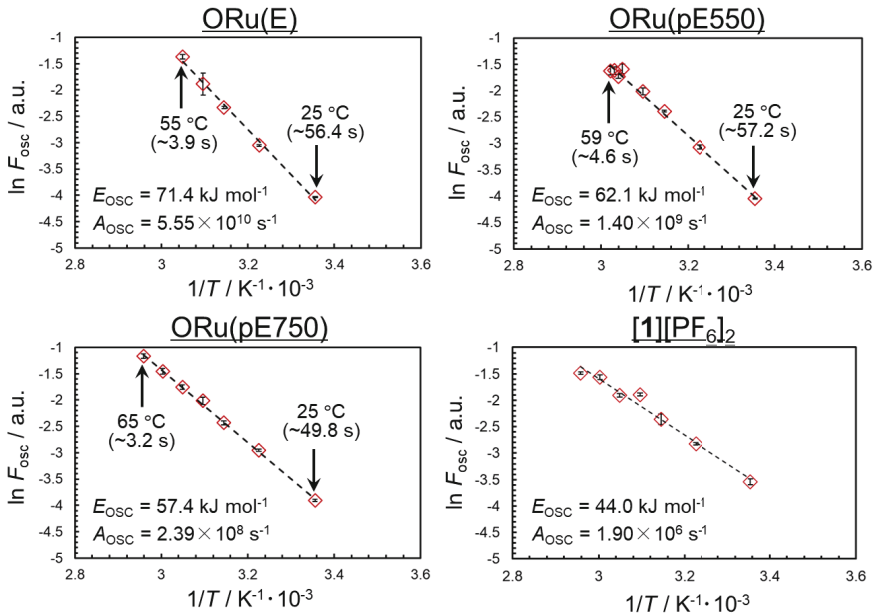

Figure 2-12. Linear relationship between the oscillation period and temperature in the BZ reactions of ORu(E), ORu(pE550), ORu(pE750), and [**1**][PF_6]$_2$ without microgels. The BZ reaction was conducted at standard reference conditions ([**1**][PF_6]$_2$ = 100 μM; [HNO_3] = 850 mM; [$NaBrO_3$] = 150 mM; [MA] = 100 mM) and the temperature was varied.

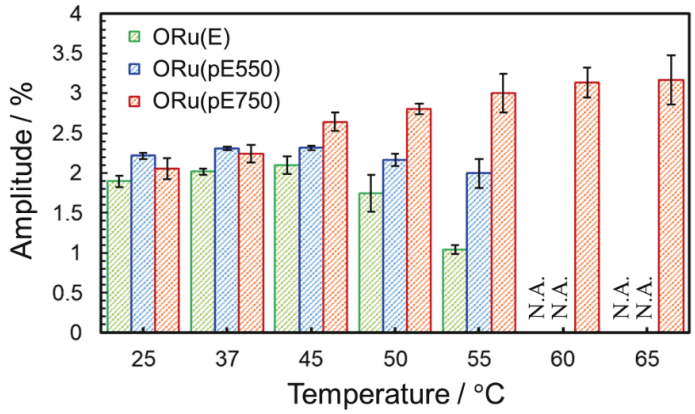

Figure 2-13. Dependence of the amplitude of the oscillation waveforms of the ORu(E), ORu(pE550), and ORu(pE750) microgels on the temperature. [**1**][PF_6]$_2$ = 100 μM; [HNO_3] = 850 mM; [$NaBrO_3$] = 150 mM; [MA] = 100 mM.

2.3.3. Controlling the short-period oscillation of the microgels

The author then attempted to achieve an oscillation period of ~1 s, which is close to that of the human heartbeat, using the oscillating pOEGMA microgels by optimizing the BZ reaction conditions. With the aim of further reducing the oscillation period, the temperature and substrate concentrations were adjusted. In particular, the ORu(pE750) microgels showed high potential for rapid oscillation, as their activation energy was low and the BZ reaction could be conducted at high temperature (**Figure 2-12**). In the chemical reaction rate equations obtained from the substrate concentration experiments, the absolute value of the exponent for each substrate indicates the magnitude of its influence on shortening the oscillation period (**Figure 2-8**; HNO_3: 0.34, $NaBrO_3$: 0.66, MA: 0.42). Therefore, the author assumed that higher concentrations of the substrates with smaller exponents would be required. Initially, a temperature of 65 °C, which is below the flocculation temperature of the microgels, and substrate concentrations of [HNO_3] = 2500 mM, [$NaBrO_3$] = 80 mM, and [MA] = 500 mM were used. In the resulting system, oscillation continued for more than 100 s without aggregation with a period of ~1.4 s (**Figures 2-14(a)** and **2-15**). The stable oscillation behavior at high temperature was attributed to the high colloidal stability of the pOEGMA microgels. As hypothesized, a rapid stimulus-response potential of the microgels was realized. However, the need for high-temperature conditions is disadvantageous from a material-handling perspective. Subsequently, the oscillation conditions at human body temperature (37 °C) were optimized. In order to shorten the

oscillation period while keeping the temperature low, it was necessary to increase the substrate concentrations. The results described above confirmed that the microgels are tolerant of high ionic strength (**Figure 2-2**) and exhibit oscillatory behavior at human body temperature (**Figure 2-13**). The substrate concentrations were set to [HNO_3] = 2500 mM, [$NaBrO_3$] = 300 mM, and [MA] = 1000 mM at 37 °C. In the resulting reaction, the oscillation continued for more than 500 s with a period of ~1.5 s. This period was almost the same as that under the high-temperature conditions, although the amplitude of the change in the transmittance decreased from ~2.0 % to ~1.5 % (**Figures 2-14(b)** and **2-16**). To provide further evidence of the short-period oscillation, a video of the turbidity changes in real time was recorded (**Movie S1)**. The oscillation waveform of the turbidity change was estimated from the gray value and showed a period of ~1.3 s (**Figure 2-14(c)**). Based on the above results, it is feasible to expect that oscillating microgels will find promising applications as heartbeat-like autonomous actuators.

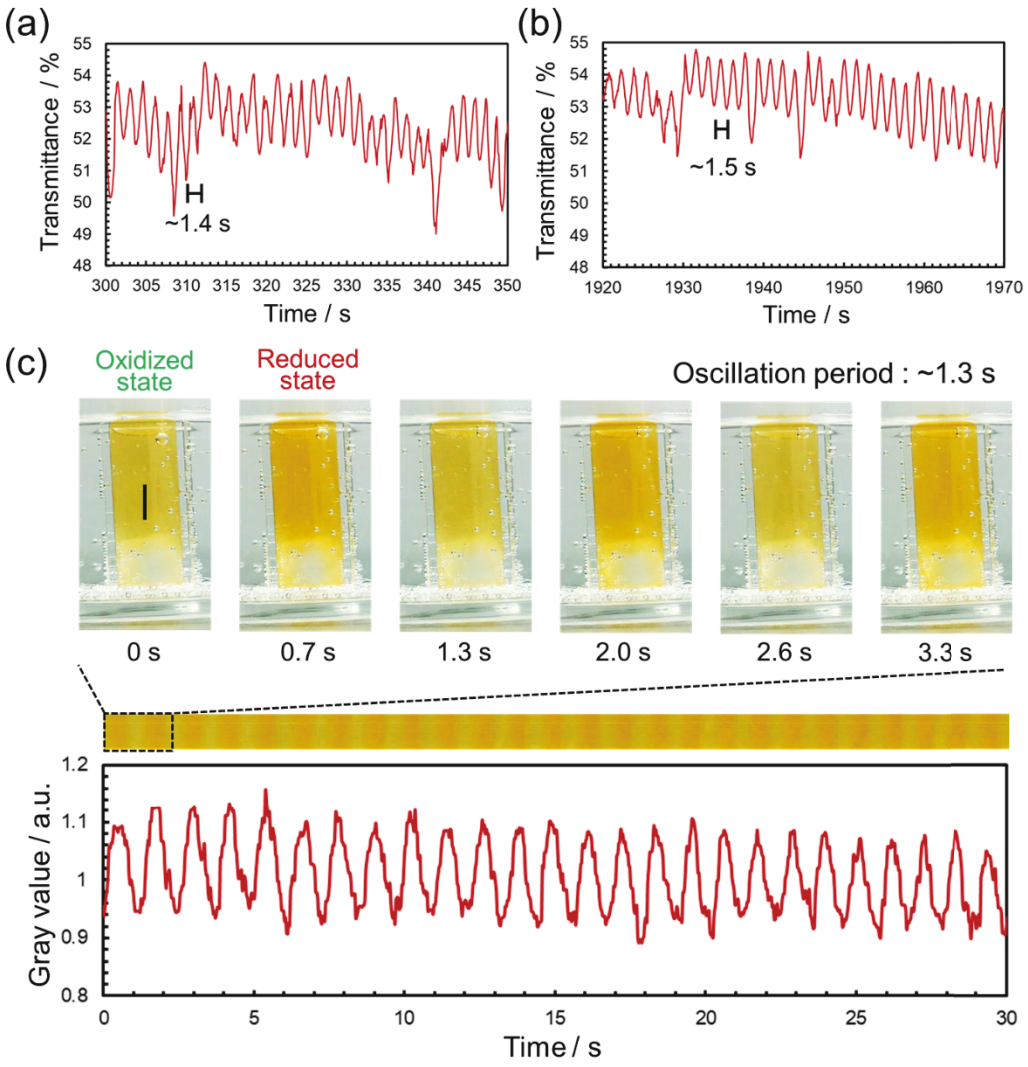

Figure 2-14. Oscillation waveforms at (a) 65 °C ([**1**][PF_6]$_2$ = 100 μM; [HNO_3] = 2500 mM; [$NaBrO_3$] = 80 mM; [MA] = 500 mM) and (b) 37 °C ([**1**][PF_6]$_2$ = 100 μM; [HNO_3] = 2500 mM; [$NaBrO_3$] = 300 mM; [MA] = 1000 mM). (c) Photographs of the short-period oscillation behavior (above) and spatiotemporal analysis graph of the turbidity change (below). The gray value was measured along the black line. [**1**][PF_6]$_2$ = 100 μM; [HNO_3] = 2500 mM; [$NaBrO_3$] = 80 mM; [MA] = 500 mM; 65 °C.

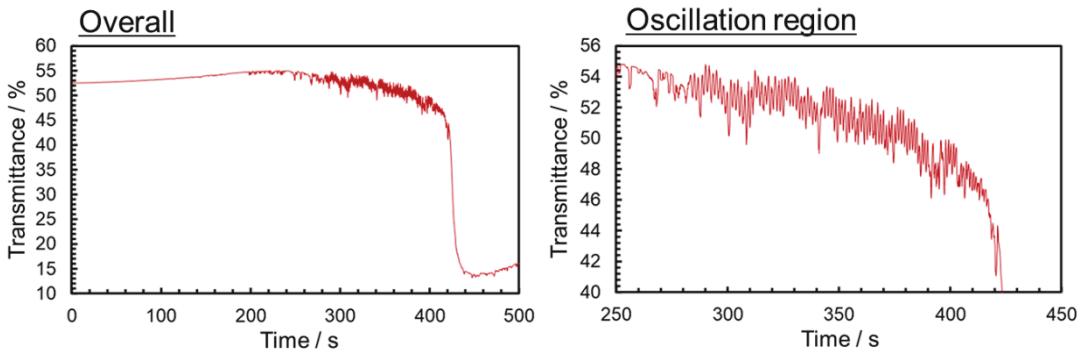

Figure 2-15. Oscillation waveform showing the short oscillation period of ORu(pE750) at 65 °C; [**1**][PF_6]$_2$ = 100 μM; [HNO_3] = 2500 mM; [$NaBrO_3$] = 80 mM; [MA] = 500 mM).

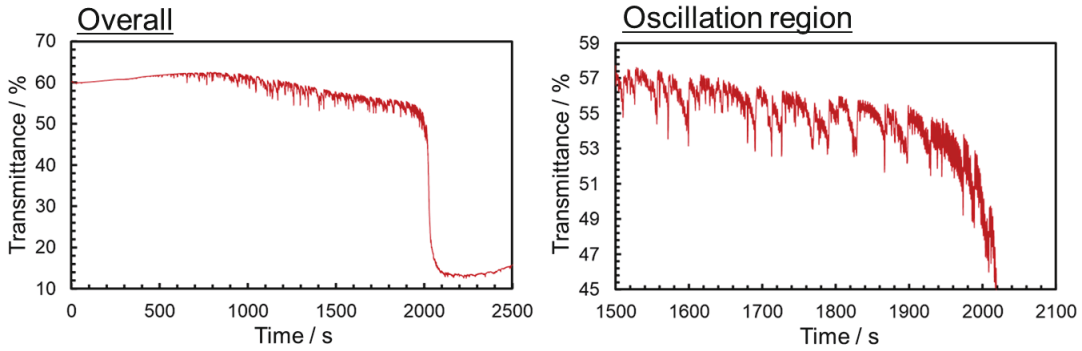

Figure 2-16. Oscillation waveform showing the short oscillation period of (ORu(pE750) at 37 °C; [**1**][PF_6]$_2$ = 100 μM; [HNO_3] = 2500 mM; [$NaBrO_3$] = 300 mM; [MA] = 1000 mM).

Finally, the oscillating microgels were applied to assemble a macrogel that acted as a heartbeat-like autonomous actuator. Compared to microgel dispersion systems, macrogels more readily present irreversible aggregation, as the microgels are adjacent to each other and are not stirred.[28] Therefore, achieving a short oscillation period in an assembled state should be particularly difficult. A microscopy image of the mm-scale macrogel produced by chemical cross-linking of the microgels is shown in **Figure 2-18(a)**. The macrogel, which was loosely but sufficiently physically cross-linked to show its volume amplitude, was too brittle to hold with tweezers (**Figure 2-17**). Observation of the macrogel under the conditions used for the dispersion system was complicated by the fact that large quantities of carbon dioxide bubbles, were generated during the BZ reaction.[29] Additionally, the change in the dimensions of the

macrogel, which depends on the oscillation period, was much smaller than the macrogel size.[35] Therefore, the swelling/deswelling measurements were performed at 37 °C under relatively mild conditions ([HNO_3] = 1000 mM; [$NaBrO_3$] = 200 mM; [MA] = 100 mM), and an oscillation period of ~6.2 s with an amplitude of ~50 μm was observed in ~1 mm macrogel (**Figure 2-18(b)**). Thus, for the first time, the swelling/deswelling oscillation with a period on the order of single seconds was accomplished in the assembled state. The oscillation period of the macrogel was short for its size from the viewpoint of the Tanaka-Fillmore equation (time is proportional to size to the power of 2)[40]. It has previously been reported that the microgel assembly has voids and that the individual microgels synchronously show swelling/deswelling oscillation, which allows the macrogel to oscillate with a high amplitude and a short period.[26] Therefore, the assembled structure of the microgels can be expected to contribute to the short-period oscillation of the macrogel in addition to the design of the oscillating pOEGMA microgels. Since the size of the macrogel is larger than the wavelength of the spatiotemporal pattern of the BZ reaction, which affects the oscillation behaviors,[57] it was expected that it would not be easy to control. Nevertheless, a short-period oscillation of ~11.7 s with an amplitude of ~0.1 mm was observed at a size as large as ~10 mm (**Figure 2-19**). Although their oscillation behavior in the assembled state is affected by the issues mentioned above, these oscillating pOEGMA microgels can be expected to play an important role as a component of autonomous actuators similar to the cardiac muscle cells in the heart.

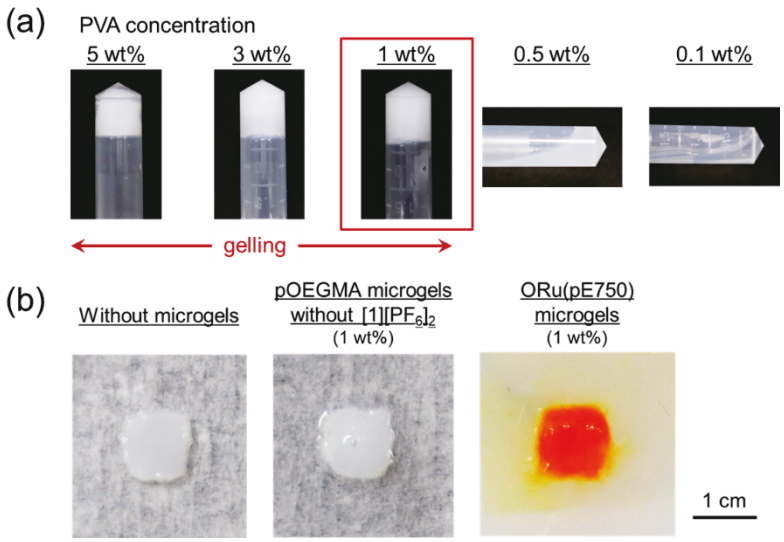

Figure 2-17. (a) Optimization of gelling conditions as a function of the PVA concentration (1 μL of 50 wt% GA is added to 1 mL PVA solution). (b) Preparation of formed macrogels (left: without microgels; center: assembled from pOEGMA microgels without $[1][PF_6]_2$; right: assembled from ORu(pE750) microgels). When the PVA concentration was 1 wt%, it was sufficient for gelation, and the shape of the macrogel was retained in the microgel assembly.

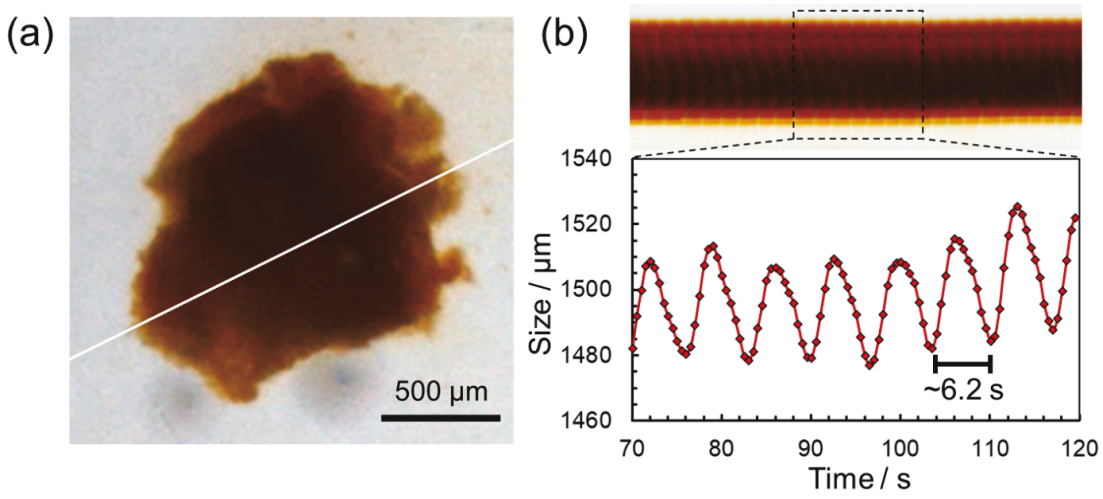

Figure 2-18. (a) Optical microscopy image of the macrogel (gel size was measured along the white line). (b) Spatiotemporal analysis of the gel size and waveform of the macrogel size ($[HNO_3]$ = 1000 mM; $[NaBrO_3]$ = 200 mM; [MA] = 100 mM; 37 °C).

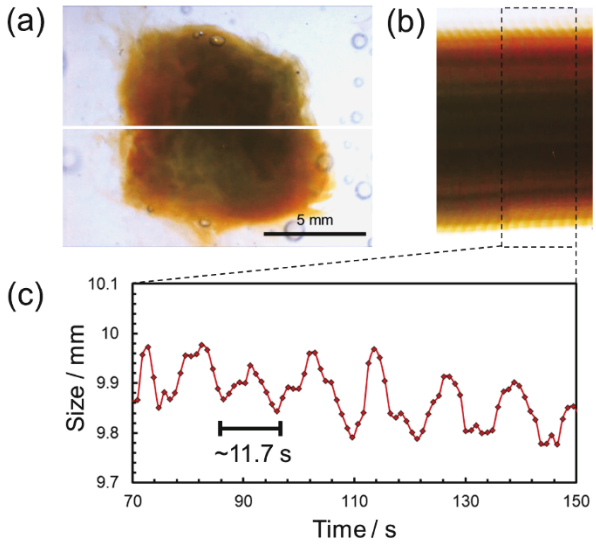

Figure 2-19. (a) Optical microscopy image of the ~10 mm macrogel (the gel size was measured along the white line). (b) Spatiotemporal analysis of the gel size and (c) oscillation waveform of the macrogel size ([HNO_3] = 1000 mM, [$NaBrO_3$] = 200 mM, and [MA] = 100 mM at 37 °C).

2.4. Conclusions

The author designed novel oscillating pOEGMA microgels that contain the catalyst [**1**][PF_6]$_2$. Aided by the high colloidal stability of pOEGMA, the BZ reaction could be carried out at high temperature (up to ~65 °C) and high substrate concentration (up to [*I*] = ~2500 mM). By optimizing the BZ reaction conditions, the author was able to achieve oscillation period as short as ~1.3 s, which is close to the frequency of the human heartbeat, and, to the best of the author's knowledge the shortest hitherto reported oscillation period for such microgels. In particular, increasing the molecular weight of the poly(ethylene glycol) cross-linker lowered the activation energy. This result suggests that the density of the polymer network in the microgels decreased, and thus did not inhibit the progress of the BZ reaction. Moreover, a mm-scale macrogel assembled from the microgels exhibited oscillatory swelling/deswelling with a period on the order of single seconds (~6.2 s) at the temperature of the human body (37 °C). It should thus be possible to use these microgels as advanced biomimetic materials in, e.g., self-oscillating micropumps that exhibit energy-efficient conversions at frequencies similar to the human heartbeat.

2.5. Reference

1. Alberts, B.; Johnson, A. D.; Lewis, J.; Morgan, D.; Raff, M.; Roberts, K.; Walter, P. *Molecular Biology of the Cell*, W. W. Norton & Company: New York, 2014.

2. Pringle, J. W. S. The Croonian Lecture, 1977 - Stretch Activation of Muscle: Function and Mechanism. *Proc. R. Soc. London, Ser. B* **1978**, *201*, 107–130.

3. Warshaw, D. M. Throttling Back the Heart's Molecular Motor. *Science* **2016**, *351*, 556–557.

4. Robison, P.; Caporizzo, M. A.; Ahmadzadeh, H.; Bogush, A. I.; Chen, C. Y.; Margulies, K. B.; Shenoy, V. B.; Prosser, B. L. Detyrosinated Microtubules Buckle and Bear Load in Contracting Cardiomyocytes. *Science* **2016**, *352*, aaf0659.

5. Needleman, D.; Dogic, Z. Active Matter at the Interface Between Materials Science and Cell Biology. *Nat. Rev. Mater.* **2017**, *2*, 17048.

6. Ricotti, L.; Trimmer, B.; Feinberg, A. W.; Raman, R.; Parker, K. K.; Bashir, R.; Sitti, M.; Martel, S.; Dario, P.; Menciassi, A. Biohybrid Actuators for Robotics: A Review of Devices Actuated by Living Cells. *Sci. Robot.* **2017**, *2*, eaaq0495.

7. Keya, J. J.; Suzuki, R.; Kabir, A. M. R.; Inoue, D.; Asanuma, H.; Sada, K.; Hess, H.; Kuzuya, A.; Kakugo, A. DNA-Assisted Swarm Control in a Biomolecular Motor System. *Nat. Commun.* **2018**, *9*, 453.

8. Singh, D. P.; Choudhury, U.; Fischer, P.; Mark, A. G. Non-Equilibrium Assembly of Light-Activated Colloidal Mixtures. *Adv. Mater.* **2017**, *29*, 1701328.

9. Katuri, J.; Ma, X.; Stanton, M. M.; Sánchez, S. Designing Micro- and Nanoswimmers for Specific Applications. *Acc. Chem. Res.* **2017**, *50*, 2–11.

10. Lin, Z.; Gao, C.; Chen, M.; Lin, X.; He, Q. Collective Motion and Dynamic Self-Assembly of Colloid Motors. *Curr. Opin. Colloid Interface Sci.* **2018**, *35*, 51–58.

11. Zhang, X.; Chen, L.; Lim, K. H.; Gonuguntla, S.; Lim, K. W.; Pranantyo, D.; Yong, W. P.; Yam, W. J. T.; Low, Z.; Teo, W. J.; Nien, H. P.; Loh, Q. W.; Soh, S.

The Pathway to Intelligence: Using Stimuli-Responsive Materials as Building Blocks for Constructing Smart and Functional Systems. *Adv. Mater.* **2019**, *31*, 1804540.

12. Fernández-Medina, F.; Ramos-Docampo, M. A.; Hovorka, O.; Salgueiriño, V.; Städler, B. Recent Advances in Nano- and Micromotors. *Adv. Funct. Mater.* **2020**, *30*, 1908283.

13. van Ravensteijn, B. G. P.; Voets, I. K.; Kegel, W. K.; Eelkema, R. Out-of-Equilibrium Colloidal Assembly Driven by Chemical Reaction Networks. *Langmuir* **2020**, *36*, 10639–10656.

14. Pelton, R. Temperature-sensitive Aqueous Microgels. *Adv. Colloid Interface Sci.* **2000**, *85*, 1–33.

15. Plamper, F. A.; Richtering, W. Functional Microgels and Microgel Systems. *Acc. Chem. Res.* **2017**, *50*, 131–140.

16. Suzuki, D.; Horigome, K.; Kureha, T.; Matsui, S.; Watanabe, T. Polymeric Hydrogel Microspheres: Design, Synthesis, Characterization, Assembly and Applications. *Polym. J.* **2017**, *49*, 695–702.

17. Karg, M.; Pich, A.; Hellweg, T.; Hoare, T.; Lyon, L. A.; Crassous, J. J.; Suzuki, D.; Gumerov, R. A.; Schneider, S.; Potemkin, I. I.; Richtering, W. Nanogels and Microgels: From Model Colloids to Applications, Recent Developments, and Future Trends. *Langmuir* **2019**, *35*, 6231–6255.

18. Umeda, Y.; Kobayashi, T.; Hirai, T.; Suzuki, D. Effects of pH and Temperature on Assembly of Multiresponsive Janus Microgels. *Colloid. Polym. Sci.* **2011**, *289*, 729–737.

19. Kureha, T.; Aoki, D.; Hiroshige, S.; Iijima, K.; Aoki, D.; Takata, T.; Suzuki, D. Decoupled Thermo- and pH-responsive Hydrogel Microspheres Cross-linked by Rotaxane Networks. *Angew. Chem., Int. Ed.* **2017**, *57*, 15393–15396.

20. Suzuki, D.; Sakai, T.; Yoshida, R. Self-Flocculating/Self-Dispersing Oscillation of Microgels. *Angew. Chem., Int. Ed.* **2008**, 47, 917–920.

21. Suzuki, D.; Yoshida, R. Temporal Control of Self-Oscillation for Microgels by Cross-Linking Network Structure. *Macromolecules* **2008**, *41*, 5830–5838.

22. Suzuki, D.; Yoshida, R. Effect of Initial Substrate Concentration of the Belousov−Zhabotinsky Reaction on Self-Oscillation for Microgel System. *J. Phys. Chem. B* **2008**, *112*, 12618–12624.

23. Suzuki, D.; Taniguchi, H.; Yoshida, R. Autonomously Oscillating Viscosity in Microgel Dispersions. *J. Am. Chem. Soc.* **2009**, *131*, 12058–12059.

24. Taniguchi, H.; Suzuki, D.; Yoshida, R. Characterization of Autonomously Oscillating Viscosity Induced by Swelling/Deswelling Oscillation of the Microgels. *J. Phys. Chem. B* **2010**, *114*, 2405–2410.

25. Suzuki, D.; Yoshida, R. Self-Oscillating Core/Shell Microgels: Effect of a Crosslinked Nanoshell on Autonomous Oscillation of the Core. *Polym. J.* **2010**, *42*, 501–508.

26. Suzuki, D.; Kobayashi, T.; Yoshida, R.; Hirai, T. Soft Actuators of Organized Self-Oscillating Microgels. *Soft Matter* **2012**, *8*, 11447–11449.

27. Matsui, S.; Kureha, T.; Nagase, Y.; Okeyoshi, K.; Yoshida, R.; Sato, T.; Suzuki, D. Small-Angle X-ray Scattering Study on Internal Microscopic Structures of Poly(*N*-isopropylacrylamide-*co*-tris(2,2′-bipyridyl))ruthenium(II) Complex Microgels. *Langmuir* **2015**, *31*, 7228–7237.

28. Matsui, S.; Inui, K.; Kumai, Y.; Yoshida, R.; Suzuki, D. Autonomously Oscillating Hydrogel Microspheres with High-Frequency Swelling/Deswelling and Dispersing/Flocculating Oscillations. *ACS Biomater. Sci. Eng.* **2019**, *5*, 5615–5622.

29. Inui, K.; Watanabe, T.; Minato, H.; Matsui, S.; Ishikawa, K.; Yoshida, R.; Suzuki, D., The Belousov–Zhabotinsky Reaction in Thermoresponsive Core–Shell Hydrogel Microspheres with a Tris(2,2′-bipyridyl)ruthenium Catalyst in the Core. *J. Phys. Chem. B* **2020**, *124*, 3828–3835.

30. Zaikin, A. N.; Zhabotinsky, A. M. Concentration Wave Propagation in Two-Dimensional Liquid-Phase Self-Oscillating System. *Nature* **1970**, *225*, 535–537.

31. Field, R. J.; Koros. E.; Noyes R. M. Oscillations in Chemical Systems. II. Thorough Analysis of Temporal Oscillation in the Bromate-Cerium-Malonic Acid System. *J. Am. Chem. Soc.* **1972**, *94*, 8649–8664.

32. Zhabotinsky, A. M.; Zaikin, A. N. Autowave Processes in a Distributed Chemical System. *J. Theor. Biol.* **1973**, *40*, 45–61.

33. Field, R. J.; Burger, M. *Oscillations and Travelling Waves in Chemical Systems*; John Wiley & Sons, Inc.: New York, 1985.

34. Toth, R.; Taylor, A. F. The Tris(2,2′-bipyridyl)ruthenium-Catalysed Belousov–Zhabotinsky Reaction. *Prog. React. Kinet. Mech.* **2006**, *31*, 59–115.

35. Yoshida, R.; Sakai, T.; Hara, Y.; Maeda, S.; Hashimoto, S.; Suzuki, D.; Murase, Y. Self-Oscillating Gel as Novel Biomimetic Materials. *J. Controlled Release* **2009**, *140*, 186–193.

36. Epstein, I. R.; Xu, B. Reaction-Diffusion Processes at the Nano- and Microscales. *Nat. Nanotechnol.* **2016**, *11*, 312–319.

37. Heskins, M.; Guillet, J. E. Solution Properties of Poly(*N*-isopropylacylamide) *J. Macromol. Sci. Chem. A.* **1968**, *2*, 1441–1455.

38. Schild, H. G. Poly(*N*-isopropylacrylamide): Experiment, Theory and Application. *Prog. Polym. Sci.* **1992**, *17*,163–249.

39. Bertram, R.; Budu-Grajdeanu, P.; Jafri, M. S. Using Phase Relations to Identify Potential Mechanisms for Metabolic Oscillations in Isolated β-cell Mitochondria. *Islets* **2009**, *1*, 87–94.

40. Tanaka, T.; Fillmore, D. J. Kinetics of Swelling of Gels. *J. Chem. Phys.* **1979**, *70*, 1214–1218.

41. Varga, I.; Szalai, I.; Mészaros, R.; Gilányi, T. Pulsating pH-Responsive Nanogels. *J. Phys. Chem. B* **2006**, *110*, 20297–20301.

42. Wrede, O.; Reimann, Y.; Lülsdorf, S.; Emmrich, D.; Schneider, K.; Schmid, A. J.; Zauser, D.; Hannappel, Y.; Beyer, A.; Schweins, R.; Gölzhäuser, A.; Hellweg, T.; Sottmann, T. Volume Phase Transition Kinetics of Smart N-n-propylacrylamide Microgels Studied by Time-Resolved Pressure Jump Small Angle Neutron Scattering. *Sci. Rep.* **2018**, *8*, 13781.

43. Bánsági Jr., T.; Leda, M.; Toiya, M.; Zhabotinsky, A. M.; Epstein, I. R. High-Frequency Oscillations in the Belousov–Zhabotinsky Reaction. *J. Phys. Chem. A* **2009**, *113*, 5644–5648.

44. Ahiabu, A.; Serpe, M., J. Rapidly Responding pH- and Temperature-Responsive Poly(*N*-Isopropylacrylamide)-Based Microgels and Assemblies. *ACS Omega* **2017**, *2*, 1769–1777.

45. Ghosh, P. K.; Spiro, T. G. Photoelectrochemistry of Tris(bipyridyl)ruthenium(II) Covalently Attached to *n*-Type SnO_2. *J. Am. Chem. Soc.* **1980**, *102*, 5543–5549.

46. Ma, X.; Li, Y.; Wang, W.; Ji, Q.; Xia, Y.; Mu, H. Dually responsive multinetworked hydrogels with improved performances by covalently bonding poly(*N*-isopropylacrylamide)-based microgels and poly(vinyl alcohol) skeleton. *Polym. Compos.* **2013**, *34*, 141–148.

47. Figueiredo, K. C. S.; Alves, T. L. M.; Borges, C. P. Poly(vinyl alcohol) Films Crosslinked by Glutaraldehyde under Mild Conditions. *J. Appl. Polym. Sci.* **2009**, *111*, 3074–3080.

48. N. Badi. Non-Linear PEG-Based Thermoresponsive Polymer Systems. *Prog. Polym. Sci.* **2017**, *66*, 54–79.

49. Sun, S.; Wu, P. On the Thermally Reversible Dynamic Hydration Behavior of Oligo(ethylene glycol) Methacrylate-Based Polymers in Water. *Macromolecules* **2013**, *46*, 236–246.

50. Kureha, T.; Suzuki, D. Nanocomposite Microgels for the Selective Separation of Halogen Compounds from Aqueous Solution. *Langmuir* **2018**, *34*, 837–846.

51. Agnihotri, P.; Raj, R.; Kumar, D.; Dan, A. Short Oligo(ethylene glycol) Chain Incorporated Thermoresponsive Microgels: From Structural Analysis to Modulation of Solution Properties. *Soft Matter* **2020**, *16*, 7845–7859.

52. Ma, X.; Cui, Y.; Zhao, X.; Zheng, S.; Tang, X. Different deswelling behavior of temperature-sensitive microgels of poly(*N*-isopropylacrylamide) crosslinked by polyethyleneglycol dimethacrylates. *J. Colloid Interface Sci.* **2004**, *276*, 53–59.

53. Kureha, T.; Hayashi, K.; Ohira, M.; Li, X.; Shibayama, M. Dynamic Fluctuations of Thermoresponsive Poly(oligo-ethylene glycol methyl ether methacrylate)-Based Hydrogels Investigated by Dynamic Light Scattering. *Macromolecules* **2018**, *51*, 8932–8939.

54. Yoshida, R.; Onodera, S.; Yamaguchi, T.; Kokufuta, E. Aspects of the Belousov–Zhabotinsky Reaction in Polymer Gels. *J. Phys. Chem. A* **1999**, *103*, 8573–8578.

55. Pullela, S. R.; Shen, J.; Marquez, M.; Cheng, Z. A Comparative Study of Temperature Dependence of Induction Time and Oscillatory Frequency in Polymer-Immobilized and Free Catalyst Belousov–Zhabotinsky Reactions. *J. Polym. Sci., Part B: Polym. Phys.* **2009**, *47*, 847−854.

56. Xiao, C.; Wu, Q.; Chang, A.; Peng, Y.; Xu, W.; Wu, W. Responsive Au@polymer hybrid microgels for the simultaneous modulation and monitoring of Au-catalyzed chemical reaction. *J. Mater. Chem. A* **2014**, *2*, 9514–9523.

57. Teng, R.; Ren, L.; Yuan, L.; Wang, L.; Gao, Q.; Epstein, I. R. Effect of Reaction Parameters on the Wavelength of Pulse Waves in the Belousov–Zhabotinsky Reaction–Diffusion System. *J. Phys. Chem. A* **2019**, *123*, 9292–9297.

3. Chapter 2

"The Belousov−Zhabotinsky Reaction in Thermoresponsive Core−Shell Hydrogel Microspheres with a Tris(2,2'-bipyridyl)ruthenium Catalyst in the Core"

*Part of this work was published in Inui, K.; Watanabe, T.; Minato, H.; Matsui, S.; Ishikawa, K.; Yoshida, R.; Suzuki, D. *The Journal of Physical Chemistry B* **2020**, *124*, 3828−3835.
Reprinted with permission from Copyright (2020) American Chemistry Society.

3.1 Introduction

The BZ reaction is a periodic oxidation/reduction reaction that uses a metal complex as a catalyst.[1-5] Overall, the BZ reaction involves the oxidation of an organic substrate, such as malonic acid, by an oxidizing agent under acidic conditions in the presence of a catalyst such as [**1**][PF_6]$_2$.[5] During the BZ reaction, the catalyst periodically changes between the reduced state ([**1**]$^{2+}$) and the oxidized state ([**1**]$^{3+}$), which creates a cyclic reaction network of intermediates (e.g., Br_2, $HBrO_2$, and BrMA). This is analogous to metabolic reactions such as the tricarboxylic acid cycle in cellular organisms.[6] The BZ reaction shows a typical oscillation behavior defined by the reaction-diffusion system. It shows spatiotemporal rhythms or patterns in a petri dish, which is similar to cellular organisms in the micro-space field (e.g., the pulsation of cardiac muscle cells[7] and signal transduction by the activity of nerve cells[8]). Thus, the BZ reaction is often compared to biological oscillation phenomena and is recognized as a model for understanding other reaction-diffusion systems.[9-12]

From the point of view of materials science, Suzuki's group has been investigating autonomously oscillating microgels, which are hybrids between a reaction-diffusion system and soft colloidal particles.[13-21] Microgels are soft and deformable particles composed of cross-linked three-dimensional networks swollen by water.[22-25] Due to their open structures, chemical species can diffuse into the interior or exterior of the microgels. In the case of oscillating microgels, the catalyst for the BZ reaction, [**1**][PF_6]$_2$ is covalently bound to a thermo-responsive polymeric main chain such as pNIPAm[26,27] (**Figure 3-1(a)**). Conventional stimuli-responsive microgels change their physicochemical properties in response to external stimuli such as changes in temperature or pH value.[28,29] In contrast, oscillating microgels show swelling/deswelling and assembling/disassembling oscillatory motions[13-15] as the microgels spontaneously convert the chemical energy of the BZ reaction into mechanical energy. Thus, oscillating microgels are useful in e.g. rheology

modifiers,[16,17] micropumps without an external device energy source,[19] and soft actuators similar to the human heartbeat.[21]

To develop oscillating microgels further, different structures and chemical species that improve the properties of the microgels have been investigated. For instance, a hydrogel shell has been added to prevent irreversible flocculation during oscillation.[18] Hydrophilic monomers (i.e., acrylamide) have been copolymerized with the microgels in order to increase the VPTT and thus to ensure the stability of the microgels when they are dispersed at high temperature,[21] which led to short microgel oscillation period (~7 s) at high temperature (~50 °C).[21] However, some problems related to oscillating microgels still remain. One impracticality is the on-off control of the oscillatory behavior. The swelling/deswelling and assembling/disassembling oscillatory motions continue until the chemical substrates for the BZ reaction have been consumed.

In the present study, the author created, on pre-existing oscillating microgels, new double-shell hydrogel structures. The first layer of the double-shell structure is a thermo-responsive hydrogel shell, while the second layer is a colloidally stable hydrogel shell. The author hypothesized that the double-shell structure would enable us to switch the BZ reaction, and therefore the microgel oscillations, from an "on" active state to an "off" inactive state. Through a series of investigations on the effects of shell thickness, the author selected the target microgels and, using these microgels and changing the temperature, the author also attempted to control the on-off switching behavior of the spatiotemporal pattern of the BZ reaction.

3.2 Experimental section

Materials

N-isopropyl acrylamide (NIPAm, purity 98%), *N,N′*-methylenebis(acrylamide) (BIS, 97%), 2,2’-azobis(2-methylpropinamidine)dihydrochloride (V-50, 95%), sodium chloride (NaCl, 99.5%), malonic acid (MA, 98%), sodium bromate ($NaBrO_3$, 99.5%), nitric acid (HNO_3, 16 M), cerium(III) sulfate *n*-hydrate ($Ce(SO_4)\cdot nH_2O$, 78–88%), and cerium(IV) sulfate tetrahydrate ($Ce(SO_4)_2\cdot 4H_2O$), were purchased from Wako Pure Chemical Industries and used as received. Poly(ethylene glycol) methyl ether methacrylate (OEGMA; M_n = 300 g/mol), and ethylene glycol dimethacrylate (EGDMA, 98%) were purchased from Sigma Aldrich and used as received. [Ruthenium(II)tris(2,2’-bipyridine)][PF_6]$_2$ ([**1**][PF_6]$_2$) monomer, [ruthenium(II)(4-vinylinyl-4’-methyl-2,2’-bipyridine)bis(2,2’-bipyridine)][PF_6]$_2$ was

synthesized according to a previously reported procedure.[30] Distilled and ion-exchanged (EYELA, SA-2100E1) water was used in all experiments.

Synthesis of core (NRu) microgels

The oscillating microgels were synthesized by surfactant-free aqueous free radical precipitation polymerization according to previously reported procedure.[13] Briefly, the polymerization was performed in a three-necked round-bottom flask (300 mL) equipped with a mechanical stirrer, a condenser, and a nitrogen gas inlet. The NIPAm monomer (95 mol%), [**1**][PF_6]$_2$ (3 mol%), cross-linker BIS (2 mol%), and NaCl (30 mM) were dissolved in deionized water (245 mL). The monomer solution was heated to 70 °C under a stream of nitrogen and constant stirring (250 rpm). The solution was sparged with nitrogen for a period of at least 30 min to remove any dissolved oxygen. Subsequently, the polymerization was initiated with V-50 (2 mM) dissolved in deionized water (5 mL). After 4 h, the microgel dispersion obtained in the flask was cooled in an ice bath to stop the polymerization. The microgels were purified by centrifugation (15 °C, 30 min, 415,000 g) (HITACHI, himac CS 100 GX), decantation, and redispersion of the precipitate in water. This purification process was conducted twice in order to remove any impurities. The dispersion was then dialyzed for 5 days with daily water replacements. The obtained core microgels are denoted as NRu. Here, N and Ru represent NIPAm and [**1**][PF_6]$_2$, respectively.

Synthesis of core-shell (NRu-N*X*) microgels

Subsequently, the thermo-responsive shells were added onto the pre-existing cores (NRu). The core-shell microgels were synthesized by aqueous free radical seeded precipitation polymerization following to previous report.[18] The polymerization was performed in a three-necked round-bottom flask (200 mL) equipped with a mechanical stirrer, a condenser, and a nitrogen gas inlet. NaCl (final concentration: 10 mM) was dissolved in deionized water, and the solution was sparged with N_2 gas for 30 min. Then, the core (NRu) microgel dispersion (final concentration: 0.4 wt%) was added to the flask (85 mL) and heated to 70 °C in an oil bath. Thereafter, the free-radical polymerization was initiated by adding V-50 (2 mM) dissolved in deionized water (5 mL). Subsequently, the monomer solution (10 mL) was immediately added to the flask. The monomer solution was prepared in advance by dissolving the NIPAm monomer (20, 40, or 60 mM; 98 mol%) and the cross-linker BIS (20, 40, or 60 mM; 2 mol%) in deionized water, followed by sparging with N_2 gas for 30 min. After 4 h, the microgel dispersion was cooled in an ice bath to stop the polymerization. The microgels were

purified by centrifugation (15 °C, 30 min, 415,000 g), decantation, and redispersion of the precipitate in water. This process was conducted twice to remove any impurities in the flask. The dispersion was then dialyzed for 5 days with daily water replacements. The obtained core-shell microgels are denoted as NRu-N*X*. Here, N and Ru represent NIPAm and [**1**][PF_6]$_2$, respectively. *X* indicates the pNIPAm monomer concentration used during the polymerization.

Synthesis of double-shell (NRu-N*X*-O) microgels

All the double-shell microgels were synthesized by aqueous seeded precipitation polymerization using the same procedure as that for the core-shell microgels. For seeds, a series of core-shell microgels synthesized in the previous section were used. The polymerization was performed in a three-necked round-bottom flask (50 mL) equipped with a mechanical stirrer, a condenser, and a nitrogen gas inlet. The core-shell (NRu-N*X*) microgel dispersion (final concentration: 0.4 wt%) was added to the flask (15 mL) and heated to 90 °C in an oil bath. Thereafter, the free-radical polymerization was initiated by adding V-50 (2 mM) dissolved in deionized water (5 mL). Subsequently, an OEGMA monomer solution (10 mL) was immediately added. This monomer solution was prepared in advance by dissolving OEGMA (98 mol%) and the cross-linker EGDMA (2 mol%) in deionized water (10 mL), followed by sparging with N_2 for 30 min. After 4 h, the obtained microgel dispersion was collected in an ice bath to stop the polymerization. The obtained microgels were purified by centrifugation (15 °C, 30 min, 415,000 g), decantation, and redispersion of the precipitate in water. This process was conducted twice to remove any impurities in the flask. The dispersion was then dialyzed for 5 days with daily water replacements. The obtained double-shell microgels are denoted as NRu-N*X*-O. Here, N, Ru, and O represent NIPAm, [**1**][PF_6]$_2$, and OEGMA, respectively. *X* indicates the monomer concentration of the pNIPAm shell.

TEM observations of the microgels

In order to confirm the formation of microgels and to evaluate the microgel size, the microgels were examined by transmission electron microscopy (TEM, JEOL2010, operated at 200 kV). Samples were prepared by deposition of microgel dispersions (1 μL, ~0.001 wt%) on to a carbon-coated copper grid (Okenshoji Co., Ltd.), followed by drying at room temperature. The diameter of the microgels was calculated based on the observed images by using Image J software (version 1.51, National Institutes of Health, USA) (N = 50).

DLS measurements of the hydrodynamic diameter (D_h) of the microgels

In order to confirm that the shells were successfully added, the temperature dependence of the hydrodynamic diameters (D_h) was measured by DLS (Malvern instruments Ltd., Zetasizer Nano S). The D_h values were calculated from the diffusion coefficient obtained using the Stokes-Einstein equation (Zetasizer software v 6.12). The microgel concentration was set to 0.01 wt%. The average value of 3 sets of 15 measurements with a 30 s acquisition time for the intensity autocorrelation was used. To fix the microgels for the oxidized $[\mathbf{1}]^{3+}$ and the reduced $[\mathbf{1}]^{2+}$ states, the microgels were dispersed in a solution of either 300 mM of HNO_3 and 1 mM of Ce^{4+} or 300 mM of HNO_3 and 1 mM of Ce^{3+}, respectively. The D_h of the microgels in the oxidized $[\mathbf{1}]^{3+}$ ($D_{h,\ Oxidized}$) and the reduced $[\mathbf{1}]^{2+}$ ($D_{h,\ Reduced}$) states were measured between 15 and 40 °C.

UV-vis spectroscopy measurements of the oscillation waveforms of the BZ reaction

In order to evaluate the effect of each microgel structure on the BZ reaction, the color changes of the $[\mathbf{1}][PF_6]_2$ redox reaction were observed by UV-vis spectroscopy (JASCO, V-630 iRM). A mixture of HNO_3 (300 mM), $NaBrO_3$ (84 mM) and microgel dispersion ($[[\mathbf{1}][PF_6]_2]$ = 50 μM) was poured into a sample holder and after thermal equilibration for 10 minutes, the BZ reaction was started by adding MA (62.5 mM) (final liquid volume: 2.5 mL). The measurement was carried out while constantly stirring at 800 rpm between 20±0.5 °C and 35±0.5 °C at a measurement wavelength of 460 nm. At this wavelength, the difference in absorbance between the reduced $[\mathbf{1}]^{2+}$ state and the oxidized $[\mathbf{1}]^{3+}$ state is at a maximum,[13] which facilitates the detection of the progress of the BZ reaction. The induction period and the oscillation period were investigated from the obtained waveforms. The induction period was calculated as the time from the start of the observation to the start of the oscillation. The oscillation period is the average time of the period between the second and the sixth oscillation.

Direct observation of the spatiotemporal pattern of the BZ reaction with a video camera

In order to observe the spatiotemporal pattern of the BZ reaction, it was recorded using a video camera (JVC KENWOOD, GZ-RX500-B) with the microgel dispersion spread in two dimensions. A 1 mm thick silicone rubber mold with a 5 cm diameter circle cut out of the center (AS ONE Corporation., Silicon rubber sheet) was produced and placed between two glass substrates (Matsunami Glass Ind., Ltd., Neo

Micro Cover Glass). Then, the reaction solution (1000 μL), in which the oscillation reaction was started by adding MA (62.5 mM) to a mixed solution of HNO_3 (300 mM), $NaBrO_3$ (84 mM), and the microgel dispersion (0.2 wt%), was poured into the container and observed. The reaction vessel was placed in a chamber that contained flowing temperature-controlled water and the observation was performed while switching the reaction temperature between 25±1 °C and 35±1 °C. The spatiotemporal analysis[19,21] was performed by placing one-line images of the BZ reaction pattern in time order using the image processing software Image J. Time-dependent gray values were obtained from these sequential images and the on-off switching of the spatiotemporal pattern was evaluated.

3.3 Results and discussion

3.3.1 Microgel synthesis

To realize an on-off switch for the BZ reaction within a core-shell microgel,[31-38] a thermo-responsive shell, which can selectively allow diffusion of the chemical substrates for the BZ reaction, was added to an oscillating-microgel core that contains the catalyst, [**1**][PF_6]$_2$ (**Figure 3-1(b)**). In addition, since the BZ reaction occurs only at high ionic strengths (> 300 mM),[21] another shell was necessary to achieve colloidal stability under strenuous conditions (**Figure 3-1(c)**). Using an oscillating microgel as the core, a two-stage seeded precipitation polymerization of polymers with different lower critical solution temperature (LCST) was performed to form the double-shell structured microgel.[39-41] A thermo-responsive pNIPAm hydrogel with an LCST of ~32 °C[26,27] was selected to form the first shell. The author hypothesized that due to changes in hydrophilicity and hydrophobicity in response to temperature, changes in substrate diffusivity[42-44] could be expected, which could potentially lead to on-off switch for the BZ reaction. In addition, poly(oligoethylene glycol methacrylate) (pOEGMA; LCST ~64 °C)[45-47] was chosen as the second shell in order to form a colloidally stable double-shell-structured microgel that prevents the flocculation of the core-shell microgels at high ionic strengths.

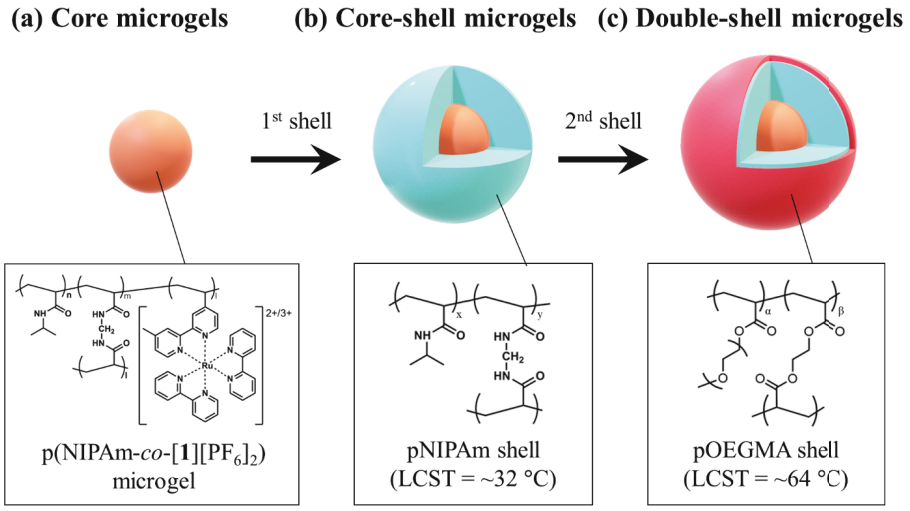

Figure 3-1. Chemical structures and schematic illustration of the (a) core, (b) core-shell, and (c) double-shell microgels used in this study.

In this study, core-shell microgels and double-shell microgels with pNIPAm shells of different thicknesses were synthesized in order to optimize the thickness of the pNIPAm shell and thus change the diffusivity of the substrates for the BZ reaction (**Table 3-1**). To confirm that the shells were added correctly, the temperature dependence of the hydrodynamic diameters (D_h) was measured using DLS. The catalyst [**1**][PF_6]$_2$ was immobilized in the microgels fixed either in the reduced state ([**1**]$^{2+}$) or the oxidized state ([**1**]$^{3+}$) using a reducing agent or an oxidizing agent,[13] respectively. The ionic strength of each microgel dispersion was set to that of the BZ reaction (> 300 mM). As can be seen in **Figure 3-2(a)**, both for the reduced and oxidized catalyst, the D_h of the core-shell microgels increases with increasing amount of monomer used during the seeded precipitation polymerization, which is consistent with previous reports on other systems.[35-38] It should be noted here that all the core-shell microgels flocculated above the LCST of pNIPAm (~32 °C), even though the core microgels maintained their colloidal stability under these conditions. This is additional evidence that supports the notion that a pNIPAm shell was added to the pre-existing core microgels; the dehydrated pNIPAm microgel surface would usually lose colloidal stability at high ionic strength due to a loss of steric hindrance.[13,18] As shown in **Figure 3-2(b)**, following the addition of the second pOEGMA shell, the D_h of the double-shell microgels, both in the reduced and

oxidized state, increased further still. It should be noted here that all of double-shell microgels did not flocculate above the LCST of pNIPAm (~32 °C). This is further evidence that the pOEGMA shell was added to the pre-existing core-shell microgels; in contrast to the pNIPAm shell of the core-shell microgels, the hydrated pOEGMA microgel surface retains colloidal stability due to a gain of steric hindrance.[47] TEM images of representative core (NRu), core-shell (NRu-N40), and double-shell (NRu-N40-O) microgels following drying at room temperature are shown in **Figure 3-2(c)**. Each microgel appeared deformed due to its softness. However, secondary particles were not confirmed and particulate matter was obtained, given the coefficient of variation obtained by evaluation for the diameters of the microgels (CV=~10%; **Figure 3-3**). Following a series of tests, double-shell microgels were synthesized for the use as an on-off switch for the BZ reaction.

Subsequently, the author determined the difference in D_h (ΔD_h) between the microgels with the reduced ($[\mathbf{1}]^{2+}$) and the oxidized ($[\mathbf{1}]^{3+}$) catalyst. As shown in **Figure 3-4**, the ΔD_h decreases upon adding shells. During the seeded precipitation polymerization, the hydrogel shell is adsorbed onto the hydrophobic or deswollen core microgels as the polymer precipitates.[35] During this synthetic process, the shell structure suppresses the swelling of the core microgels,[32-34] i.e., the decrease in ΔD_h is derived from the synthetic method. Due to the lack of oscillatory motions, the ΔD_h of the microgels with additional shells is smaller than that of the individual core. Therefore, the double-shell structure can provide stability and stop the oscillatory function of the microgels, albeit that this benefit comes together with a trade-off in the form of a decrease in ΔD_h. Further discussion of this point would be beyond the focus of this study, even though it will be an issue to improve in future research.

Table 3-1. The synthetic conditions, the diameter (*D*) determined from TEM images, and the critical flocculation temperatures (CFTs) of the core, core-shell, and double-shell microgels.

Core	Monomer conc. [mM]	NIPAm [mol%]	**[1]**[PF_6]$_2$ [mol%]	BIS [mol%]	*D* [nm] (CV / %)	CFT [°C]	
						[1]$^{2+}$	**[1]**$^{3+}$
NRu	75	95	3	2	91±12 (13.0 %)	27	> 40

Core-shell	Seed [wt%]	Monomer conc. [mM]	NIPAm [mol%]	BIS [mol%]	*D* [nm] (CV / %)	CFT [°C]	
						[1]$^{2+}$	**[1]**$^{3+}$
NRu-N20	0.4 (NRu)	20	98	2	106±8.9 (8.4 %)	28	31
NRu-N40	0.4 (NRu)	40	98	2	110±14 (13.1 %)	29	31
NRu-N60	0.4 (NRu)	60	98	2	157±16 (9.9 %)	30	32

Double-shell	Seed [wt%]	Monomer conc. [mM]	OEGMA [mol%]	EGDMA [mol%]	*D* [nm] (CV / %)	CFT [°C]	
						[1]$^{2+}$	**[1]**$^{3+}$
NRu-N20-O	0.4 (NRu-N20)	40	98	2	113±15 (13.1 %)	> 40	> 40
NRu-N40-O	0.4 (NRu-N40)	40	98	2	129±15 (11.7 %)	> 40	> 40
NRu-N60-O	0.4 (NRu-N60)	40	98	2	174±34 (19.7 %)	> 40	> 40

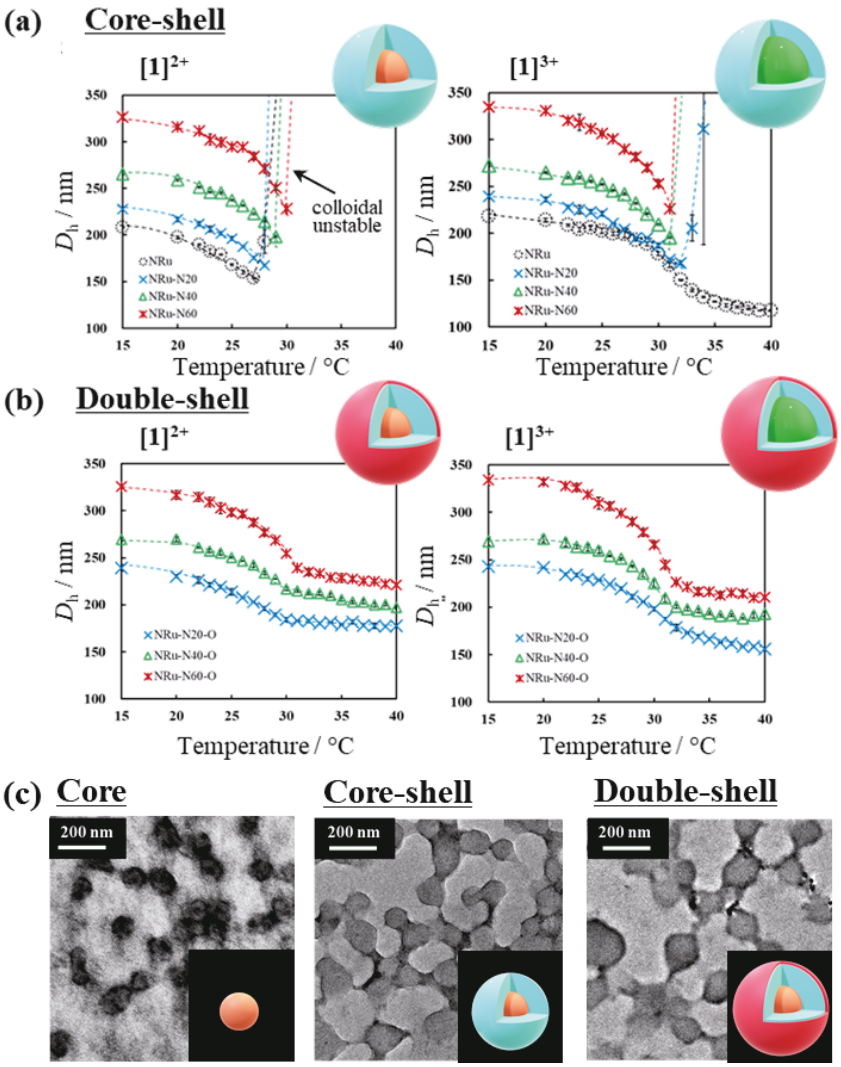

Figure 3-2. Temperature dependence of the hydrodynamic diameter (D_h) of (a) the core microgel (NRu), the core-shell microgels (NRu-N20, NRu-N40, and NRu-N60), and (b) the double-shell microgels (NRu-N20-O, NRu-N40-O, and NRu-N60-O) for reduced $[\mathbf{1}]^{2+}$ (1 mM Ce^{3+} and 300 mM HNO_3) and oxidized $[\mathbf{1}]^{3+}$ (1 mM Ce^{4+} and 300 mM HNO_3). (c) TEM images of the core microgel (NRu), a core-shell microgel (NRu-N40), and a double-shell microgel (NRu-N40-O).

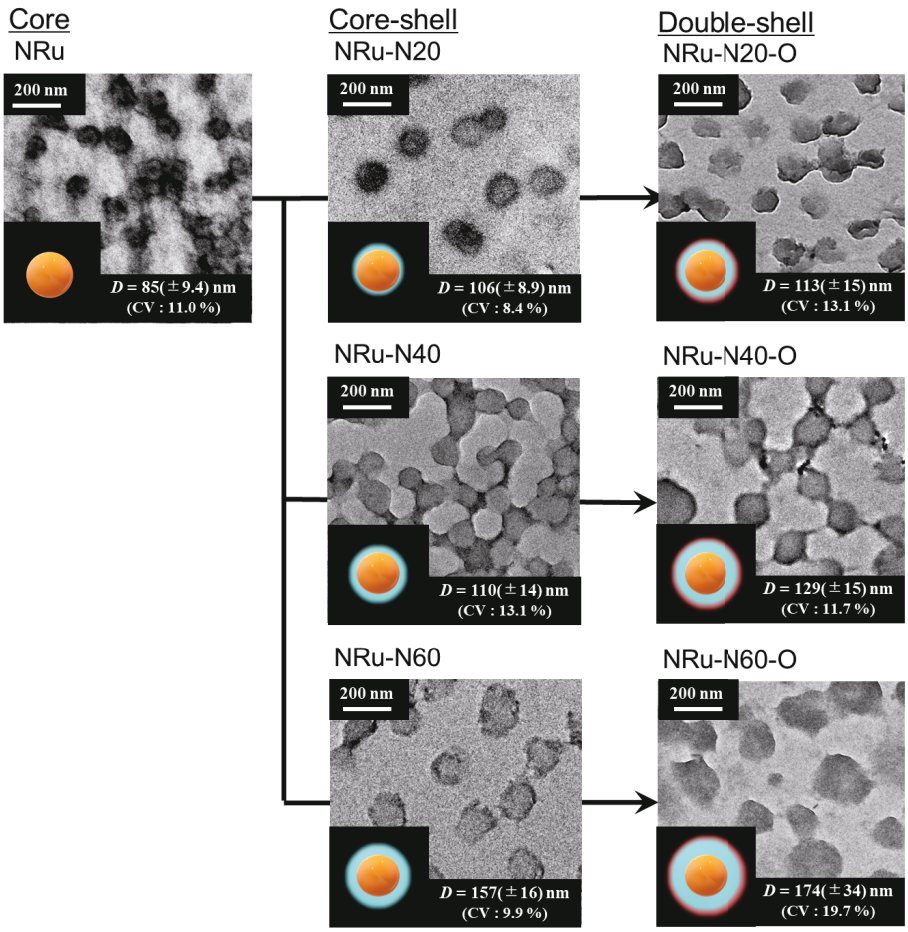

Figure 3-3. TEM images of the core microgels (NRu), the core-shell microgels (NRu-N20, NRu-N40 and NRu-N60), and the double-shell microgels (NRu-N20-O, NRu-N40-O and NRu-N60-O) dried on a carbon-coated copper grid at room temperature. From the images, the diameter (D) of the microgels was measured using the Image J software. The coefficients of variation (CV) were determined from the D values ($N = 50$).

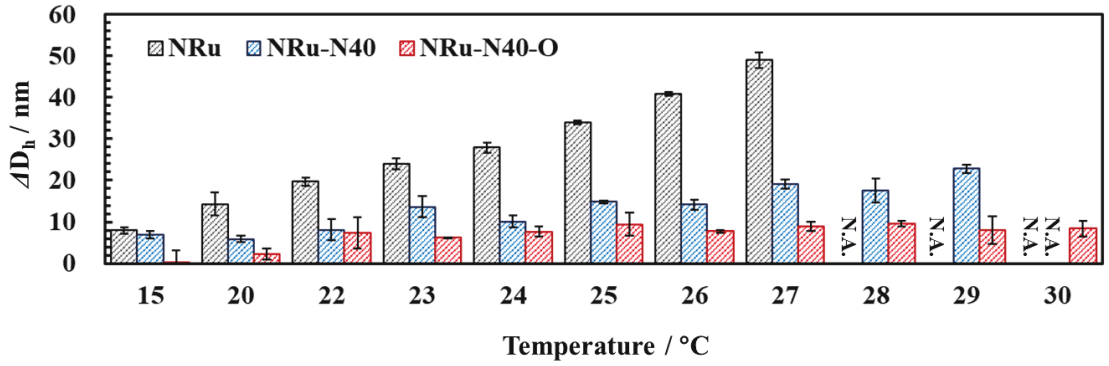

Figure 3-4. Temperature dependence of ΔD_h for the core, the core-shell, and the double-shell microgels, which shows that ΔD_h decreases upon applying the shells. ΔD_h is the difference in D_h between the microgels with the reduced $[\mathbf{1}]^{2+}$ state catalyst and those with the oxidized $[\mathbf{1}]^{3+}$ state catalyst. ΔD_h values were calculated from **Figures 2(a)** and **2(b)**.

3.3.2. Oscillation study using various microgels

Next, the BZ reaction was performed using the obtained microgels. In order to confirm if these microgels can stop the BZ reaction upon changing the temperature, the temperature dependence of their oscillatory behavior under constant substrate concentration and stirring was measured via optical transmittance using UV-vis spectroscopy. The oscillation waveforms of the core, the core-shell, and the double-shell microgels showed different behavior depending on the temperature (**Figures 3-5, 3-6, 3-7**). When the core microgels were exposed to low temperatures, for example 20 °C and 25 °C (**Figure 3-5(a)**), the transmittance changed periodically within a certain range. This indicates a change in the redox state of $[\mathbf{1}]^{2+}/[\mathbf{1}]^{3+}$ immobilized in the microgels where the change of color of $[\mathbf{1}][PF_6]_2$ synchronized with the progress of the BZ reaction. However, upon increasing the temperature to 30 °C, the oscillation waveform became disordered and the value of transmittance continued to increase as the BZ reaction proceeded (**Figure 3-5(a)**). This result indicates that the microgel formed aggregates due to a decrease in colloidal stability caused by the rising temperature (**Figure 3-8(a)**). Similar oscillation behavior (**Figure 3-5(b)**) and irreversible aggregation (**Figure 3-8(b)**) was also observed for the core-shell microgel at high temperature (30 °C). In contrast, as confirmed by both optical transmittance measurements (**Figure 3-5(c)**) and visual inspections (**Figure 3-9**),

the double-shell microgels successfully completed the BZ reaction without aggregation even at 35 °C. This result confirms that the pOEGMA outer shell effectively maintains the colloidal stability at high ionic strength and at high temperature.

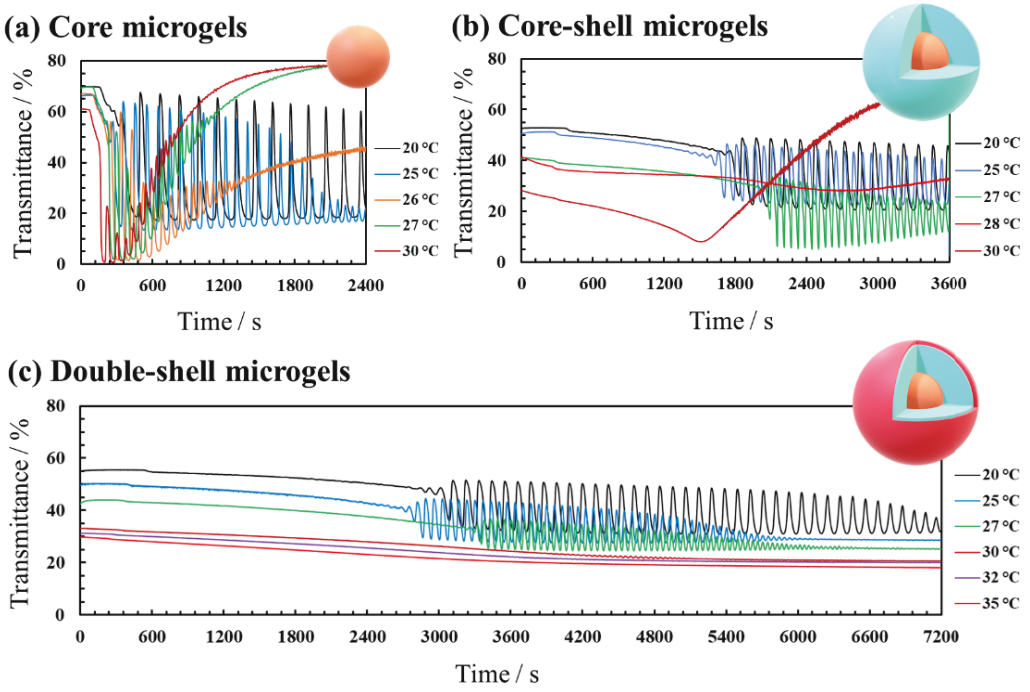

(d)

Microgel code		Temperature / °C					
		20	25	27	30	32	35
Core	NRu	○	○	×	×	-	-
Core-shell	NRu-N20	○	○	×	×	-	-
	NRu-N40	○	○	○	×	-	-
	NRu-N60	○	○	○	×	-	-
Double-shell	NRu-N20-O	○	○	○	○	○	○
	NRu-N40-O	○	○	○	○	●	●
	NRu-N60-O	○	○	○	●	●	●

Figure 3-5. Temperature-dependent oscillation waveforms of the BZ reaction for (a) the core (NRu), (b) the core-shell (NRu-N40), and (c) the double-shell (NRu-N40-O) microgels detected by UV-vis spectroscopy (λ = 460 nm; [**1**][PF_6]$_2$ = 50 μM; [HNO_3] = 300 mM; [$NaBrO_3$] = 84 mM; [MA] = 62.5 mM). (d) Summary of the temperature-dependent oscillation behavior for all microgels. Each symbol indicates the

oscillation behavior upon increasing the temperature from 25 °C to 35 °C during the UV-vis measurements (◯ = oscillating; ● = almost no change in transmittance; × = microgel aggregated).

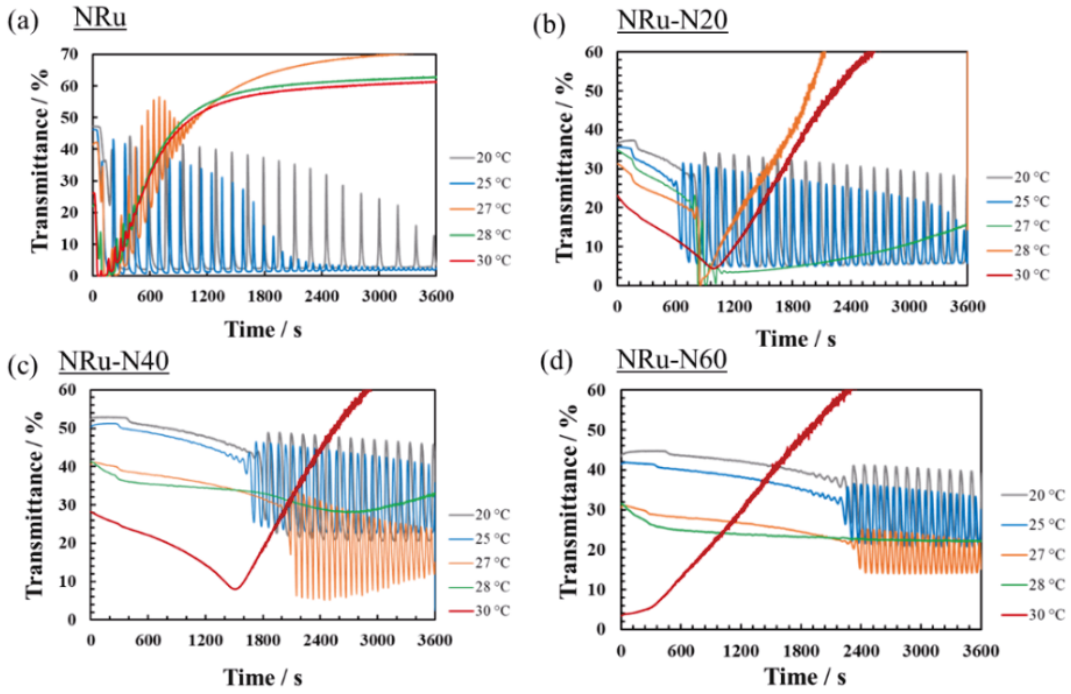

Figure 3-6. Typical oscillation waveforms for (a) NRu, (b) NRu-N20, (c) NRu-N40, and (d) NRu-N60 microgels ([**1**][PF_6]$_2$ = 50 μM; [HNO_3] = 300 mM; [$NaBrO_3$] = 84 mM; [MA] = 62.5 mM). Addition of a pNIPAm shell showed irreversible aggregation at the LCST of pNIPAm.

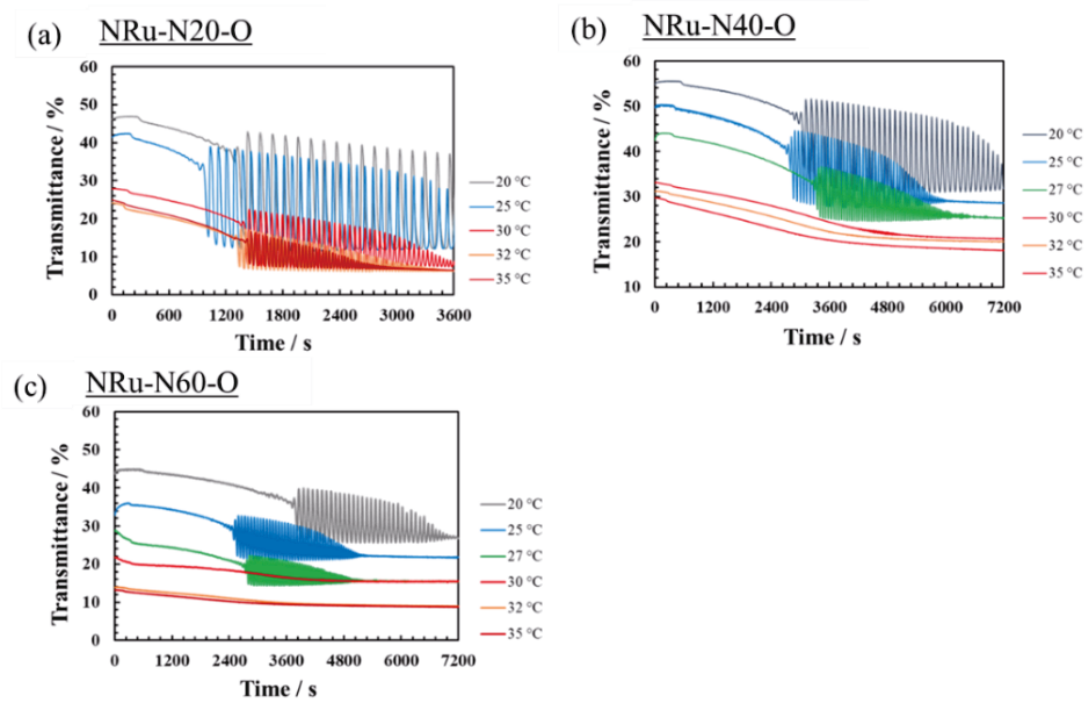

Figure 3-7. Typical oscillation waveforms for (a) NRu-N20-O, (b) NRu-N40-O, and (c) NRu-N60-O microgels ([**1**][PF_6]$_2$ = 50 μM; [HNO_3] = 300 mM; [$NaBrO_3$] = 84 mM; [MA] = 62.5 mM). The double-shell microgels NRu-N40-O and NRu-N60-O are able to stop the BZ reaction at the LCST of pNIPAm, but this is not possible when the pNIPAm shell is thinner (c.f. NRu-N20-O microgels). This indicates that stable on-off switches require a specific pNIPAm shell thickness.

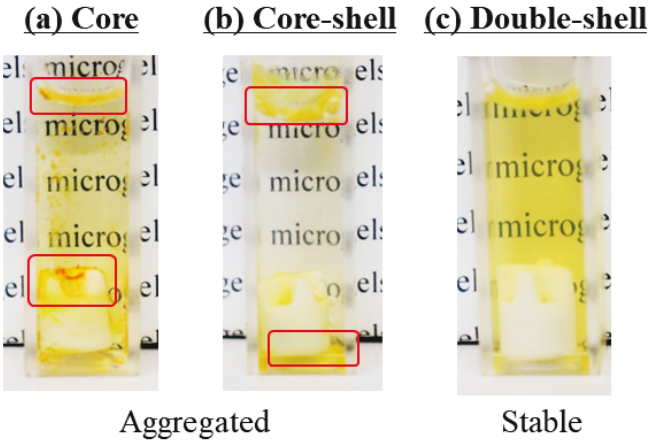

Figure 3-8. Visual appearance of the (a) core (NRu), (b) core-shell (NRu-N40), and (c) double-shell (NRu-N40-O) microgels in the cell following UV-vis measurements at 30 °C. The core and the core-shell microgels aggregated, while the double-shell microgels maintained colloidal stability.

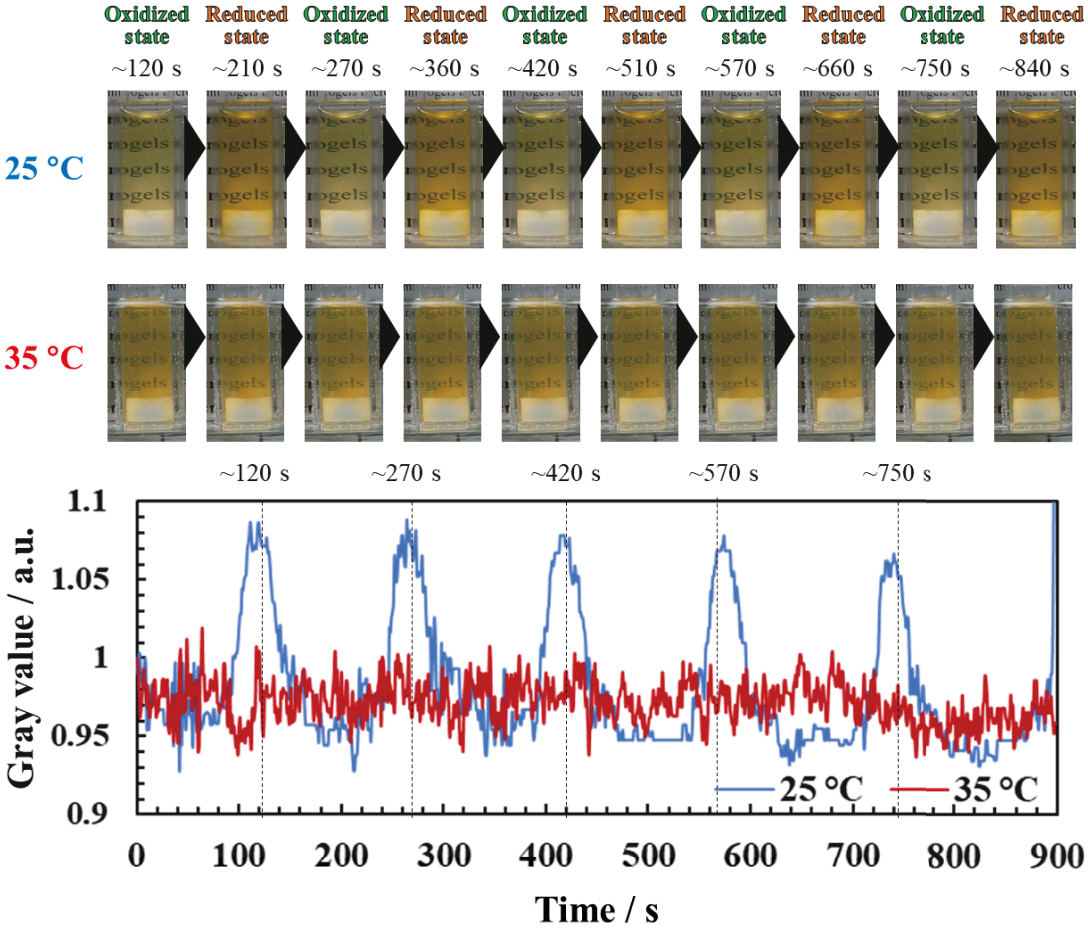

Figure 3-9. Time-lapse video images of the double-shell (NRu-N40-O) microgels in the cell taken during the BZ reaction (0 s refers to the time when the observation of the BZ reaction was started). The sample preparation procedure is the same as that used for the UV−vis spectroscopy oscillation study, which is described in the experimental section ([**1**][PF_6]$_2$ = 50 μM; [HNO_3] = 300 mM; [$NaBrO_3$] = 84 mM; [MA] = 62.5 mM at 25 °C or 35 °C under constant stirring at 800 rpm). The BZ reaction proceeded at 25 °C and stopped at 35 °C.

The author also found that the thickness of the pNIPAm shell is an important factor to control the on-off switching of the BZ reaction. When the microgels have a thin pNIPAm shell (NRu-N20-O), the BZ reaction could not be stopped above the LCST of pNIPAm (32 °C) (**Figure 3-5(d)**). On the other hand, it was possible to stop the BZ reaction by increasing the temperature when the NRu-N40-O and NRu-N60-O core-shell microgels were used (**Figure 3-5(d)**). In addition, the presence of the pNIPAm shell affected the oscillation period, the induction period, and the oscillation mechanism of the BZ reaction, which provides more evidence that substrate diffusion is inhibited (**Figures 3-10**, **3-11**, **3-12**, **3-13**, and **3-15**; **Tables 3-2**, **3-2**, and **3-3**). Based on these tests, it can thus be concluded that double-shell oscillating microgels with a suitably thick shell can control the on-off switching behavior of the BZ reaction without aggregation of the microgels.

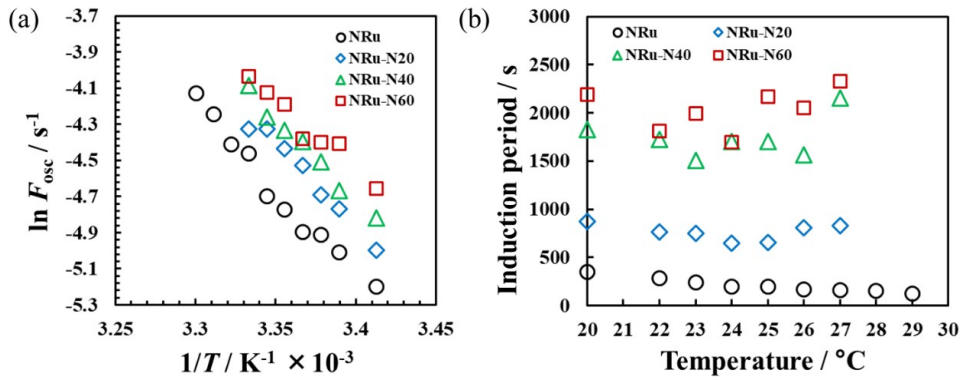

Figure 3-10. Temperature dependence of (a) the oscillating frequency (F_{osc} is the reciprocal of the oscillation period) and (b) the induction period for the core-shell (NRu-N*X*) microgels. *X* indicates the monomer concentration of NIPAm used in the synthesis of the core-shell microgels. F_{osc} almost linearly correlates with the operating temperature, which means the oscillatory motions of any oscillating microgels are synchronized with the BZ reaction (i.e., an Arrhenius plot).[1] The thicker the pNIPAm shell, the longer the induction period and the shorter the oscillation period. Therefore, the addition of the pNIPAm shell affects the substrate diffusion.

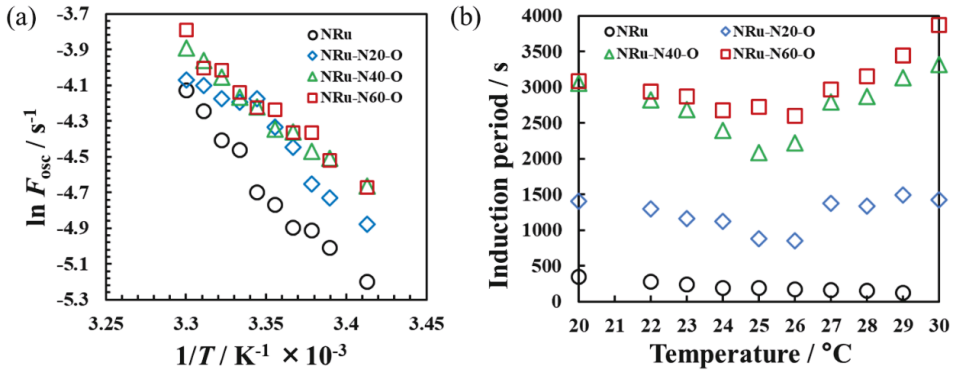

Figure 3-11. Temperature dependence of (a) the oscillating frequency (F_{osc} is the reciprocal of the oscillation period) and (b) the induction period for the double-shell (NRu-N*X*-O) microgels. *X* indicates the concentration of NIPAm used in the synthesis of the double-shell microgels. Like the core-shell microgels, F_{osc} almost linearly correlates with the operating temperature, which means that the oscillatory motions of any oscillating microgels are synchronized with the BZ reaction (i.e. an Arrhenius plot). Furthermore, the thicker the pNIPAm shell, the longer the induction period and the shorter the oscillation period. Therefore, the addition of the pNIPAm shell affects the substrate diffusion in the double-shell microgels.

In order to consider the influence of the double-shell structure in more detail, we examine here the cycle of the BZ reaction. The mechanism of the BZ reaction can be understood using the Field-Körös-Noyes (FKN) mechanism,[2,14] and be subdivided into three main reaction processes: the Br^- consumption reaction (A); the autocatalytic reaction of $HBrO_2$ (B); and the Br^- generation reaction (C).

A: $BrO_3^- + 2\ Br^- + 3\ H^+ \rightarrow 3\ HOBr$

B: $BrO_3^- + HBrO_2 + 2\ [\mathbf{1}]^{2+} + 3\ H^+ \rightarrow 2\ HBrO_2 + 2\ [\mathbf{1}]^{3+} + H_2O$

C: $2\ [\mathbf{1}]^{3+} + BrMA \rightarrow f Br^- + 2\ [\mathbf{1}]^{2+}$ + other products

Following the FKN mechanism, the waveforms can be divided into processes A, B, and C. Here, each process is defined as follows: the region where transmittance settles (A); the region where transmittance increases (B); and the region where transmittance decreases (C). Between 20 °C and 28 °C (values > 28 °C were neglected for discussion because changes in the values were too small), the time each reaction process takes per reaction cycle was investigated. Processes B and C were focused on as these reactions involve the $[\mathbf{1}][PF_6]_2$ catalyst. For the double-shell microgels (**Figure 3-12** and **Table**

3-2), there were relatively few changes in the amount of time process B took in the reaction cycle (B/P_{osc}), which, when the temperature was increased from 20 °C to 28 °C, only increased by 10%. This might originate from the autocatalytic reaction. Thus, it was concluded that the substrate involved in the oxidization reaction (process B) did not contribute much to stopping the oscillation. However, the amount of time taken by process C in the reaction cycle (C/P_{osc}), upon increasing the temperature from 20 °C to 28 °C, dramatically increased by 24%. In contrast, for the core and core-shell microgels large changes in the C/P_{osc} value were not observed. As the temperature was increased from 20 °C to 28 °C, C/P_{osc} changed by 10% and 7% for the core and core-shell microgels, respectively (**Figures 3-13** and **3-14**; **Tables 3-3** and **3-4**). Process C involves the consumption of BrMA and previous reports have suggested that the polymer network might prevent the diffusion of BrMA.[1] In this case, it was assumed that the deswollen pNIPAm shell inhibits the diffusion of BrMA or other reaction intermediates during the progress of the BZ reaction as observed during the induction period in previous studies.[14] When the temperature was raised above 28 °C the pNIPAm shell possibly becomes more hydrophobic, which would severely hamper the supply of substrates such as BrMA and thus stop the BZ reaction.

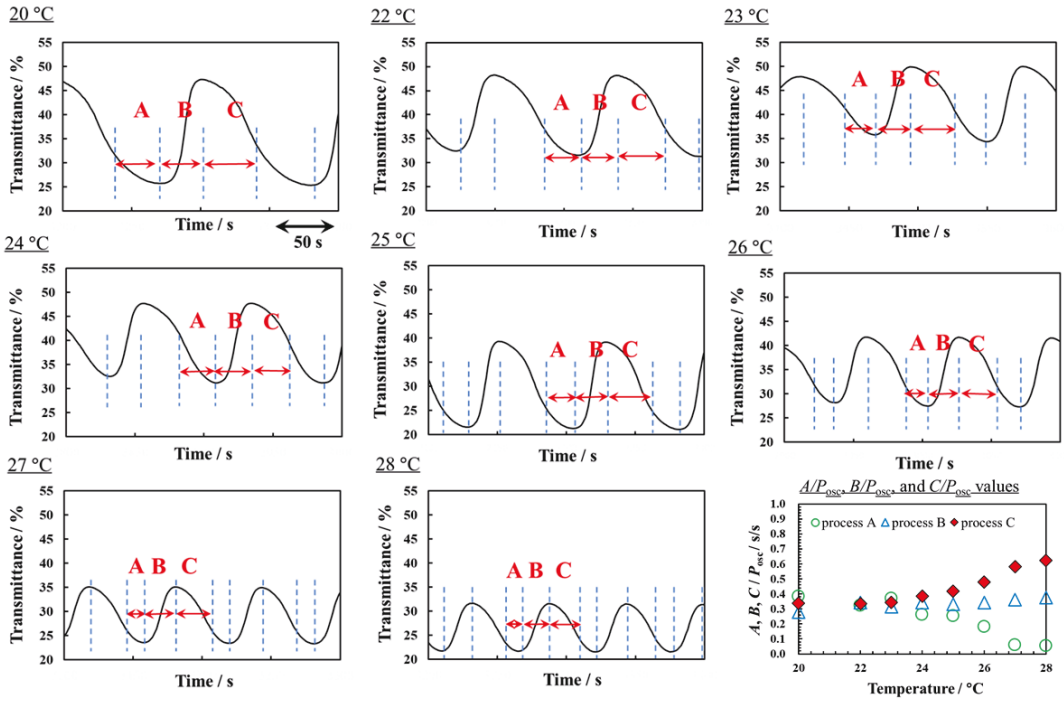

Figure 3-12 Typical oscillation waveforms in double-shell microgels at various temperatures ([**1**][PF_6]$_2$ = 50 μM; [HNO_3] = 300 mM; [$NaBrO_3$] = 84 mM; and [MA] = 62.5 mM). Based on the FKN mechanism, the waveforms are divided into processes A, B, and C. The plot at the bottom right shows the values of A/P_{osc}, B/P_{osc}, and C/P_{osc} as a function of temperature.

Table 3-2. A/P_{osc}, B/P_{osc}, and C/P_{osc} values as a function of temperature for the double-shell microgels. The oscillation periods P_{osc}, the durations of processes A-C, and the values of A/P_{osc}, B/P_{osc} and C/P_{osc} are summarized.

Temp, °C	P_{osc}, s	A, s	B, s	C, s	A/P_{osc}	B/P_{osc}	C/P_{osc}
20	109.0	42.0	30.0	37.0	0.38	0.28	0.34
22	88.7	28.7	30.3	29.7	0.33	0.34	0.33
23	81.3	29.3	25.0	27.0	0.34	0.32	0.34
24	77.0	20.3	26.7	30.0	0.28	0.34	0.38
25	76.6	19.3	25.3	32.0	0.25	0.33	0.42
26	66.4	12.0	22.7	31.7	0.18	0.34	0.48
27	62.0	3.7	22.3	36.0	0.06	0.36	0.58
28	58.0	3.0	20.7	34.3	0.05	0.38	0.57

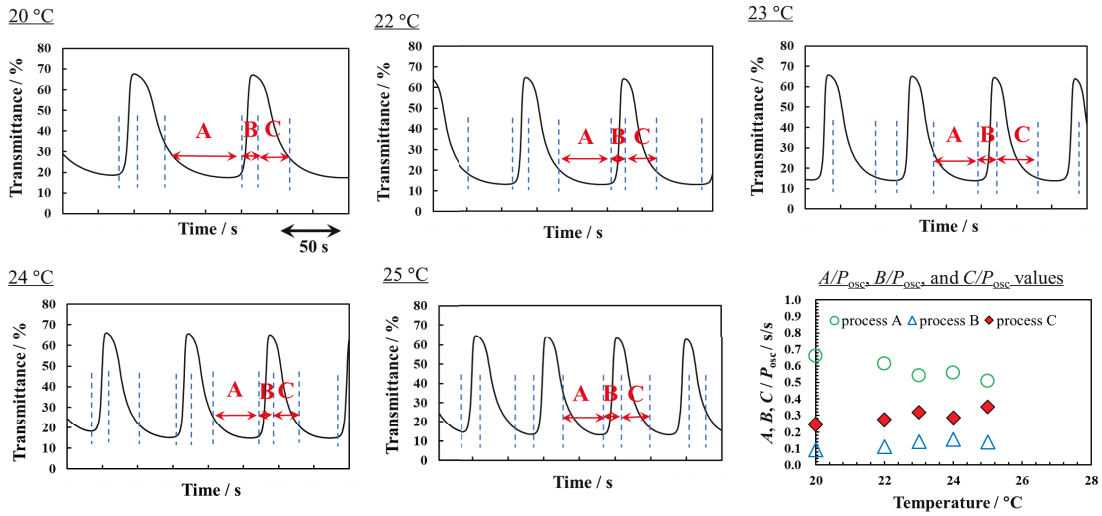

Figure 3-13. Typical oscillation waveforms in core microgels at various temperatures ([**1**][PF_6]$_2$ = 50 μM; [HNO_3] = 300 mM; [$NaBrO_3$] = 84 mM; [MA] = 62.5 mM). Based on the FKN mechanism, the waveforms are divided into processes A, B, and C. The plot at the bottom right shows the values of A/P_{osc}, B/P_{osc}, and C/P_{osc} as a function of temperature.

Table 3-3. A/P_{osc}, B/P_{osc}, and C/P_{osc} values as a function of temperature for the core microgels. The oscillation periods P_{osc}, the durations of processes A-C, and the values of A/P_{osc}, B/P_{osc} and C/P_{osc} are summarized.

Temp, °C	P_{osc}, s	A, s	B, s	C, s	A/P_{osc}	B/P_{osc}	C/P_{osc}
20	185.0	122.3	17.3	45.7	0.66	0.09	0.25
22	152.0	93.3	17.0	41.7	0.62	0.11	0.27
23	136.0	73.3	19.3	43.0	0.54	0.14	0.32
24	135.0	75.3	21.0	38.7	0.56	0.15	0.29
25	116.2	59.0	16.3	41.0	0.51	0.14	0.35

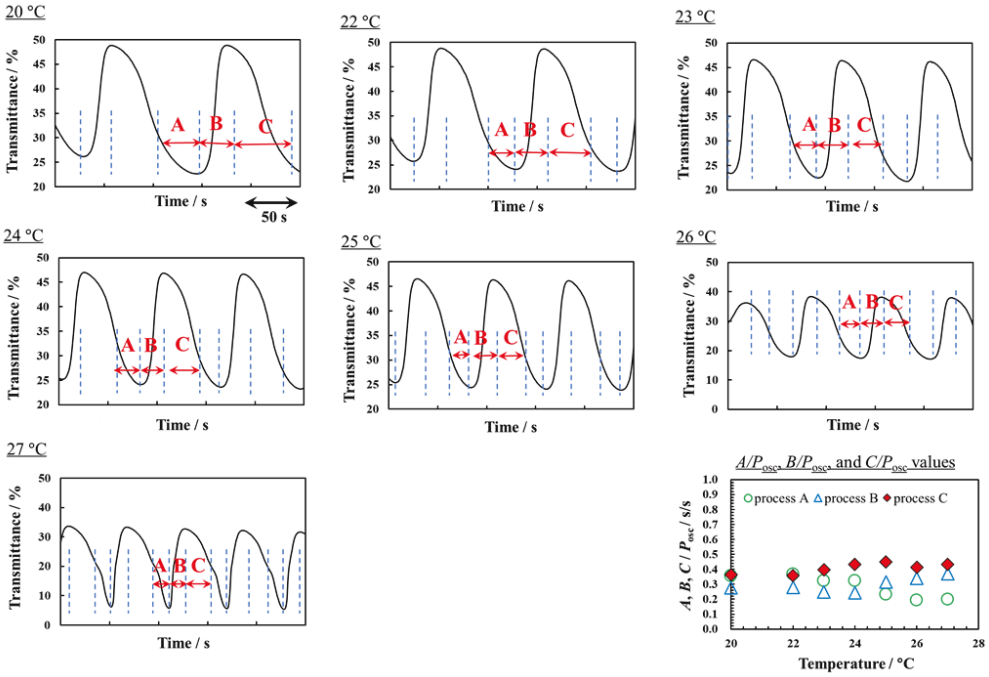

Figure 3-14. Typical oscillation waveforms in core-shell microgels at various temperatures ([**1**][PF_6]$_2$ = 50 μM; [HNO_3] = 300 mM; [$NaBrO_3$] = 84 mM; [MA] = 62.5 mM). Based on the FKN mechanism, the waveforms are divided into processes A, B, and C. The plot at the bottom right shows the values of A/P_{osc}, B/P_{osc}, and C/P_{osc} as a function of temperature.

Table 3-4. A/P_{osc}, B/P_{osc}, and C/P_{osc} values as a function of temperature for the core-shell microgels. The oscillation periods P_{osc}, the durations of processes A-C, and the values of A/P_{osc}, B/P_{osc} and C/P_{osc} are summarized.

Temp, °C	P_{osc}, s	A, s	B, s	C, s	A/P_{osc}	B/P_{osc}	C/P_{osc}
20	119.0	42.7	33.0	43.3	0.36	0.28	0.36
22	105.0	38.3	29.3	37.3	0.36	0.28	0.36
23	90.0	29.0	22.3	35.7	0.35	0.25	0.40
24	81.0	26.0	19.7	35.0	0.33	0.24	0.43
25	76.3	17.7	24.0	34.3	0.24	0.31	0.45
26	74.3	14.3	25.3	30.7	0.19	0.34	0.47
27	58.7	11.7	21.7	25.3	0.20	0.37	0.43

3.3.3. Temperature-controlled On-Off switching behavior of the BZ reaction in microgels

Next, the temperature dependence of the BZ reaction in each microgel was investigated (**Figure 3-15**). When the core (NRu) or the core-shell (NRu-N40) microgels were used as the reactor for the BZ reaction, the oscillation waveform appeared disordered and the transmittance increased with increasing the temperature from 25 °C to 35 °C (**Figure 3-15(a, b)** and **Figure 3-16**), indicating that the microgels had aggregated (**Figure 3-5(a, b)**). Conversely, when double-shell (NRu-N40-O) microgels were used as the reactor, the oscillation behavior immediately stopped upon raising of the temperature. Moreover, the oscillation behavior quickly restarted upon cooling the solution, i.e., the microgels returned to their swollen state (**Figure 3-15(c)** and **Figure 3-16**). Conversely, the oscillation did not stop when a [**1**][PF_6]$_2$ monomer solution was heated and then cooled **(Figure 3-15(d))**, which confirms that the observed on-off switching behavior is due to the properties of the double-shell microgels. Furthermore, the BZ reaction could be switched on and off repeatedly (**Figure 3-15(c)**).

However, the amplitude of the BZ reaction (A_{ave}: average oscillation amplitude) gradually decreased over several oscillation cycles, given that the substrate for the BZ reaction was consumed (**Figure 3-15(c)**). To overcome this problem, the author investigated the effect of the addition of more substrate on the on-off switching behavior of the BZ reaction. After switching the BZ reaction on and off twice under the same reaction conditions as those used in **Figure 3-15(c)**, additional substrate (0.5 mL; [HNO_3] = 1.5 M) was injected into the reaction system in one step using a pipette. Subsequently, the transmittance increased immediately, followed by restoration of the oscillation of the reaction and the cycles of on-off switching were extended (**Figure 3-15(e)** and **Figure 3-17**). These results indicate that the double-shell microgels could potentially find applications as a high-performance catalyst for the BZ reaction that can stop the oscillation behavior on demand.

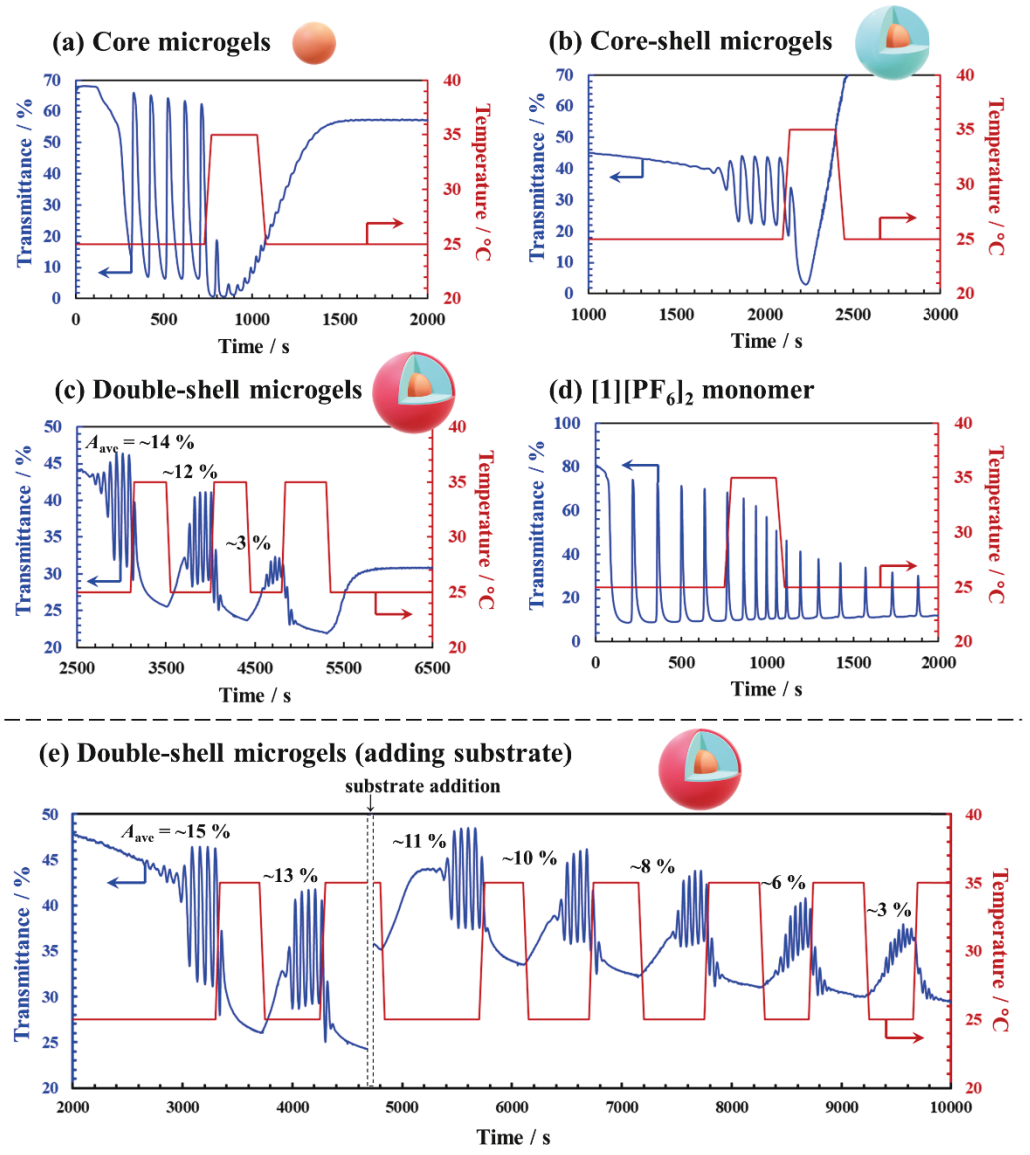

Figure 3-15. Oscillation waveforms for (a) the core (NRu), (b) the core-shell (NRu-N40), and (c) the double-shell (NRu-N40-O) microgels, as well as (d) the [**1**][PF_6]$_2$ monomer when the temperature was changed for ~300 s ([**1**][PF_6]$_2$ = 50 μM; [HNO_3] = 300 mM; [$NaBrO_3$] = 84 mM; [MA] = 62.5 mM). The reaction was heated to 35 °C and cooled to 25 °C. (e) Oscillation waveform obtained using the double-shell microgels when substrate was added after the BZ reaction was switched on and off twice (reaction conditions identical to those above). 0.5 mL of the substrate solution ([HNO_3] = 1.5 M) was added to 2.5 mL of the BZ reaction solution.

(a)

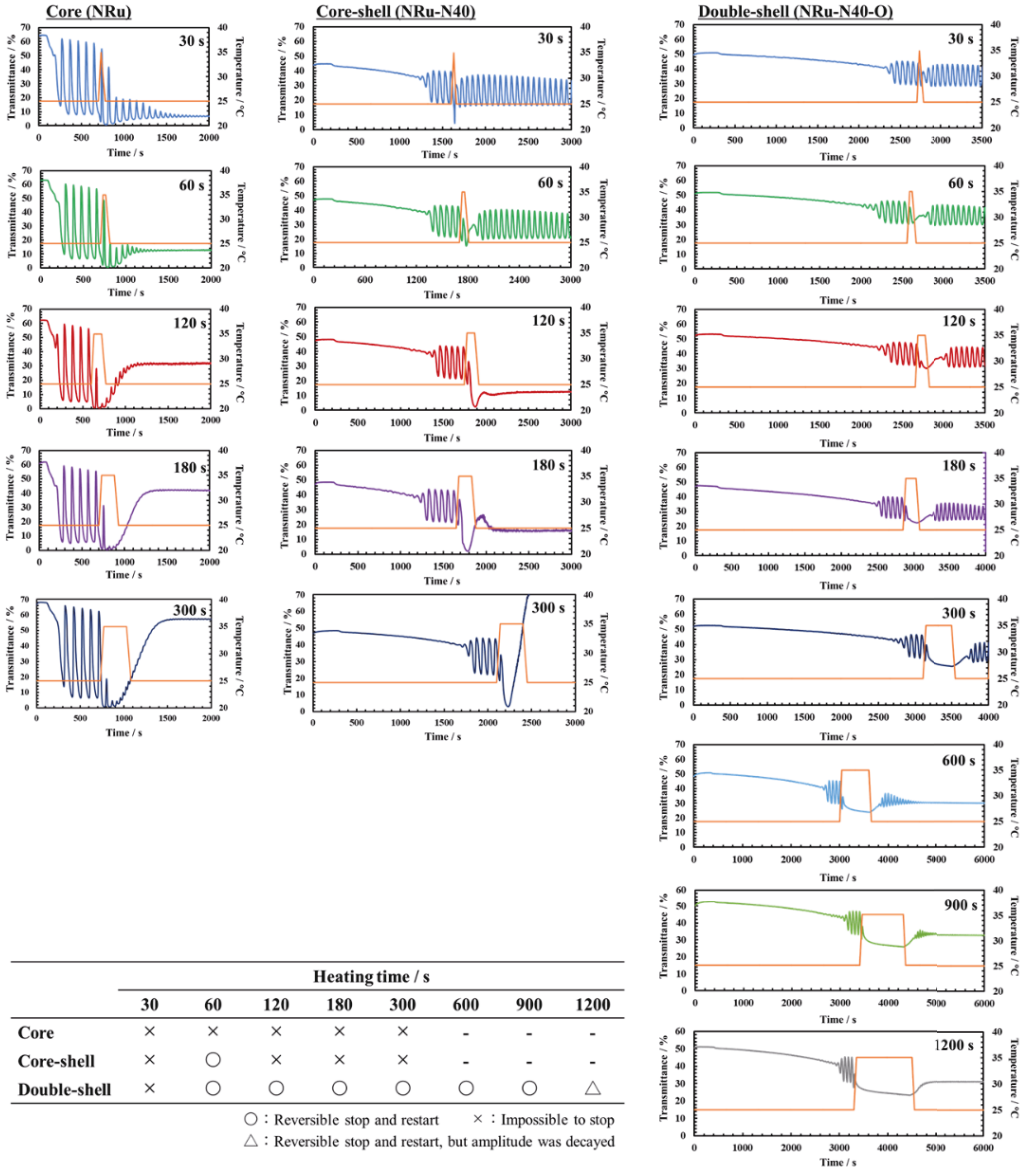

(b)

	Heating time / s							
	30	60	120	180	300	600	900	1200
Core	×	×	×	×	×	-	-	-
Core-shell	×	○	×	×	×	-	-	-
Double-shell	×	○	○	○	○	○	○	△

○ : Reversible stop and restart × : Impossible to stop
△ : Reversible stop and restart, but amplitude was decayed

Figure 3-16. (a) The oscillation waveforms obtained following time-dependent heating of the core (NRu), core-shell (NRu-N40), and double-shell (NRu-N40-O) microgels ([**1**][PF_6]$_2$] = 50 μM; [HNO_3] = 300 mM; [$NaBrO_3$] = 84 mM; [MA] = 62.5 mM. The reaction was heated to 35 °C and cooled to 25 °C). The time allowed for heating and cooling of the reaction was either 30 s, 60 s, 120 s, 180 s, 300 s, 600 s, 900 s, or 1200 s. (b) Summary of the oscillation behavior of the microgels following heating of the reaction to 35 °C and cooling to 25 °C over various time periods. Even though the core (NRu) and core-shell (NRu-N40) microgels showed irreversible aggregation at heating

times ≥ 120 s, it was possible to restart the BZ reaction when using the double-shell (NRu-N40-O) microgels due to their high colloidal stability. Above 1200 s, restarting the reaction was not possible due to substrate consumption.

The BZ reaction in this experiment was performed in a closed system, which means that the substrate would eventually be consumed as the BZ reaction proceeded. Therefore, to extend the oscillations of the BZ reaction, addition of more substrate is required. This was attempted with conventional oscillating microgels, although that the ionic strength increased upon adding the substrate, which lowered the colloidal stability. Therefore, it was difficult to restart the oscillation by addition of more substrate (**Figure 3-17(a)**). However, the double-shell microgels are designed to have not only the desirable ability to be able to control the substrate diffusion into the gel fixed with the catalyst, but also high colloidal stability. In contrast, when the double-shell microgels were used the colloidal stability was maintained and the oscillation of the reaction continued even after two additions of further substrate (0.5 mL; $[HNO_3]$ = 1.5 M) (**Figure 3-17(b)**). The amplitude of the transmittance decreased from ~19% initially to 12% following each addition of the substrate, which was tentatively attributed to the dilution of the [**1**][PF_6]$_2$ concentration. The BZ reaction was extended by addition of more substrate due to the colloidal stability imparted by the pOEGMA shell, which is a characteristic of the double-shell microgels. Therefore, the addition of more substrate was adopted as a solution to the problem that the number of times the reaction could be switched on and off were limited.

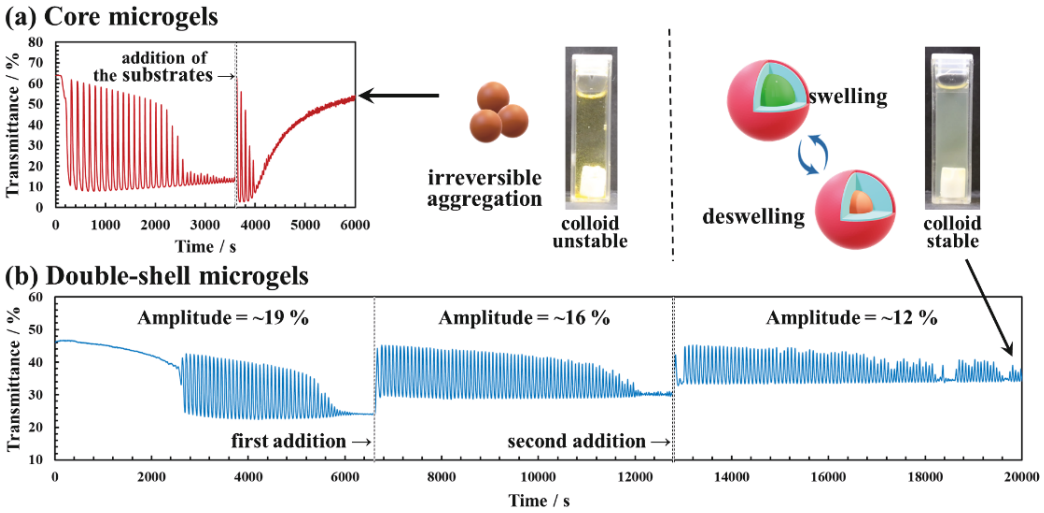

Figure 3-17. Oscillation waveforms of (a) the core (NRu) microgels and (b) the double-shell (NRu-N40-O) microgels when substrate was added after the oscillation had decayed ([**1**][PF_6]$_2$] = 50 μM; [HNO_3] = 300 mM; [$NaBrO_3$] = 84 mM; [MA] = 62.5 mM). 0.5 mL of the substrate solution ([HNO_3] = 1.5 M) was added to 2.0 mL of the BZ reaction solution.

In order to obtain further evidence for the on-off switching behavior of the double-shell microgels, the author investigated the thermal responsivity of the double-shell microgels by observing how the spatiotemporal pattern synchronized with the redox reactions of the [**1**][PF_6]$_2$ catalyst,[1-5] (**Figure 3-18**). A 0.2 wt% dispersion of the double-shell (NRu-N40-O) microgel was poured into a silicone rubber mold, placed between glass substrates, and then observed with a video camera. At room temperature (25 °C), a traveling pattern occurred spontaneously (**Figure 3-18(a)**; ~0 s to ~12 s) and the average oscillation period was determined to be ~150 s (**Figure 3-18(b)**). Upon increasing the temperature to 35 °C, the spatiotemporal pattern disappeared (**Figure 3-18(b)**; ~12 s to ~18 s). The spatiotemporal pattern was not observed for ~300 s at 35 °C. However, the BZ reaction, i.e., the spatiotemporal pattern was reactivated by cooling the microgel dispersion to 25 °C and the oscillation period was determined to be ~100 s, which is similar to the oscillation observed initially (**Figure 3-18 (b)**; ~18 s to ~25 s). Therefore, these results clearly indicate that the double-shell microgels can be used to stop the BZ reaction regardless of the stirring conditions. Typically, in catalysis studies using nanocomposite microgels, including metal nanoparticles, the diffusion kinetics of low molecules are affected by the properties of the microenvironment, such as the hydrophilicity/hydrophobicity and polymer density.[41-44] Suzuki's group has already demonstrated that the cross-linking density and the chemical composition of

microgels affect the induction period of the BZ reaction.[14,18,21] However, it still remains unclear whether the swelling state of pNIPAm affects the diffusion of the key substrates (e.g., Br_2, $HBrO_2$, and BrMA) for the BZ reaction. In this context, the results obtained in the present study constitute the first report of the effect of the thermal responsivity of pNIPAm microgels on a chemical oscillation reaction, which is important for the understanding and design of complex chemical reactions, such as the BZ reaction, in the presence of microgels.

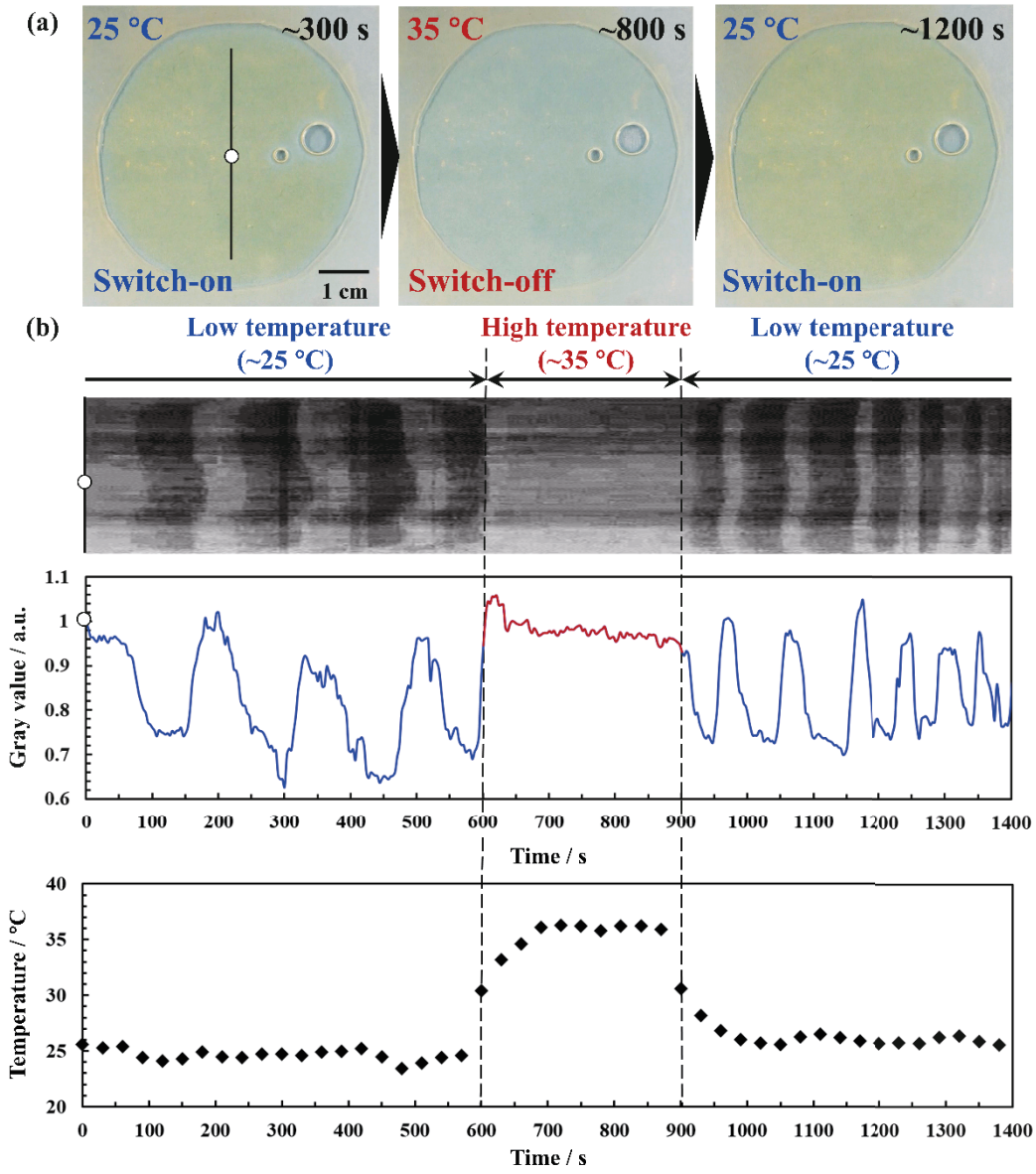

Figure 3-18. (a) Representative frames taken from movie showing the oscillating wave pattern of the BZ reaction at different time points. The bubbles observed in this case are carbon dioxide generated during the BZ reaction. (b) Gray value image of the spatiotemporal analysis (top), the oscillation waveform corresponding to the same analysis (middle), and temperature of the reaction vessel (bottom) ([microgel] = 0.2 wt%; [HNO_3] = 300 mM; [$NaBrO_3$] = 84 mM; [MA] = 62.5 mM. The reaction was heated to 35 °C and cooled to 25 °C).

3.4. Conclusions

The author has demonstrated the effect of the thermal responsivity of autonomously oscillating hydrogel microspheres, which contain the catalyst [ruthenium(II)tris(2,2'-bipyridine)][PF_6]$_2$ ([**1**][PF_6]$_2$), on the BZ reaction. To realize both molecular selectivity in response to temperature, and high colloidal stability of the microgel catalyst, microgels with a double-shell structure were prepared by seeded precipitation polymerization in the presence of the oscillating core microgels. The first shell is a thermo-responsive pNIPAm hydrogel, while the second shell consists of a more hydrophilic pOEGMA hydrogel. Due to the change in molecular interactions between the pNIPAm shell layer and the substrates of the BZ reaction, the BZ reaction that occurs in the microgel dispersion can be stopped or initiated on demand by changing the temperature. Moreover, the hydrated pOEGMA layer ensures that the double-shell microgels maintain their colloidal stability under high ionic concentrations (> 300 mM) and at high temperatures, i.e., above the VPTT of pNIPAm, which leads to reversible oscillation switching. The on-off switching behavior of the BZ reaction was confirmed by optical transmittance analysis of the microgel dispersion (**Figure 3-15(e)**) and by observation of the spatiotemporal pattern of the BZ reaction (**Figure 3-18**). Although the amplitude of the swelling and deswelling of the microgel catalyst was decreased by construction of the double-shell structure, the thermally responsive hydrogel shell can change the molecular selectivity and permeability of the microgels toward to the components of the complex chemical reaction system of the BZ reaction. The author believes that the core result of this study, i.e., a method to switch the BZ reaction on and off, will be beneficial for the development of advanced bioinspired materials with potential applications in e.g. self-oscillating micropumps,[19,21] high-performance catalytic carriers,[41-44,48] and reaction-diffusion models of biological oscillation phenomena[10-12]

3.5. References

1. Zaikin, A. N.; Zhabotinsky, A. M. Concentration wave propagation in two-dimensional liquid-phase self-oscillating system. *Nature* **1970**, *225*, 535-537.

2. Field, R. J.; Koros. E.; Noyes R. M. Oscillations in chemical systems. II. Thorough analysis of temporal oscillation in the bromate-cerium-malonic acid system. *J. Am. Chem. Soc.* **1972**, *94*, 8649-8664.

3. Zhabotinsky, A. M.; Zaikin, A. N. Autowave processes in a distributed chemical system. *J. Theor. Biol.* **1973**, *40*, 45-61.

4. Field, R. J.; Burger, M. *Oscillations and Travelling Waves in Chemical Systems*; John Wiley & Sons, Inc.: New York, 1985.

5. Toth, R.; Taylor, A. F. The tris(2,2′-bipyridyl)ruthenium-catalysed Belousov–Zhabotinsky reaction. *Prog. React. Kinet. Mech.* **2006**, *31*, 59-115.

6. Bertram, R.; Budu-Grajdeanu, P.; Jafri, M. Using phase relations to identify potential mechanisms for metabolic oscillations in isolated β-cell mitochondria. *Islets* **2009**, *1*, 87-94.

7. Bason, P. T.; Celler, B. G. Control of the Heart Rate by External Stimuli. *Nature* **1972**, *238*, 279-280.

8. O'Leary, T.; Marder, E. Temperature-Robust Neural Function from Activity Dependent Ion Channel Regulation. *Current Biology* **2016**, *26*, 2935–2941.

9. Yoshida, R.; Sakai, T.; Hara, Y.; Maeda, S.; Hashimoto, S.; Suzuki, D.; Murase, Y. Self-oscillating gel as novel biomimetic materials. *J. Controlled Release* **2009**, *140*, 186-193.

10. Pullela, S. R.; Cristancho, D.; He, P.; Luo, D.; Hall, K. R.; Cheng. Z. Temperature dependence of the Oregonator model for the Belousov-Zhabotinsky reaction. *Phys. Chem. Chem. Phys*. **2009**, *11*, 4236-4243.

11. Taylor, A. F.; Tinsley, M. R.; Wang, F.; Huang, Z.; Showalter, K. Dynamical Quorum Sensing and Synchronization in Large Populations of Chemical Oscillators. *Science* **2009**, *323*, 614-617.

12. Epstein, I. R.; Xu. B. Reaction-diffusion processes at the nano-and microscales. *Nature Nanotech.* **2016**, *11*, 312-319.

13. Suzuki, D.; Sakai, T.; Yoshida, R. Self-flocculating/self-dispersing oscillation of microgels. *Angew. Chem., Int. Ed.* **2008**, 47, 917–920.

14. Suzuki, D.; Yoshida, R. Temporal control of self-oscillation for microgels by cross-linking network structure. *Macromolecules* **2008**, *41*, 5830–5838.

15. Suzuki, D.; Yoshida, R. Effect of initial substrate concentration of the Belousov−Zhabotinsky reaction on self-oscillation for microgel system. *J. Phys. Chem. B* **2008**, *112*, 12618–12624.

16. Suzuki, D.; Taniguchi, H.; Yoshida, R. Autonomously oscillating viscosity in microgel dispersions. *J. Am. Chem. Soc.* **2009**, *131*, 12058–12059.

17. Taniguchi, H.; Suzuki, D.; Yoshida, R. Characterization of autonomously oscillating viscosity induced by swelling/deswelling oscillation of the microgels. *J. Phys. Chem. B* **2010**, *114*, 2405–2410.

18. Suzuki, D.; Yoshida, R. Self-oscillating core/shell microgels: effect of a crosslinked nanoshell on autonomous oscillation of the core. *Polym. J.* **2010**, *42*, 501–508.

19. Suzuki, D.; Kobayashi, T.; Yoshida, R.; Hirai, T. Soft actuators of organized self-oscillating microgels. *Soft Matter* **2012**, *8*, 11447–11449.

20. Matsui, S.; Kureha, T.; Nagase, Y.; Okeyoshi, K.; Yoshida, R.; Sato, T.; Suzuki, D. Small-angle X-ray scattering study on internal microscopic structures of poly(*N*-isopropylacrylamide-*co*-tris(2,2′-bipyridyl))ruthenium(II) complex microgels. *Langmuir* **2015**, *31*, 7228–7237.

21. Matsui, S.; Inui, K.; Kumai, Y.; Yoshida, R.; Suzuki, D. Autonomously Oscillating Hydrogel Microspheres with High-Frequency Swelling/deswelling and Dispersing/flocculating Oscillations. *ACS Biomater. Sci. Eng.* **2019**, *5*, 5615-5622.

22. Pelton, R. Temperature-sensitive aqueous microgels. *Adv. Colloid Interface Sci.* **2000**, *85*, 1-33.

23. Plamper, F. A.; Richtering, W. Functional microgels and microgel systems. *Acc. Chem. Res.* **2017**, *50*, 131-140.

24. Suzuki, D.; Horigome, K.; Kureha, T.; Matsui, S.; Watanabe, T. Polymeric hydrogel microspheres: design, synthesis, characterization, assembly and applications. *Polym. J.* **2017**, *49*, 695-702.

25. Karg, M.; Pich, A.; Hellweg, T.; Hoare, T.; Lyon, L. A.; Crassous, J. J.; Suzuki, D.; Gumerov, R. A.; Schneider, S.; Potemkin, I. I.; Richtering, W. Nanogels and Microgels: From Model Colloids to Applications, Recent Developments, and Future Trends. *Langmuir* **2019**, *35*, 6231-6255.

26. Heskins, M.; Guillet, J. E. Solution Properties of Poly(*N*-isopropylacylamide) *J. Macromol. Sci. Chem. A.* **1968**, *2*, 1441-1455.

27. Schild, H. G. Poly(*N*-isopropylacrylamide): experiment, theory and application *Prog. Polym. Sci.* **1992**, *17*,163-249.

28. Umeda, Y.; Kobayashi, T.; Hirai, T.; Suzuki, D. Effects of pH and Temperature on Assembly of Multiresponsive Janus Microgels *Colloid. Polym. Sci.* **2011**, *289*, 729-737.

29. Kureha, T.; Aoki, D.; Hiroshige, S.; Iijima, K.; Aoki, D.; Takata, T.; Suzuki, D. Decoupled Thermo- and pH-responsive Hydrogel Microspheres Cross-linked by Rotaxane Networks *Angew. Chem., Int. Ed.* **2017**, *57*, 15393-15396.

30. Ghosh, P. K.; Spiro, T. G. Photoelectrochemistry of tris(bipyridyl)ruthenium(II) covalently attached to *n*-type SnO_2. *J. Am. Chem. Soc.* **1980**, *102*, 5543-5549.

31. Jones, C. D.; Lyon, A. L. Synthesis and Characterization of Multiresponsive Core-Shell Microgels. *Macromolecules* **2000**, *33*, 8301-8306.

32. Jones, C. D.; Lyon, A. L. Shell-Restricted Swelling and Core Compression in Poly(*N*-isopropylacrylamide) Core-Shell Microgels *Macromolecules* **2003**, *36*, 1988-1993.

33. Jones, C. D.; Lyon, A. L. Dependence of Shell Thickness on Core Compression in Acrylic Acid Modified Poly(*N*-isopropylacrylamide) Core/Shell Microgels. *Langmuir* **2003**, *19*, 4544-4547.

34. Berndt, I.; Pedersen, J. S.; Richtering, W. Temperature-Sensitive Core–Shell Microgel Particles with Dense Shell. *Angew. Chem., Int. Ed.* **2006**, *118*, 1769-1773.

35. Nayak, S.; Lyon, L. A. Soft nanotechnology with soft nanoparticles. *Angew. Chem., Int. Ed.* **2005**, *44*, 7686-7708.

36. Lu, Y.; Ballauff, M. Thermosensitive core–shell microgels: from colloidal model systems to nanoreactors. *Prog. Polym. Sci.* **2011**, *36*, 767-792.

37. Smith, M. H.; Lyon. L. A. Multifunctional Nanogels for siRNA Delivery *Acc. Chem. Res.* **2012**, *45*, 985-993.

38. Hellweg, T. Responsive core–shell microgels: Synthesis, characterization, and possible applications. *J. Polym. Sci. Part B: Polym. Phys.* **2013**, *51*, 1073-1083.

39. Suzuki, D.; McGrath, J. G.; Kawaguchi, H.; Lyon, L. A. Colloidal Crystals of Thermosensitive, Core/Shell Hybrid Microgels. *J. Phys. Chem. C* **2007**, *111*, 5667-5672.

40. Hu, X.; Tong, Z.; Lyon, L. A. Multicompartment Core/Shell Microgels *J. Am. Chem. Soc.* **2010**, *132*, 11470-11472.

41. Richtering, W.; Potemkin, I. I.; Trautwein. C. Could multiresponsive hollow shell–shell nanocontainers offer an improved strategy for drug delivery? *Nanomedicine* **2016**, *11*, 2879-2883.

42. Gelissen, A. P. H.; Scotti, A.; Turnhoff, S. K.; Janssen, C.; Radulescu, A.; Pich, A.; Rudov, A. A.; Potemkin, I. I.; Richtering, W., An anionic shell shields a cationic core allowing for uptake and release of polyelectrolytes within core–shell responsive microgels. *Soft Matter* **2018**, *14*, 4287-4299.

43. Carregal-Romero, S.; Buurma, N. J.; Pérez-Juste, J.; Liz-Marzán, L. M.; Hervés, P. Catalysis by Au@pNIPAM Nanocomposites: Effect of the Cross-Linking Density. *Chem. Mater.* **2010**, *22*, 3051-3059.

44. Wu, S.; Dzubiella, J.; Kaiser, J.; Drechsler, M.; Guo, X.; Ballauff, M.; Lu, Y. Thermosensitive Au-PNIPAYolk–Shell Nanoparticles with Tunable Selectivity for Catalysis *Angew. Chem., Int. Ed.* **2012**, *52,* 2229-2233.

45. Sun, S.; Wu, P. On the Thermally Reversible Dynamic Hydration Behavior of Oligo(ethylene glycol) Methacrylate-Based Polymers in Water. *Macromolecules* **2013**, *46*, 236-246.

46. Maeda, Y.; Kubota, T.; Yamauchi, H.; Nakaji, T.; Kitano, H. Hydration Changes of Poly(2-(2-methoxyethoxy)ethyl Methacrylate) during Thermosensitive Phase Separation in Water. *Langmuir* **2007**, *23*, 11259-11265.

47. Kureha, T.; Suzuki, D. Nanocomposite Microgels for the Selective Separation of Halogen Compounds from Aqueous Solution, *Langmuir* **2018**, *34*, 837-846.

48. Kureha, T.; Nagase, Y.; Suzuki, D. High Reusability of Catalytically Active Gold Nanoparticles Immobilized in Core-Shell Hydrogel Microspheres. *ACS Omega.* **2018**, *3*, 6158-6165.

4. Summary

In this thesis, the author aimed to create new functional particles that exhibit bio-inspired oscillatory motion by synthesizing the particles and controlling their behavior via chemical reactions. For this purpose, microgels swollen by water, which are soft and deformable, were used. Immobilizing a transition-metal-based catalyst inside the gel endowed it with an energy-conversion mechanism by which it spontaneously exhibited swelling/deswelling oscillations in synchronization with the BZ reaction. The diffusion of the substrate into the microgels is important, as it controls the oscillation behavior of the microgels. The effects of physicochemical properties of the microgels, such as the chemical composition and microgel structure, on the BZ reaction were investigated.

First, the author developed new microgels that oscillate with a short period similar to that of the heartbeat. By synthesizing microgels with high colloidal stability and optimizing the BZ reaction conditions, a short period of ~1.3 s was achieved. As a further application, assembly of the microgels enabled short-period (~6.2 s) volume oscillations at near-biological temperature (37 °C). Such microgels with short oscillation periods are expected to find applications in autonomous materials such as artificial hearts or micropumps.

Second, the author developed new microgels in which the oscillation can be switched on and off as desired in response to temperature changes. This was achieved by synthesizing microgels with a temperature-responsive hydrogel shell that can regulate substrate diffusion into the gels. The author thus developed a guideline for the design of high-performance catalysts and autonomous materials that can be controlled by changes in the external environment.

The author succeeded in precisely controlling the oscillation behavior of the microgels, thus endowing them with higher functionality approaching that of living systems. The control of the oscillation behavior should find applications in biomimetic polymer materials, particles for catalytic reactions, and the control of spatio-temporal patterns for the BZ reaction. Thus, the results of this study are expected to contribute to the development of the fields of polymer, colloid, and interface chemistry. For further developments, the author believes that it is important to understand the oscillation behavior of microgels at the single-particle level and to control the assembly structure. In recent years, techniques for the synthesis, evaluation, and self-assembly of microgels have been developed. In addition, since microgels act as the catalyst of the BZ reaction,

understanding the BZ reaction is also important for their control. The BZ reaction has been examined from the perspectives of physical chemistry and nonlinear science, and appropriate mathematical models of chemical reactions have been reported. The author expects that the development of basic research into microgels and the fusion of different fields will lead to better control over the collective motion of microgel systems comparable to that of living organisms.

List of Publications

1. Inui, K.; Watanabe, T.; Minato, H.; Matsui, S.; Ishikawa, K.; Yoshida, R.; Suzuki, D.
   "The Belousov-Zhabotinsky Reaction in Thermoresponsive Core-Shell Hydrogel Microspheres with a Tris(2,2'-bipyridyl)ruthenium Catalyst in the Core"
   The Journal of Physical Chemistry B **2020**, *124*, 3828−3835.
   DOI: 10.1021/acs.jpcb.0c02238

2. Inui, K.; Saito, I.; Yoshida, R.; Minato, H.; Suzuki, D.
   "High-Frequency Swelling/Deswelling Oscillation of Poly(Oligoethylene Glycol) Methacrylate Based Hydrogel Microspheres with a Tris(2,2'-bipyridyl)ruthenium Catalyst"
   ACS Applied Polymer Materials, **2021**, *3*, 3298–3306.
   DOI: 10.1021/acsapm.1c00153

Other Publications

1. Matsui, S.; Inui, K.; Kumai, Y.; Yoshida, R.; Suzuki, D.
   "Autonomously Oscillating Hydrogel Microspheres with High-Frequency Swelling/deswelling and Dispersing/flocculating Oscillations"
   ACS Biomaterials Science & Engineering **2019**, *5*, 5615-5622.
   DOI: 10.1021/acsbiomaterials.8b00850

Reviews

1. 乾滉平、松井秀介、鈴木大介
   「ソフトゲル微粒子の自己組織化」
   日本油化学会「オレオサイエンス」、第 17 巻、第 2 号、pp55-62 (2017)

2. 鈴木大介、乾滉平
   「化学反応で動く人工ナノプラスチック」
   現代化学、2021 年 12 月号、No.609、pp60-64 (2021)

Oral Presentations

1. ○乾滉平、松井秀介、鈴木大介
   “時計タンパク質様集合挙動を示す人工微粒子の創製”
   新学術領域研究「動的秩序と機能」第 4 回若手研究会、アイアイランド、大阪、11 月 8 日(2017)

2. ○乾滉平、松井秀介、熊井有希、吉田亮、鈴木大介
   “動的な秩序機能を示すハイドロゲル微粒子の振動周期制御”
   第 69 回コロイドおよび界面化学討論会、筑波大学、茨城、9 月 19 日(2018)

3. ○乾滉平、松井秀介、渡邊拓巳、吉田亮、呉羽拓真、柴山允弘、鈴木大介
   “自律駆動高分子微粒子のコアシェル化による振動の on-off 制御”
   第 50 回中部化学関係学協会支部連合秋季大会、信州大学松本キャンパス、11 月 10 日(2019)、口頭(2K10)

4. ○乾滉平、渡邊拓巳、湊遥香、松井秀介、石川圭人、吉田亮、鈴木大介
   “$Ru(bpy)_3$ 金属触媒を担持したゲル微粒子の合成と化学振動反応の制御”
   第 71 回コロイドおよび界面化学討論会、オンライン開催、9 月 14-15 日(2020)、口頭(D-40)

5. ○乾滉平、渡邊拓巳、湊遥香、松井秀介、石川圭人、吉田亮、鈴木大介
   “温度応答性コアシェル型ゲル微粒子による化学振動反応のオン-オフ制御”
   第 69 回高分子討論会、オンライン開催、9 月 16 日(2020)、口頭(1K17)

6. ○乾滉平、鈴木大介
   “化学振動反応を駆動源とするゲル微粒子のコアシェル化による機能創出”
   2020 年度東海高分子研究会学生発表会、オンライン開催、11 月 7 日(2020)、口頭(2-12)

7. ○Inui, K.; Watanabe, T.; Minato, H.; Matsui, S.; Ishikawa, K.; Yoshida, R.; Suzuki, D.
   “Control of Chemical Oscillation Behaviors using Core-shell Hydrogel Microspheres”
   3rd G’L’owing Polymer Symposium in KANTO、オンライン開催、11 月 28 日(2020)、口頭(C08)

8. ○乾滉平、湊遥香、吉田亮、鈴木大介
“自律駆動ゲル微粒子の集団運動制御”
第 30 回日本 MRS 年次大会、オンライン開催、12 月 9 日(2020)、口頭(P-O9-012)

9. ○乾滉平、渡邊拓巳、湊遥香、松井秀介、石川圭人、吉田亮、鈴木大介
“自律駆動ソフトナノアクチュエータの階層化による運動機能のオン-オフ制御”
第 70 回高分子討論会、オンライン開催、9 月 8 日(2021)、口頭(3R02)

10. ○乾滉平、齋藤生真、吉田亮、湊遥香、鈴木大介
“心臓のように高速で振動する人工微粒子の創成”
第 72 回コロイドおよび界面化学討論会、オンライン開催、9 月 15 日(2021)、口頭(1D12)

11. ○乾滉平、佐野航季、吉田亮、湊遥香、鈴木大介
“化学反応で動くゲル微粒子集積体の運動制御”
第 21 回高分子ミクロスフェア討論会、オンライン開催、3 月 11 日(2022)、口頭(3-05A)

Patents

1. 鈴木大介、乾滉平、松井秀介、湊遥香
「細胞機能体及びその製造方法」
特願 2017-117591、出願日 6 月 15 日 (2017)
特開 2019-001902、公開日 1 月 10 日 (2019)

Awards

1. 針塚賞 (2016 年度信州大学繊維学部化学･材料系応用化学課程主席卒業)
2. ポスター賞 (第 69 回コロイドおよび界面化学討論会)
3. オンライン学生講演賞 (第 71 回コロイドおよび界面化学討論会)
4. 東海高分子研究会優秀口頭発表賞 (2020 年度東海高分子研究会学生発表会)
5. Award for Encouragement of Research (30th Annual Meeting of MRS-J)
6. 優秀ポスター賞 (第 70 回高分子討論会)
7. 優秀ポスター賞 (第 2 回発動分子科学研究会)
8. 学生優秀発表賞 (第 21 回高分子ミクロスフェア討論会)

5. Acknowledgements

First of all, I am deeply grateful to my supervisor Prof. Dr. Daisuke Suzuki (Shinshu University) for a lot of support and encouragement during my research. The advice and comments given by him has been a great help in developing the research. Without his guidance and persistent help this thesis would not have been possible.

I greatly thank to Emeritus Prof. Dr. Haruma Kawaguchi (Keio University), Prof. Dr. Ryo Yoshida (The University of Tokyo), Prof. Dr. Mitsuhiro Shibayama (The University of Tokyo), Prof. Dr. Takuma Kureha (Hirosaki University), Prof. Dr. Kenji Urayama (Kyoto Institute of Technology), Prof. Dr. Yoshitake Akiyama (Shinshu University), Prof. Dr. Yutaka Sumino (Tokyo Univ. of Science), Kazuki Murai (Shinshu University), Tohru Moriyama (Shinshu University), for useful comments, discussions, and suggestions.

I am also grateful to the Suzuki lab members. I have had the support and encouragement of them. They always influenced me positively, and thus I was able to continue to enjoy my research in the lab. I wish the Suzuki lab members many more successful.

Finally, I would like to thank my gratitude to my family, Naruhiro, and Chikako. Thank you for everything you have done for me. I can never thank you enough.

Kohei Inui
乾　滉平